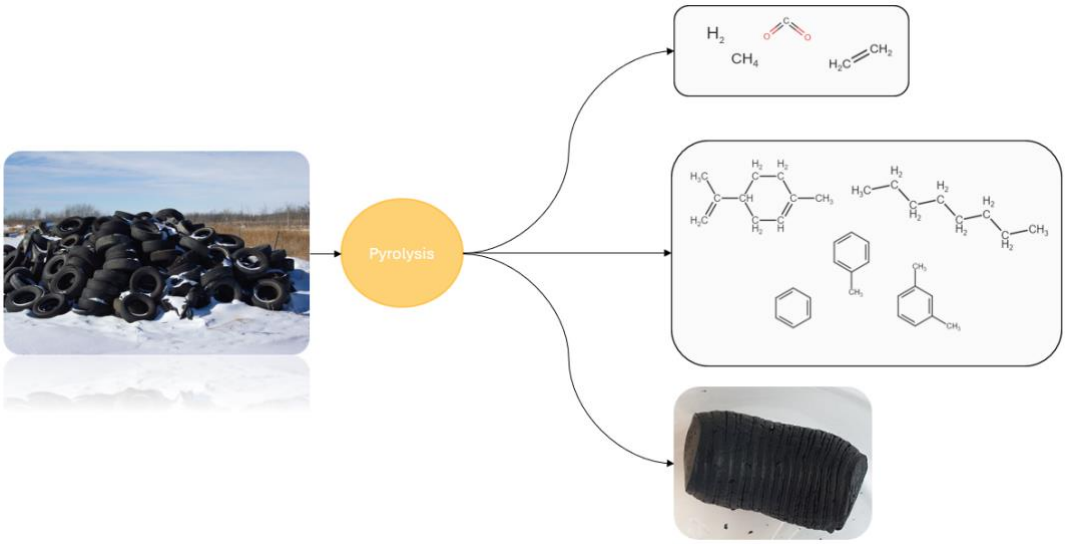

Thermochemical recycling of complex polymers

General decomposition pathways for pyrolysis of end-of-life tires

Master's thesis in Sustainable Energy Systems

Adam Sköld

DEPARTMENT OF Space, Earth and Environment

Division of Energy Technology

CHALMERS UNIVERSITY OF TECHNOLOGY

DEPARTMENT OF Space, Earth and Environment
Division of Energy Technology
CHALMERS UNIVERSITY OF TECHNOLOGY
Gothenburg, Sweden 2024
www.chalmers.se
Gothenburg, Sweden 2024
www.chalmers.se

MASTER'S THESIS 2024

Thermochemical recycling of complex polymers

General decomposition pathways for pyrolysis of end-of-life-tires.

Adam Sköld

CHALMERS
UNIVERSITY OF TECHNOLOGY

DEPARTMENT OF Space, Earth, and Environment
Division of Energy Technology
CHALMERS UNIVERSITY OF TECHNOLOGY
Gothenburg, Sweden 2024

Thermochemical recycling of complex polymers
General decomposition pathways for pyrolysis of end-of-life tires.
ADAM SKÖLD

Supervisor: Renesteban Forero Franco, Department of Space, Earth and Environment
Examiner: Martin Seemann, Department of Space, Earth and Environment
Part of a collaboration with Scandinavian Enviro Systems within the frame of Klimateledande Processindustri

Master's Thesis 2024
Department of Space, Earth and Environment
Division of Energy Technology
Chalmers University of Technology
SE-412 96 Gothenburg
Telephone +46 31 772 1000

Abstract
With an increasing population of the world, our reliance on tires in transportation and production of goods is following suit. As tires are relying on fossil fuels to produce both synthetic rubbers and the filler carbon black, recycling the material in end-of-life tires (ELTs) and closing the carbon loop is of great importance for continuing the production of tires in a sustainable fashion. Thermochemical conversion using pyrolysis is a viable option and has been proven to be commercially viable as the company *Scandinavian Enviro System* has shown by using the recovered carbon black in new tires, and the oils as feedstock to the petrochemical industry. To be able to predict the results from pyrolysis of ELTs, understanding the process is a must. In this work, the behaviour of the solid and volatile products was investigated using prior experiments, literature review and followed by modelling, done using both an empirical model as well as a simplified reactor model (SRM) using kinetics based radical reactions. The empirical model investigated the feasibility of using key species, i.e. species providing significant information about the process to be used in an implicit fashion to decrease the complexity of both models and analysis in experiments. The solid behaviour indicates the significance of how the particle is heated, as this dictates how if the particle is swelling or shattering as the volatile compounds are leaving the material. The interaction between the solid and volatile vapours leaving the sample was investigate further in a literature review, where the influence of heating rate was shown to affect the amount of carbonisation in the solid yield, where lower heating rates favoured carbonisation. The heating rate was also shown to influence the secondary reactions as yields of aromatic content increase with heating rate at the expense of aliphatic content, along with slightly higher gas production. The empirical model took heating rate into account when predicting the carbon conversion to species in both the oil and gas using a key specie. The models showed the promise of utilizing key species, while the species chosen, ethylene and styrene, should be investigated further in future research. By increasing the complexity in the simplified reactor model, additional insight regarding radical rearrangement could be gleaned, however, significant focus should be put on the kinetic parameters of the different reactions to create a more holistic decomposition model.

Keywords: Tire pyrolysis, ELTs, Carbon black, Pyrolysis, Aromatic hydrocarbons, Empirical modelling

Acknowledgments

As is the case for many things in life, one person’s work is not produced in a vacuum, but is a collaborative effort. I would like to express my gratitude to my supervisor Renesteban Forero Franco for supporting me during this endeavour with fruitful insights and discussions.

I would like to thank my examiner Martin Seemann for providing perspective and support, which has helped me to think differently as a researcher.

While this work was contained in my last semester at Chalmers, experiments done prior to it laid the groundwork for my understanding of the subject. With this I would like to thank both Nidia Diaz Perez and Jessica Bohwalli for their help and patience during the experimental trials.

Finally, I would like to thank my dear friend Eliette Emma Lacaze-Masmonteil, for her unwavering support, discussions, and critique.

Adam Sköld, Gothenburg, June 2024

Contents

List of figures

List of tables

List of abbreviation and nomenclature

ELT	*End-of-life tire*
HR	Heating rate, °C/min
NR	Natural rubber
Br	Butadiene rubber
SBR	Styrene-butadiene rubber
CFB	Circulating fluidised bed
CC	Carbon conversion
HC	Hydrogen conversion
SC	Sulphur conversion
OC	Oxygen conversion
H/C	Hydrogen to carbon ratio

Nomenclature

In this thesis the use of several definitions which needs further explanation is used and presented here:

- Solid residue yield

While char is a commonly used name for the solid yield, the solid residue also encapsulates the cases where full conversion has not occurred due to low temperatures.

- Carbon number.

It can be C2, C3, C4 etc. which refers to hydrocarbons which has two, three and four carbon atoms in their molecules, regardless of the bonds present in a compound. So propane is a C3, butane a C4 etc.

- Calculated by difference.

A mass balance is closed by difference, meaning if the solid and oil yield is 40%w_daf and 55w%_daf respectively, the gas yield calculated by difference would be 5%w_daf. By using this, we implicitly apply the assumption of no losses in the system.

1 Introduction

In our everyday lives tires are used extensively, either directly in personal vehicles public transport, or indirectly from use in agriculture or truck transport which enables our current lifestyle. The wear and tear of tires makes them an integral consumable in today's society. Due to the stable nature of tires at ambient conditions, they become a waste issue, making end-of-life solutions an important endeavour. While landfills might be seen as an option, the impact has on its local environment and its inhabitants is not to be understated. While end-of-life tires (ELTs) are mainly stable at ambient conditions, they do decompose into toxic compounds when exposed to UV radiation, which leaks into the surrounding environment. Landfills pose additional challenges as small puddles of water can be sustained within the pile of tires. These puddles are breeding grounds for mosquitos, adding to the issue with malaria and dengue fever in the local communities[1], [2].

Tires are a complex composite, containing rubbers (natural and synthetic), metals, fabrics (Polyester, Rayon etc.), fillers such as silica and carbon black, vulcanization agents and additives[3]. Due to this complexity, recycling poses a challenge as the materials are stable and interconnected, making removal of each individual material impractical. Some of the materials may be recovered using mechanical recycling by shredding the tires and separating out the metals and fabrics, leaving a crumble of rubber. The crumble can be re-used as fillers in asphalt or sports courts[2]. However, this only re-uses, or downcycles, the materials, essentially wasting the potential for recycling where new products can be created with the same properties as those produced by virgin feedstock.

Thermochemical treatment in the form of pyrolysis is a robust alternative where the feedstock is broken down into recyclable products by heating the sample in an oxygen-free environment, achieving a higher recovery rate of material. The solid phase (recovered carbon black, rCB) can be reused in tire manufacturing, while the liquid phase can be used to make tire derived fuels (TDFs) or as feedstock for the petrochemical industry due to the high aromatic content[2], [4].

Pyrolysis of ELTs is currently being demonstrated at a commercial level by *Scandinavian Enviro Systems*, who is selling the recovered Carbon Black (rCB) for reuse in the production of new tires. Recently their pyrolysis oil was successfully processed by the finish company *Neste* into "*high-quality raw materials for chemicals and plastics"*[5]. As development of new facilities is progressing, understanding the fundamental process is key. By furthering the understanding, designs of the process can be produced with a higher accuracy, making the overall procedure to have a *design*-based approach, rather than having to adjust an already built process in an *incremental*-based approach. Modelling can be used to understand the physical phenomenon occurring in the process, providing insight and enables predictions and estimations to be performed for the process.

1.1 Aim

The main purpose of this thesis is to provide insight into the decomposition patterns of end-of-life tires (ELTs) and to investigate the feasibility to model this process. This overall aim can be broken into parts to specify the issue:

- *Investigate the impact of thermal particle size on the characteristic of the solid yield after pyrolysis.* The impact of particle size influences how the particle behaves under different heating conditions, where the thermal size of the particle changes. This will be done by using data from prior experimental work.
- *Investigate what products can be found in a product stream from pyrolysis of ELTs.* This will include impact of end temperatures, heating rate and feedstock to show the yields of solid, liquid and gas products.
- *Evaluate the useability of empirical modelling.* By using empirical modelling a complex process, such as pyrolysis, can be simplified by the use of statistical correlations. The model can be used in both a predictive measure when designing a reactor, and as a reference point when doing experiments.
- *Evaluate the feasibility of explicit modelling of the radical reactions occurring during pyrolysis of ELTs.* By modelling the reactions explicitly, the model might result in a higher level of accuracy for the complex process.

1.2 Limitations

Limitations imposed on this thesis comes in many forms, some of which will
Due to the complexity of ELTs, some simplifications will be necessary, imposing limitation of the thesis:

1. The data used is provided from literature along with some results from previous research done by the author and Dr. Nidia Diaz Perez.
2. No new experimental campaigns were done.
3. Data collected from literature is limited to the data found during the period to the best of the authors ability.
4. All data was assumed to be true.
5. Temperatures below 800 °C was included from literature.
6. Condensation and re-evaporation of the products not accounted included.
7. No internal mass transport was included in models.

1.3 Specification of the issue

Tire pyrolysis is a broad field where experiments and modelling have been presented in different studies with different focuses, while still falling under the umbrella of ELT pyrolysis. The present work follows an increase of resolution of the process itself, starting from a broader view and zooming in, into the process as the thesis progresses. It can be divided into four parts:

1) The first part discusses the behaviour of the solids behaviour during pyrolysis as well as serving as an introduction to the procedures used in many of the studies.
2) The second part looks at the data found in literature to shed light into generic trends which as present for the process.
3) The third part uses the data and trends found to investigate how well the process can be modelled using an empirical model, which is evaluated against experiments found in literature.
4) The final part presents a study in the decomposition pathways of the monomers in rubbers by utilizing kinetic modelling to assess the feasibility of using such model in a predictive manner. The aim is to describe production of key species.

2 Background

In most peoples' everyday lives, tires play an important role in everything from production of goods to transportation. As tires are spent, they become an end-of-life tire (ELT) and needs to be disposed of. While there is a great variation of materials within one single tire, depending on the section of the tire, the variation of materials between two tires for different applications becomes even greater. Adding to this, manufacturers have their own recipes to produce tires with specific properties. This shows the heterogeneity of this feedstock, introducing issues when considering end-of-life options.

2.1 Material composition of tires

Tires mainly consists of several types of rubbers, fabrics, metals, additives, and fillers (such as silica and carbon black)[3], with proportions between different materials vary depending on the use case and manufacturer. In Table 1 some examples of compositions for different tires are shown to indicate the variance of tires[1].

Table 2-1. Common compositions of tires depending on application

Material wt.%	*Personal vehicle*	*Truck*
Rubbers	47	45
Carbon black	21.5	22
Metals	16.5	21.5
Textiles	5.5	-
Zinc oxide	1	2
Sulphur	1	1
Additives	7.5	5

Depending on the ratios between these products, the ELTs properties will be influenced. Two important parameters used in solid fuel conversion and thus in pyrolysis is the proximate and ultimate analysis. These properties of the feedstock provide some information regarding the decomposition (proximate analysis) and the mass fraction of some element (elemental composition). An example of the proximate and ultimate analysis for an ELT are shown in Table 2-2 as a reference point, note the fixed carbon(FC) and the volatile matter(VM) content as these will be referenced in the following section[6].

Table 2-2. Proximate and ultimate analysis of an ELT.

	Ultimate analysis, DAF, wt.%						*Proximate analysis, wt.%*		
	C	H	N	S	O	Ash	Volatile matter	Fixed carbon	Moisture
ELT	88.0	8.2	0.4	1.0	2.4	2.4	66.5	30.3	0.8

2.1.1 Rubbers

The main component of tires are rubbers, as they provide the elasticity and grip needed to dampen impact, adjust to the underlaying surface all while minimizing the abrasion on the road/surface. There are three main rubbers, all which are used in tandem to create the desired mechanical properties of the tires.

1. Natural rubber, consisting of isoprene, C_5H_{10}.
2. Butadiene rubber, a synthetic rubber consisting of Butadiene, C_4H_6.
3. Styrene-Butadiene rubber, a synthetic rubber created by copolymerization of Butadiene and Styrene, C_8H_8.

The monomer of natural rubber is 2-methyl-butadiene, or more commonly called isoprene, showed in Figure 1. In the figure, n indicates an arbitrary number of monomers to create the polymer polyisoprene when synthesised.

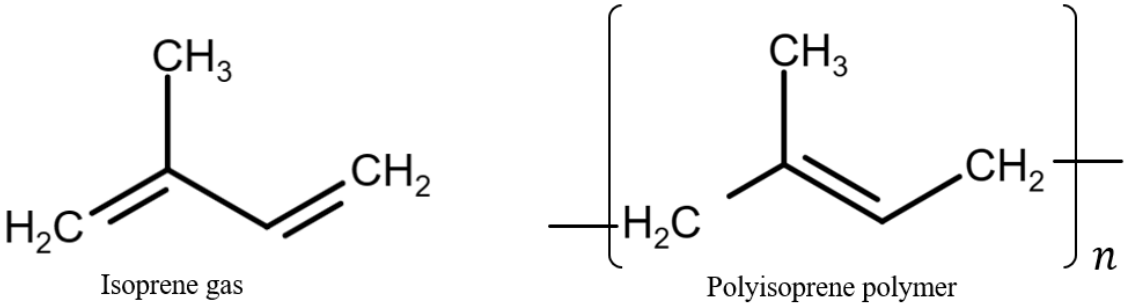

Figure 1. Monomer in natural rubber, polyisoprene.

The two most common synthetic rubbers are butadiene and styrene-butadiene rubbers. The first is (poly-) butadiene rubbers (BR) consist of a polymerisation of 1,3-butadiene gas, as seen in Figure 2, creating a rubbery solid with high abrasion and fatigue resistance [3], [7].

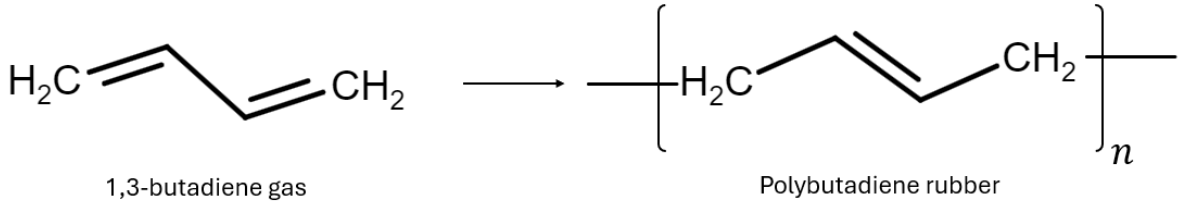

Figure 2. 1,3-butadiene monomers and polybutadiene rubber

When butadiene is copolymerized with styrene, the second synthetic rubber is created, (poly-) styrene-butadiene rubber, SBR for short, seen in Figure 3. The copolymerisation consists of random sequences of the two monomers. This irregularity makes then not crystalise upon stretching, thus needed reinforcement from carbon black or other pigments to be used in applications[7]. The amount of butadiene in the polybutadiene polymer is defined by m for each polymer, n, in Figure 3. The mass fraction of styrene in SBR varies depending on the type of SBR with some rubbers having 23.5-25 wt.% styrene while others have a styrene fraction of 40 wt.%[8], [9].

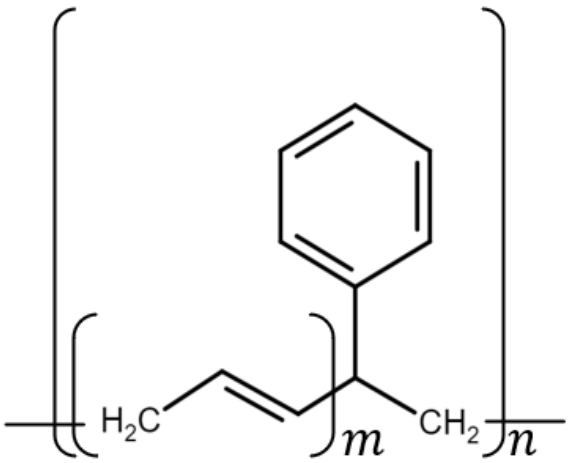

Figure 3. Styrene-butadiene rubber.

The rubbers are mixed in specific ratios depending on the manufacturer's recipe, however, the rubber themselves have specific characteristics. The ultimate and proximate analysis for natural rubber and SBR is shown in Table 2-3[10], in which some trace compounds such as nitrogen, sulphur and oxygen is shown. While these are not present in the monomers, they are present in the rubbers as well as being commonly reported for ultimate analysis of ELTs, as previously shown in Table 2-2. The table shows value for non-vulcanised rubbers, indicated by a very low sulphur content. Note the high amount of volatile matter compared to the ELT in Table 2-2, which indicates a decomposition of the polymers with low amounts of carbon left behind. The solid yield of both vulcanised and non-vulcanised rubber has shown a solid residue of around 2-3%wt_daf, while the rubbers themselves has a fixed carbon content is close to 0%wt_daf [11]. Compare these values to those of the ELT presented earlier and the influence of additives, such as carbon black, on the fixed carbon becomes evident.

Table 2-3. Ultimate and proximate analysis of natural rubber and SBR

	Ultimate analysis, DAF, wt.%						*Proximate analysis, wt.%*		
	C	H	N	S	O	Ash	Volatile matter	Fixed carbon	Moisture
NR	86.31	12.1	0.47	0.28	0.84	0.22	98.94	0.48	0.36
SBR	89.14	10.52	0.08	0.17	0.09	0.13	98.81	0.67	0.39

The rubbers themselves do not provide sufficient support for most applications and must be hardened in a process called vulcanisation. In this process several compounds are used, such as ZnO used as an accelerator and sulphur acting as the vulcanisation agent. The impact of vulcanisation on the products produced was studied by Liu et al. They noted that the impact was mainly seen at lower temperatures, where a vulcanised rubbers will produce more oil than a non-vulcanised rubber. They attribute this to the vulcanisation process, where the rubbers are mixed with the additives and heated to break the longer polymers, after which the sulphur will bond and crosslink the longer chains. This partial breakage of bonds during the process was assumed to be linked to the higher production of oil at lower temperature, as the polymers already had been slightly broken down, if the sulphur was not bonding and crosslinking. They also look at the sulphur distribution between the solid residue, oil, and gas when pyrolyzing the vulcanised rubbers. Above 400 °C, the sulphur will be in the oil (50-70%) and gas phase (50-30%)[11].

2.1.2 Carbon black, fillers, and additives

In tires the use of fillers is essential to achieve the desired performance. Carbon black contribute with abrasion resistance and silica aid with rolling resistance. Carbon black can be recovered when pyrolysis ELTs to be either reused in new tires or activated and be further used as activated carbon in filter for engineering applications.

2.1.3 Metal and fabrics reinforcements

A tire is used every day for extended periods, putting immense pressure on the tire as it spins. Because of this, additional reinforcements must be used to ensure the integrity of the tire is kept. The reinforcements along the inner edge of the tire are made from steel cable, while underneath the treads, woven meshes of steel and fabrics are used. The fabrics used in tires are usually Rayon, Polyester or Nylon[3].
The impact of fabrics can change the composition of the products in the gases. In experiments done by the author and Dr. Nidia Diaz Perez using a fixed bed reactor, gas composition provided some insight into this effect. Using pure rubber produced no CO at 550°C and 650°C, while CO_2 went from 1%wt to 12 %wt in the gas phase. When using samples which included

a large amount of fabric, the CO and CO_2 content in the gas phase was 12%wt and 43%wt at 550 °C and 14 %wt and 21 %wt at 650°C. This increase in oxygenated products is linked to the fabric content of the feedstock.

2.2 Recycling options

With an increasing world population, the number of tires is rising, and due to the stable nature of the materials at normal conditions, disposal of end-of-life tires (ELTs) becomes more important. End-of-life option might include energy recovery (combusting), grounding into granulates used for synthetic turf or asphalt[2] or landfilling. In the EU 2019 3.55 Mt of ELTs was produced, where was disposed of via either energy recovery, material recycling or other options such as pyrolysis or use in steel mills, to name a few. The material recovery (granulation) can be further divided up into subgroup as shown in Figure 4[12], indicated by the green colours.

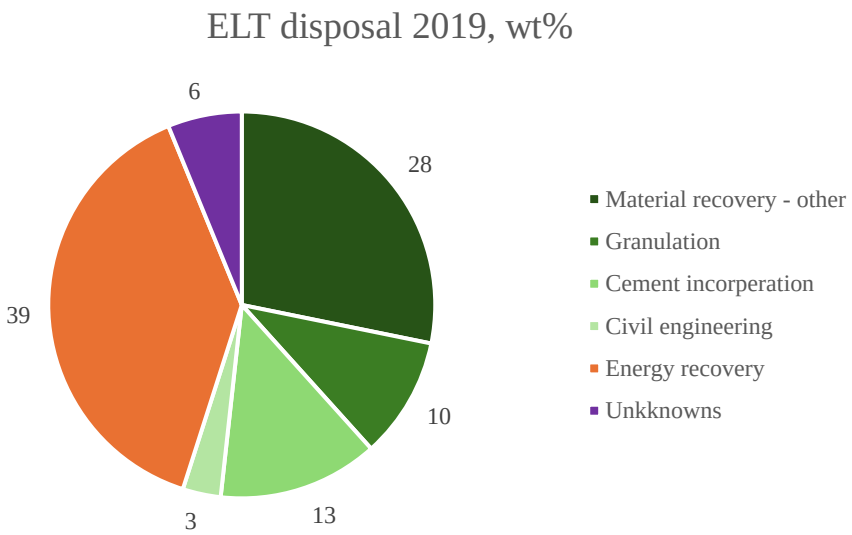

Figure 4. Disposal of ELTs in EU according to ETRMA 2019. All green colours indicate material recovery

2.2.1 Energy recovery

Energy recovery of the tires is widely used both in the form of using granulates as fuels in cement kilns, but the use of tire derived fuels (TDFs) from pyrolysis is also practiced as these are easier to handle than solid fuels. TDFs can also be used to replace some of the coal used today, as they have a higher heating value, while can also be defined as biofuel. TDFs is also used as cooking oil in Nigeria, something which greatly affects the health of the population using them, as the oil contain high amounts of carcinogens[2].

2.2.2 Material recovery

Materials, such as the metal bead and fabrics can be separated out, after granulation has been done. While the metal can be reused, Nylon or other fabrics is usually landfilled, adding to the issue with plastic waste in landfills. The remaining materials will be blend of rubbers, fillers, and additives, which can be used as granulates in construction, either in roads and sports fields, or in astroturf where rubber beads are used[2].
This is a partial solution to the issue of waste tires; however, the use of tires in construction materials as an end-of-life option has been demonstrated to be harmful for the health and environment due to leaching of toxic compounds. In leaching tests for crumb rubber asphalt concrete, metals such as aluminium and mercury have been found to be above the limit to be

deemed toxic in aquatic toxic tests, which indicates the potential to be harmful. Other compounds such as benzothiazole, a highly toxic accelerator used in the vulcanization process of rubber, was also found at high concentrations in the tests[13].
This highlights some of the issues with using ELTs in construction projects, making the implementation a trade-off where knowledge of the risks must be accurately understood.

2.2.3 Landfilling

Landfilling is an alternative which brings a host of issues for the local environment. The impact of landfilling comes in many shapes, with issue such as spread of harmful gases due to decomposition caused by UV-light exposure, leaching of heavy metals and toxic compounds into the ground. The heating value of tires is equivalent or higher than that of coal at 35-40 MJ/kg, making an outbreak of fire a very hard task to control. The fumes produced during a landfill greatly impact the local environment with its high contain of harmful compounds.
Other issue arises from the geometry of the tires, as they can hold small puddles of water, which can act as incubation of mosquito larvae. The landfills become breeding grounds for mosquitos, exacerbating the spread of malaria and dengue fever in regions with these issues. [14]

2.3 Pyrolysis

As mentioned, some parts of the tire can be separated, like the metal bead. Mechanically separating out each of the parts might not introduce any large benefits, as the fabrics might be landfilled and still leaves the crumb of rubber an end-of-life option.
To achieve a recovery of the material intended for reuse in new products with equal properties to those made from virgin feedstocks, pyrolysis is a viable option. This allows for recovery of solids (mainly carbon black(rCB)), oil and gas, where the solids can be reused in new tires and oils can be further refined to tire derived fuels (TDFs) or used as feedstock for the petrochemical industry, while the gas could be used locally to cover some of the heating demand [15].

3 Theory

3.1 Pyrolysis of ELTs

The pyrolysis step is an integral part of solid fuel conversion, in which the fuel is being evaporated due to high temperatures. The vapours (volatile matter) leaving the fuel can either be oxidized (combustion) or collected, making material recovery possible. In combustion air is used to combust the vapours leaving the fuel, providing heat to keep the combustion process going. In the case of material recovery, oxygen is not present in the reactor by using a carrier gas, usually nitrogen, which also removes the heat provided by the combustion cycle. Since the aim with the process is to recover the vapours, the fuel must be heated externally, as the pyrolysis step is endothermic. To ensure continuity in this work, pyrolysis refers to the process of material recovery using thermochemical conversion by externally supplied heat. The process is shown in Figure 5, where the pyrolysis process route is indicated by "material recovery".

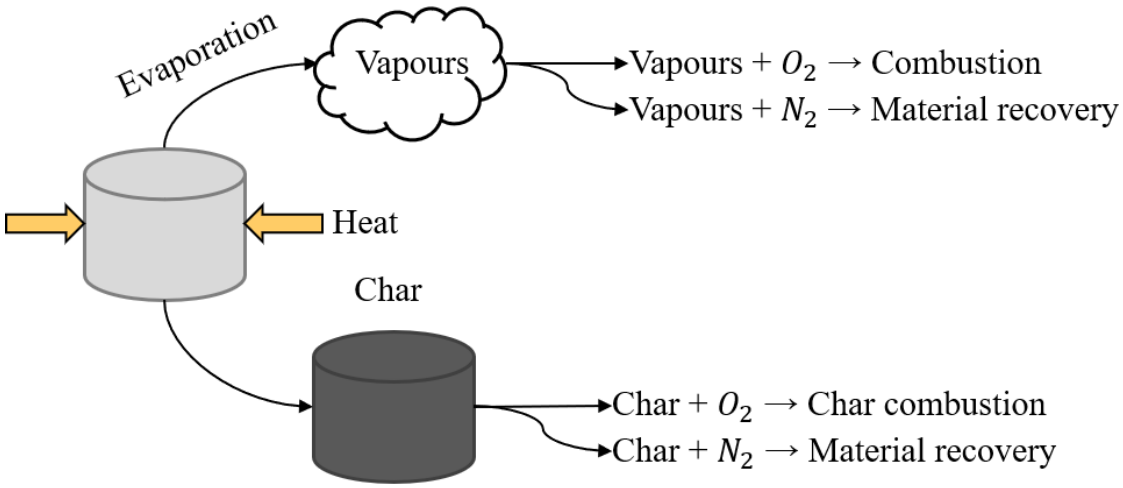

Figure 5. Pyrolysis step in solid fuel conversion with combustion and material recovery paths shown.

There are two distinct steps in pyrolysis of tires, presented by Yang et al., where the first step is the breaking of the bond to form a viscous tar, which is evaporated in the second step. Measurements done in Differential Thermal Analysis (DTA) to measure the energy consumed during the reaction shows the formation of the tar is an exothermic reaction, and the evaporation is an endothermic reaction. The energy required for the second step is more than what is being supplied by the first step, making the overall conversion endothermic[16].

The process of the pyrolysis of ELTs is a heat transfer-constrained process, where an almost linear increase in particle size, increases the time it takes for the sample to reach 90%w of its initial weight [17]. For larger particle sizes, the energy supplied will have to evaporate more oil to reach the same 90%w, leading to the linear correlation.

Yang et al. proposed a scheme of how the tar is transported within the sample. They defined three zones, a non-reacted, a reacting and a reacted zone, which can be seen in Figure 6, which is a modified version of what they showed in their study. The front of the reaction propagates inwards as the temperature of the sample is increasing due to the energy supplied from the reactor, Qr. The tars produced are evaporated continuously as heat is continuously supplied, forming bubbles. Yang et al. reported that the main internal mass transfer was done by bubble transport.

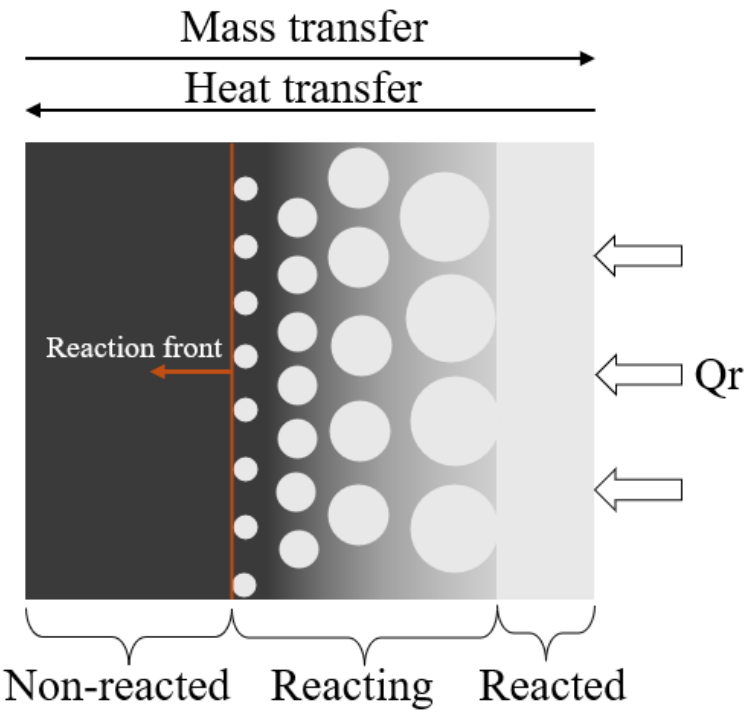

Figure 6. Internal mass transport of tars during pyrolysis, modified from Yang et al[18].

The general decomposition of ELTs has been studied using a *Thermal Gravimetric Analyser* (TGA), which continuously weighs a sample as it is heated up in a controlled environment. The most important process parameters are the end temperature, also called hold temperature °C, and the heating rate, which is the rate of which the temperature is increasing °C/min. The heating rate can also be seen as the energy supplies to the system. The decomposition of the different rubbers is affected by the heating rate, as higher heating rates seems to shift the major decomposition to higher temperatures, as shown by Lah et al. [19]. This influence was shown by the decomposition for the whole tire starting at 180 °C at ending at 510 °C when using a heating rate of 5 °C/min, while a for a heating rate of 25 °C/min the decomposition started at 260 °C and ending at 650 °C. This shift has been attributed to differences in heat transfer for different heating rates together with the kinetics of the reactions[6].
Bhowmick et al. looked at the decomposition of natural rubber tires and concluded that in air, the decomposition starts at 230 °C, while in nitrogen it starts at 330 °C, when using a heating rate of 10 °C/min[20]. Williams et al. supported the start of decomposition at around 330 °C for NR, while SBR and BR starts to 370 °C at 20°C/min. SBR undergoes two stages in as it decomposes, making the exact decomposition temperature harder to accurately describe[6].

The decomposition of ELTs has been studied by the author together with Dr. Nidia Diaz Perez, by using different end temperatures and heating rate. In Figure 7 the decomposition of three different types of tires is shown, alluding to the difference in behaviour of depending on the mixtures of materials, such as fabrics, metals, and rubbers.
The first stage is the drying phase, best indicated by the grey line, which has a slight decrease in mass as the sample is drying. Since tires have very small moisture contents compared to something like biomass, this step is usually not distinct enough to identify.
The decomposition has small “bumps”, such as the one indicated by the arrow, which shows another material starts to decompose within the sample. As tires contain a mixture of rubbers, fabrics, and additives, which decompose at different temperatures, these bumps might be attributed to another material starting to decompose.

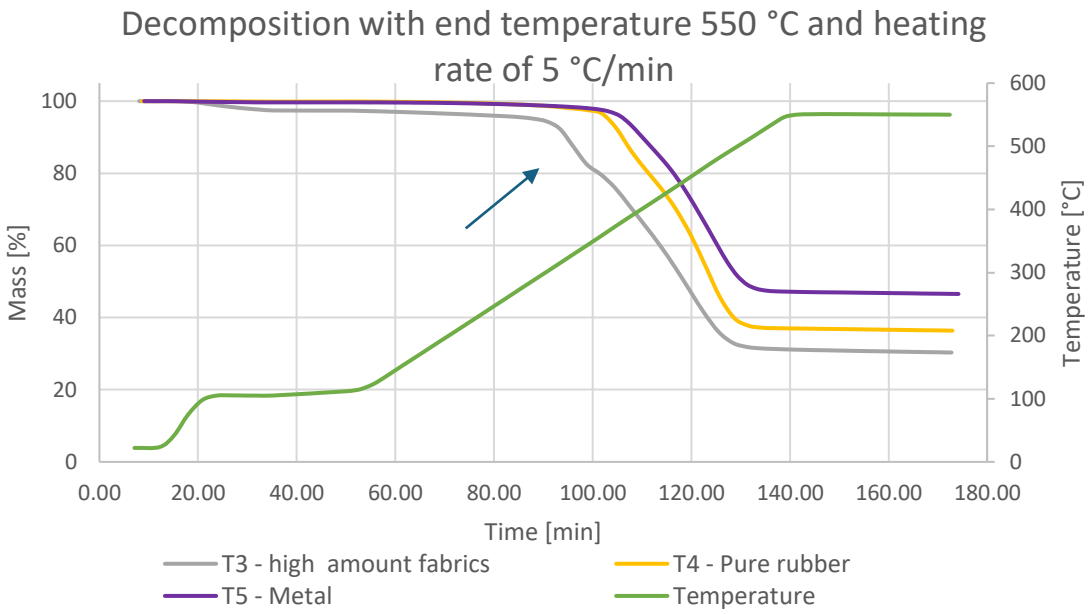

Figure 7. Decomposition of ELTs in nitrogen filled atmosphere.

3.2 Primary and secondary reactions

When polymeric materials undergo thermal decomposition, the products can be influenced by to what extent primary and secondary reactions has occurred. Primary reactions are directly linked to the polymer structure, i.e. the monomers of the chain, thus linked to the ratio between the rubbers in the ELT. This first breakage is the primary reaction, followed by radical rearrangement, resulting in primary products. Secondary reactions are the process of taking the primary products and breaking them down to more stable products, which is favoured by higher temperatures and is time dependent[21].

3.3 Key specie modelling

To simplify a complex process, such as pyrolysis, key species can be used. They can be integrated in both modelling and in experiments. A key specie is assumed to be an integral part of the reaction paths during conversion. When implemented correctly, the mass balance of carbon can be accounted for to a high degree by only analysing/modelling one specie. This enables easy implementation of analysis equipment in experiments, meaning only the key specie(s) needs to be determined to provide insight about process and reactions themselves. This can also be incorporated in modelling to simplify the system, reducing the demand for explicitly accounting for all reactions in the pyrolysis process, reducing computational resources.

3.4 Solid residence time

Bouvier et al. looked at the impact of particle size, mainly in the form of how the time to reach a sample weight of 90 %w was influenced. With larger sizes, the time increased in a linear relationship, as there is a higher amount of material needed to be evaporated to reach the 90%w. The impact on the compounds was also investigated where a larger size was shown to increase lighter compounds such as the H_2 and CH_4 at the expense of C_2 and C_{3+}. This was attributed to breakdown of larger compounds and cyclisation due to the elevated temperatures [17]. One key factor is the heat supplied to the sample as pyrolysis is a heat transfer-based process. The heat supplied to the surface will increase with increased heating rate, where one extreme is the fluidized bed, and another is a fixed bed reactor with a low heating rate.

3.5 Feedstock characteristics

Feedstocks used in any process, whether it's for combustion processes or pyrolysis, can be partially characterized by the proximate analysis and elemental composition (ultimate analysis).

The ultimate analysis shows the weight percentage of key elements, which doe ELTs are carbon(C), hydrogen(H), oxygen(O), nitrogen(N) and sulphur(S), the ash content might be included in the ultimate analysis.

An important key ratio in a sample is the H/C ratio, which relates the amount of moles of hydrogen to carbon within a sample. H/C numbers for aromatics are lower, benzene for example has a H/C = 1, while aliphatics it is always above 2 due to them being saturated with hydrogen. Smaller aliphatic compounds such as ethane has H/C = 3, while larger, such as hexane has H/C=2.3. As the aliphatic compounds increase in size, their H/C value decreases, trending towards 2. Thus, if the H/C value of the fuel is known, it can shed some insight into the polymeric composition.

The proximate analysis provides information about the feedstock as it undergoes conversion. It can be derived from using a TGA to determine the moisture (M), volatile matter (VM), fixed carbon (FC) and ash content (A) of the feedstock. The process has 4 distinct steps, of which the first 3 are done in an inert atmosphere. It starts with a drying phase followed by a rapid decrease in mass (devolatilization) after which a stable solid residue is left. The final step introduces oxygen into the reactor, combusting away the fixed carbon, only leaving the ashes of the sample behind. In Figure 8, a sample of ELT was used to find the proximate analysis in prior work done by the author and Dr. Nidia Diaz Perez.

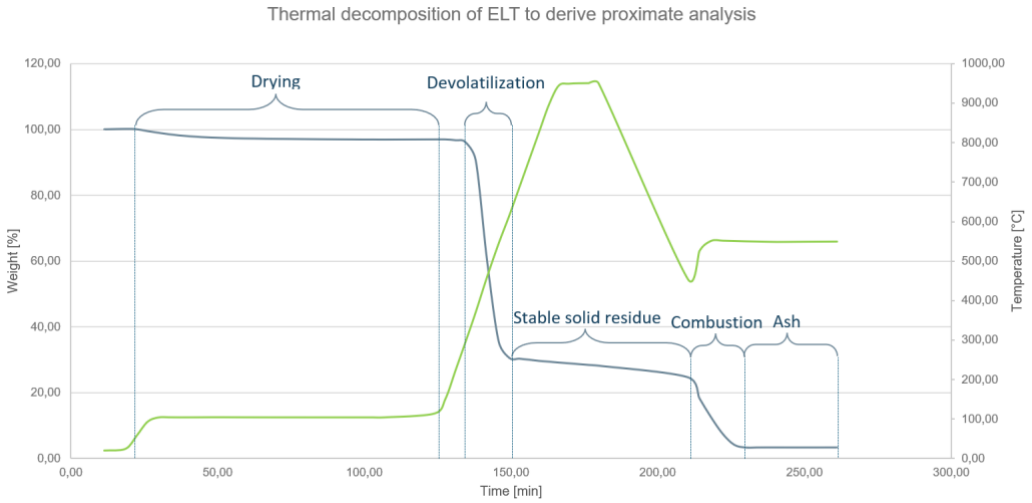

Figure 8. TGA run to find the proximate analysis of a sample.

The sample can be described by the amount of mass which has left in the different steps, as shown in eq. 1-5.

$$Y_{feedstock} = 100\% = Y_M + Y_{VM} + Y_{FC} + Y_{ash} \quad 1$$

$$Y_M = 100\% - Y_{sample}(t = drying) \quad 2$$

$$Y_{VM} = Y_{sample}(t = drying) - Y_{sample}(t = stable\ solid\ residue) \quad 3$$

$$Y_{FC} = Y_{sample}(t = stable\ solid\ residue) - Y_{sample}(t = end) \quad 4$$

$$Y_{ash} = Y_{sample}(t = end) \quad 5$$

Samples can differ even when the same feedstock is used, so describing the sample used in an experiment as generic as possible can be done by reporting the dry-ash-free (DAF) values of the ultimate and proximate analysis. As opposed to a DAF sample, a sample can be reported on as-received basis (AR), which is a non-processed sample, leading to high moisture contents in the case of biomass. In the case of tire, the amount of silica or steel can affect the composition of the reported samples, as these are variables which might not be reported but will increase the ash content in the sample. Figure 9 shows a schematic (modified from Neves et al.) of a sample as individual constituents, where the ash and moisture can be excluded to get the yield on DAF basis[22].

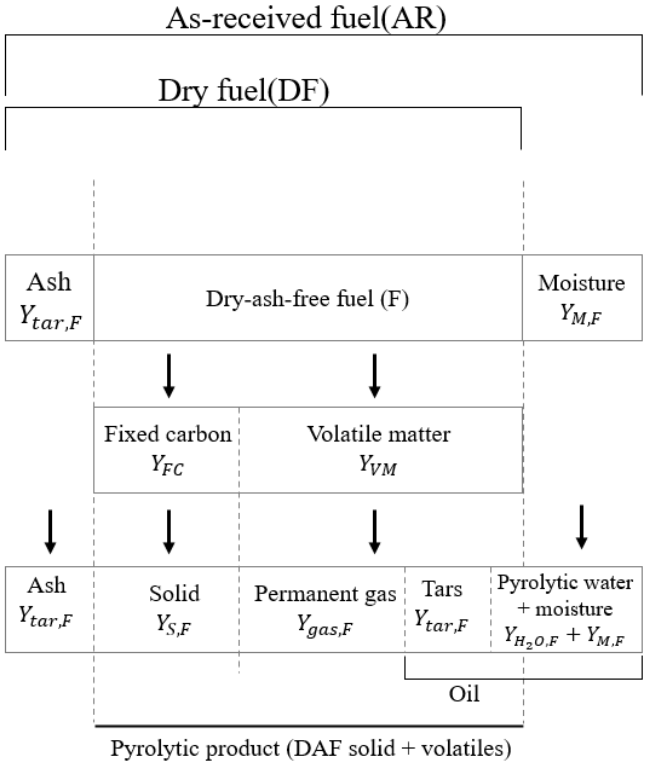

Figure 9. Sections of feedstock, based on Neves et al.[22].

3.6 Biot number

When a particle is heated, as is the case for pyrolysis, the size and the material of the particle affects how the particle is behaving during conversion, thus affecting the products. The Biot number, shown in eq. 6, provides insight into this by describing a thermal size of the particle, which relates the internal to the external heat transfer.

$$Bi = \frac{h_{ext}\, L}{k} \tag{6}$$

The conductivity, k, is material dependent and provides together with the characteristic length, L, the internal heat transfer. The external heat transfer, h_{ext}, is of great importance when determining the thermal size of the particle, as it will change depending on the type of heating occurring. The external heat transfer is dependent on the flow regime surrounding the particle. For systems where convective flow is present, such as in a fixed bed reactor, the Nusselt number, shown in eqn. 7 can be used to provide this [23]. For cylindrical particles entrained in convective flow, the Churchill-Bernstein relation can be use, as is shown in eqn. 8. [24].

$$Nu = \frac{h_{ext}\, L}{k_g} \rightarrow h_{ext} = \frac{Nu\, L}{L} \tag{7}$$

$$u = 0.3 + \frac{0.62\, Re_D^{1/2}\, Pr^{1/3}}{[1 + (0.4/Pr)^{2/3}]^{1/4}} \left[1 + \left(\frac{Re_D}{28200}\right)^{5/8}\right]^{4/5} \tag{8}$$

3.7 Reaction rate - Kinetics parameters

When modelling any reaction, the rate at which the reaction is happening is important. This will relate both the products produced, while also describing how something is consumed, an important parameter for any conversion.

The rate of a reaction is commonly described by using the Arrhenius expression where the rate is defined by its activation energy (E_a) and pre-exponent factor (A). Kinetic parameters represent experimental data and is used to explain the rate of which the reaction is occurring, depending on time and temperature. As an example, the oxidation of carbon is used:

$$C + O_2 \rightarrow CO_2$$

The reaction rate constant of the reaction, k[s^{-1}], is shown in equation 9, where A and E_a is connected to the reaction itself, and temperature in kelvin, T, is system dependent. R is the universal gas constant. It describes the conversion of reactants to products per second.

$$k_{C \rightarrow CO_2} = A \exp\left(\frac{-E_a}{RT}\right) \tag{9}$$

The transient conversion can be described by using k together with the consumption of reactants. In equation 10-11, the oxidation of carbon is used to demonstrate the consumption within a timestep, i. The amount of carbon and oxygen going into the timestep is the output from the previous timestep, $i - 1$, as mass can be created not destroyed. A schematic overlook is show in Figure 10.

$$\frac{d(n_C)}{dt_i} = k * n_{C,i-1} \tag{10}$$

$$n_i = n_{i-1} + \frac{d(n_{i-1})}{dt} * dt \qquad 11$$

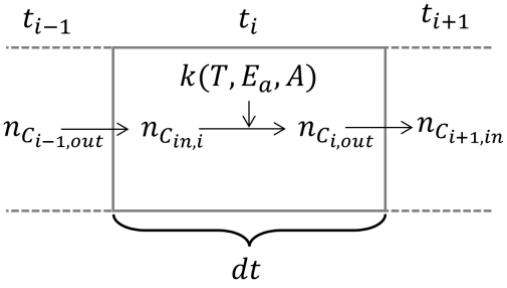

Figure 10. Transient consumption of carbon schematic

3.8 Diels Adler reaction

Pyrolysis of ELTs produce significant amounts of aromatic hydrocarbon and one path to produce them is the Diels Adler reaction, introduced here to provide an undelaying understanding of this process.

Diels Adler reaction is a way to create cyclic compounds from reactions of a diene and dienophile, creating cyclohexane, as seen in Figure 11. The carbon number (1-6) are shown in the figure. The double bond of ethylene breaks to form a single bond between carbon 1 and 2, followed by the breaking of the next bond creating a double bond between 3 and 4, propagating the breaking of the last double bond, and finalizing the formation of the single bond between 5 and 6. This reaction is rather slow compared to the radical reactions to form cyclic compounds[25]. Aromatic rings are created by dehydrogenation of the cyclohexene, producing hydrogen gas, as is shown in Figure 12.

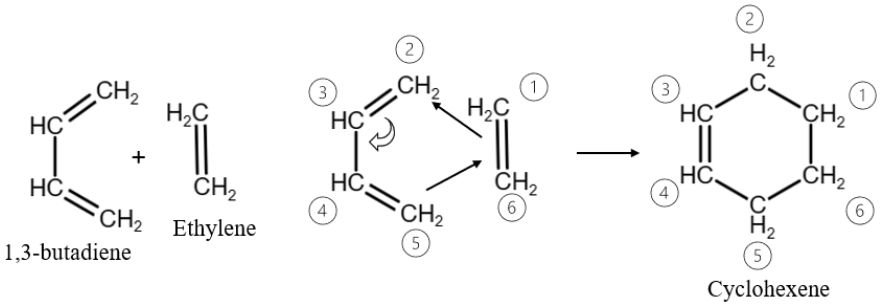

Figure 11. Diels Adler reaction of 1,3-butadiene and ethylene

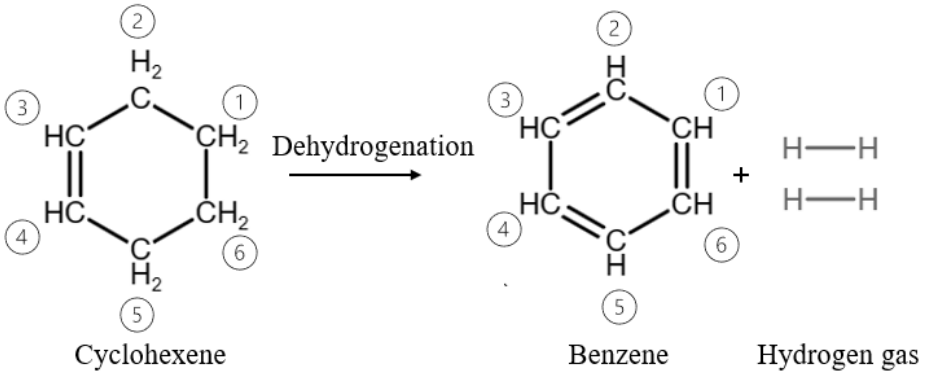

Figure 12. Dehydrogenation of cyclohexene to produce benzene and hydrogen gas

4 Methodology

The methodology follows a process, starting with focus on the char production and heating implications, followed by a literature review to deduce patterns of product yields which is used to empirically estimate the yields, and is concluded by a simple reactor model utilizing kinetic expression.

4.1 Char yield, thermal size, and heat transfer.

Prior work done by the author together with Dr Nidia Diaz Perez was used to look the characteristics of the solid as it undergoes conversion. Prior work focused on the surface area of the char, an aspect which will not be covered in this work. The focus in this work was to allude to the changes of the char as different heating conditions, i.e. energy supplied. The sampled used contained only rubber from tires, i.e. no reinforcements in the form of fabrics or metals were included.
A TGA reactor and a tubular reactor with a fixed bed (T-FXBR) was used for the same type of feedstock, which of one is shown in Figure 13, in different heating conditions.

Figure 13. Sample used in TGA and Fixed bed reactor.

The TGA uses conduction dominated heat transfer via walls of crucibles and the T-FXBR has a convective dominated heat transfer. The to evaluate the impact of the heating regime, the Biot-number was calculated for the two reactors a run at 550 °C. The three runs operating parameters are shown in Table 4-1.

Table 4-1. Operating conditions for experimental trials

	Heat transfer regime	*End temperature °C*	*Heating rate °C/min*	*Flow rate l/min*
TGA-1	Conductive	550	5	10
TGA-2	Conductive	550	20	10
T-FBR	Convective	550	Inf	10

Do determine the thermal size of the sample in the different reactors, the Biot number was calculated. For the TGA the external thermal heat transfer coefficient was calculated by using a series coupling of the conduction of the crucible wall and the stagnant nitrogen fluid. As there is little to no fluid movement within the crucible as is it sealed, the heat transfer through the fluid will also be by conduction. The crucible and nitrogen gas were assumed to have a thermal conductivity of 3.1 and 54e-3 W/mK [28] respectively.

4.2 Literature data collection

The literature data collection aimed to find information about the feedstock, yields of products and specific compounds. Sources used was publishers such as Elsevier or ACS publications, along with material data from PubChem and communication documentation from institutions

such as ETRMA. The sources used was [29], [30], [31], [32], [33], [34], [35], [36], [37], [38], [39], [40], [41], [42], [43]. A table of the data found is shown in Appendix
Appendix A. Few authors reported the species found in the gas, where some included compounds up to C6, while others did only include H_2, CO, CO_2 and CH_4. Similarly, the oil composition was reported differently between authors. Due to this lack of data available, two more reactors were included in the dataset, a fluidized bed for the gas phase[41] and a rotary kiln for the oil phase[44].
To be able to see the influence of operating conditions, common parameters was used to present data in literature. Due to differences in how feedstock, operating conditions, and products was reported, the number of datapoints varied.
Parameters which were commonly found at was:

- End temperature (°C)
- Particle size (mm)
- Elemental and proximate analysis of the feedstock
- Type of reactor

Parameters which were not always reported but was of great interest was:

- Heating rate (°C/min)
- Elemental and proximate analysis of the products, either oil or solid.
- Species of the oil and gas phase

To find some common parameters about the feedstock, averages, and deviations of both the ultimate and proximate analysis was determined. Experiments have an inherent variation, leading to deviations between experiments using the same operating conditions. To overcome this issue, normalization of the data collected was vital. A few important normalisations were made, such as taking particle size into consideration for evaluating the yield of solid, liquid and gas. Two additional procedures which need explanation were made: dry-ash-free basis and carbon conversion.

4.2.1 Dry-ash-free basis

Some authors reported the elemental composition of the solid yield which includes the ash yield, making the adjustment to DAF in more accurate, where the weight for both ash and moisture is removed. This was however not done by all authors, so to keep consistency, all ash in the parent duel was assumed to remain in the solid residue, which is in accordance when pyrolyzing biomass according to Neves et al[22]. By using this assumption, the solid residue could be adjusted by using eq. 12 to get ($Y_{sol,F}$,kg DAF solid/kg fuel).

$$Y_{sol,F} = \frac{Y_{S,R} - Y_{a,R}}{1 - Y_{a,R}} \qquad 12$$

The remaining phases was determined using eq.13. ($Y_{liq,F}$,kg DAF liquid/kg fuel, ($Y_{gas,F}$,kg DAF gas/kg fuel).

$$Y_{liq,F} = \frac{Y_{L,R}}{1-Y_{a,R}} \qquad Y_{gas,F} = \frac{Y_{G,R}}{1-Y_{a,R}} \qquad 13$$

4.2.2 Carbon conversion (CC)

Yields of a specific specie, such as ethylene or benzene, was usually reported as a mass fraction. Since there is a connection between polymeric content in the feedstock and the primary products, as described in section 3.2, taking this inherent variation into account was deemed important. To do this, the carbon conversion (CC) to the compounds was used. The carbon conversion refers to the mole fraction of carbon in the feedstock is being converted to the compound. Similar procedure can be done for any element of interest to see the influence of the operating conditions on the products.

4.3 Empirical modelling

Pyrolysis is a complex process with many reactions occurring in tandem, thus modelling of the process might be favoured by less resolution, while still providing estimations of interest. This can be achieved by utilising empirical modelling, which is built upon normalised data found in literature. The empirical modelling builds upon this data to derive more generic expressions to provide the predictions of interest, such as CC to a specie, or the yield of solid.

4.3.1 Solid, liquid and gas correlations

Correlations for the yields of solid, liquid and gas based on temperature and the H/C-value of the feedstock on dry-ash-free basis. The yields were assumed to be at full conversion, meaning the polymeric content was broken down and vapourised, only leaving char behind. The estimation of solid and liquid was done explicitly, while the gas phase was estimated using the other phases and assume no mass is lost. The decomposition was assumed to be complete at 500°C, meaning data with lower temperatures was not included in the correlations. Similarly, the elemental composition of the oil was estimated based on the pyrolysis temperature. The correlations are shown in Appendix C.

4.3.2 Specie yield correlations

To estimate the yield of specific species, key species was used as an intermediate step to the estimation. By doing this, the feasibility of using key species was also evaluated. Due to their inclusion in many different reactions in the process as well as being connected to the monomers in the rubbers, ethylene and styrene was used as key species. Styrene was selected due to its present in the synthetic rubbers and can also be produced from a Diels-Adler reaction of monomers of the rubbers. Ethylene was selected as it assumed to be produced from the secondary reactions or longer compounds and splitting of the monomers in the rubbers, as well as being a part of the Diels-Adler reaction to create cyclo-hexane, the first step to produce aromatic compound. Correlations for the CC to ethylene and styrene was derived from normalised data with regards to temperature and heating rate, as the data produced distinct trends with regards to these operating parameters. Due to data availability, products in the permanent gases were estimated using ethylene, while styrene was used for compounds in the oil.

Many of the compounds are hydrocarbons, thus providing a clear path between a key species and a compound of interest. This is not true for CO, CO_2 and H_2, as these are not constrained by the carbon balance. CO and CO_2 contribute to the carbon balance but was assumed to be constrained by the oxygen content instead, thus the oxygen conversion to these compounds was determined only based on pyrolysis temperature.

The CC to a compound was plotted against the CC to a key specie, ethylene for the gas-phase and oil-phase. From this, functions of heating rate and the CC to ethylene or styrene was derived to provide the correlations of CC to a compound. The key species and compound

investigated in the two phases can be seen in Table 4-2. Note: C3s are molecule which has 3 carbon atoms, such as propane or propylene, the same procedure is true for C4, C5 and C6s.

Table 4-2. Key species and compounds of interest used for estimation of yields.

	Gas	*Oil*
Key specie	Ethylene	Styrene
Compounds of interest	Ethane	Benzene
	C3s	Toluene
	C4s	Xylenes
	C5s	C9s
	C6s	(PAHs)
		Limonene

The total accounted for carbon content, i.e. known species corresponding to that carbon content, in both oil phase was estimated using the carbon content in the oil, which was estimated using a correlation with temperature. This way the unknown fraction of the oils could be quantified.

4.4 Simplified reactor model (SRM)

A simplified reactor model (SRM) was used to supplement the empirical modelling, by increasing the resolution of the reactions during the process. Since the experimental samples found in literature was small, the goal with the SRM was to provide more data and to model the process explicitly. The SRM was built in *MATLAB* and based on kinetic expression using the Arrhenius function, which describes the reaction rate with regards to temperature. The reaction was assumed to be of the first order. A simple decomposition model was implemented based on the assumption that the feedstock consisted of only carbon black and rubbers (NR, BR, SBR) and the carbon black was not reacting with the volatile compounds as the exited the solid residue.

4.4.1 System definition

The system used was based on a fixed bed reactor with a single tire particle and nitrogen as the working gas. The temperature was assumed to increase in a uniform way in the whole system (particle and reactor). The particle has a known polymeric content, i.e. a mix between rubbers. The system is shown in Figure 14, with two zones, indicated by ① and ②. The two zones (primary and secondary decomposition zones) provide different stages in the decomposition. In the primary zone the particle resides and is decomposed as temperature is increasing, where the vapours leaving the particle does not interact with the solid residue. This can be liked to a bag, releasing its compounds as they are over time described by kinetic relations. The input parameters required to estimate the yields are shown in Table 4-3. In the primary zone the primary reactions, i.e. splitting of the polymers into products are occurring.

Table 4-3. Model input parameters.

Feedstock related parameters		
Natural Rubber	X_{NR}	wt.%
Styrene-butadiene rubber	X_{SBR}	wt.%
Butadiene-rubber	X_{BR}	wt.%
Carbon black	X_{CB}	wt.%
Ash	X_{ash}	wt.%
Reactor related parameters		
Volumetric flow	$\dot{V}_{N_2}$	$\frac{l}{min}$
Reactor diameter	D_R	m
Reactor height	l	m
Temperature	T	°C
Heating rate	Hr	°C/min

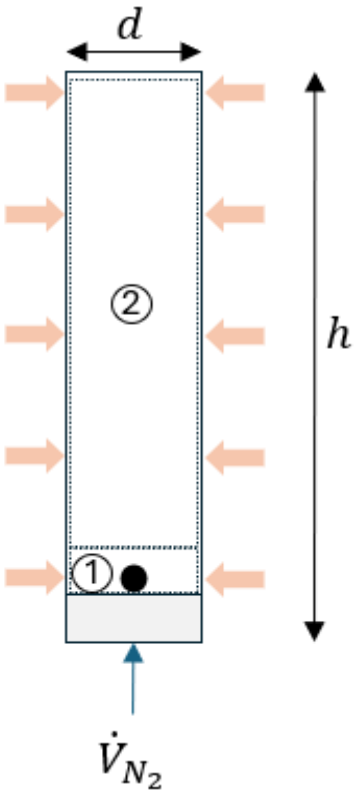

Figure 14. Simplified reactor schematic

In the secondary zone, the products from zone 1 is reacting via the radical rearrangement mentioned in section 3.2 is occurring. The carrier gas is preheated before entering zone one and is assumed to be isothermal due to the electric heating in zone 2. This decomposition is assumed to not include any interactions between the compounds produced by the different polymers; hence the model is only looking at the individual decomposition of the rubbers.

4.4.2 Natural rubber decomposition

As the polymer is heated up, several paths can take place during the decomposition. Wei et al. proposed four different paths (5-8) which are applicable in the primary decomposition of the polymer, when breaking of the single bond between two isoprene monomers occurs. The decomposition pathways are shown in the Figure 15, where path 8b was assumed to rely on an additional isoprene molecule to be available.

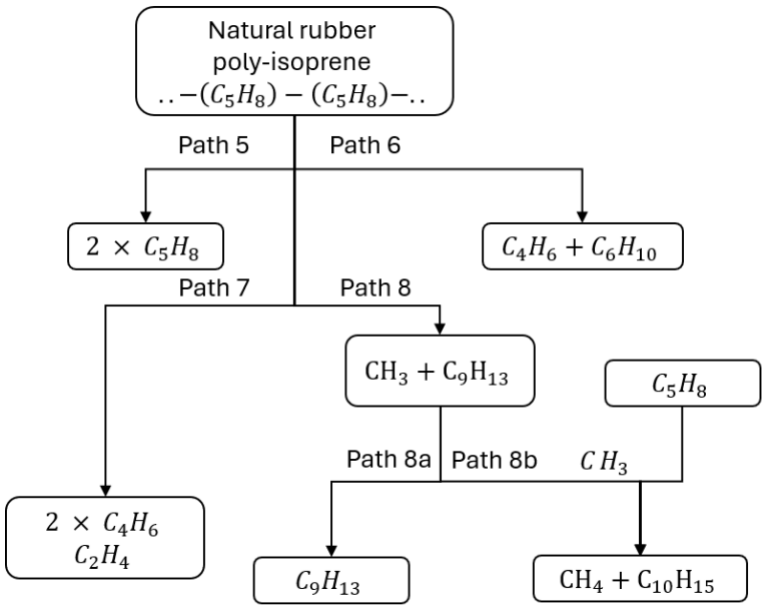

Figure 15. Primary decomposition pathways for natural rubber, polyisoprene.

In Table 4-4Table 2-1 the kinetic parameters presented by Wei et al. for which the reaction rate constant, k, was calculated to provide an indication of which reaction was the fastest, and thus would dominate/constrain the decomposition of the polyisoprene. Note the small deviation of reaction rate constants between the paths.

Table 4-4. Kinetic parameters for primary decomposition of natural rubber.

	Pre-exponent factor [1/s]	*Activation energy [kJ/mole]*	*Reaction rate constant, k, at 500 °C [1/s]*
Path 5	Not presented, set to 1	278.4	9.58E+18
Path 6	Not presented, set to 1	314	9.52E+17
Path 7	Not presented, set to 1	308.2	9.53E+17
Path 8	Not presented, set to 1	353.5	9.46E+17

In the secondary zone, i.e. radical rearrangement, Wei et al. proposed four paths, out of which the path called *path 1* was deemed the most probable one, shown in Figure 16. This path was presented to be the most likely due to having the lowest activation energy compared to other paths proposed, which was significantly higher. The path shows interactions between radicals and the production of monomers[45].

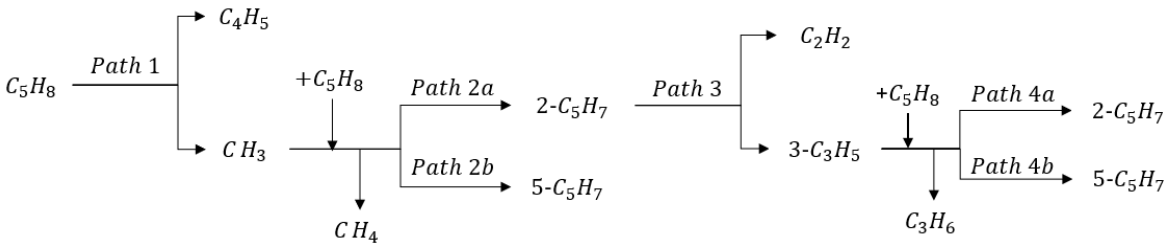

Figure 16. Secondary decomposition of natural rubber, isoprene.

The kinetic parameters for the primary and radical rearrangement of NR are shown in Table 4-5. The reaction rare constant was estimated to provide insight into which reaction might dominate/constrain the decomposition.

Table 4-5.Kinetic parameters for decomposition of isoprene and its radical rearrangement for decomposition of natural rubber.

	Pre-exponent factor [1/s]	*Activation energy [kJ/mole]*	*Reaction rate constant, k, at 500 °C [1/s]*
Path 1	5.5E+18	360.5	2.42 E-6
Path 2a	3.2E+13	63.4	1.67E+9
Path 2b	6.1E+12	35.7	2.36E+10
Path 3	2.4E+14	185.2	7.37E+1
Path 4a	2.3E+14	93.2	1.16E+7
Path 4b	1E+13	47.9	5.8E+9

In Table 4-5, path 1 is shown to be significantly slower than the other reactions, thus path 1 was assumed to be the constraining reaction, effectively determining the overall conversion. This meant that as soon as one isoprene monomer is decomposed into a methyl-group and C4-radical, the rest of the chain would react. Additional isoprene monomers used in path 2 and 4 was assumed to be abundant and would be attacked by the radicals upstream in the reaction. The impact of higher temperature only determined the yields of products produced by the path 2a and 4a, as these was slower than 2b and 4b respectively but is increased at higher temperatures, due to their higher activation energy.
With these assumptions, the radical rearrangement was simplified to only use the reaction rate of path 1, as shown in eq. 14, where k_{p1} indicates the reaction rate (k) for path 1 (p1). The downstream compounds were determined as a fraction (defined as α and β in eq.15 and in Figure 17) their reaction rates, which was seen as a function of temperature, resulting in the reactions shown in eq. 14-18 . The reaction from 4a was assumed to be go into path 2a until all $2C_5H_8$ radicals was consumed. This loop is indicated by i, in Figure 17.

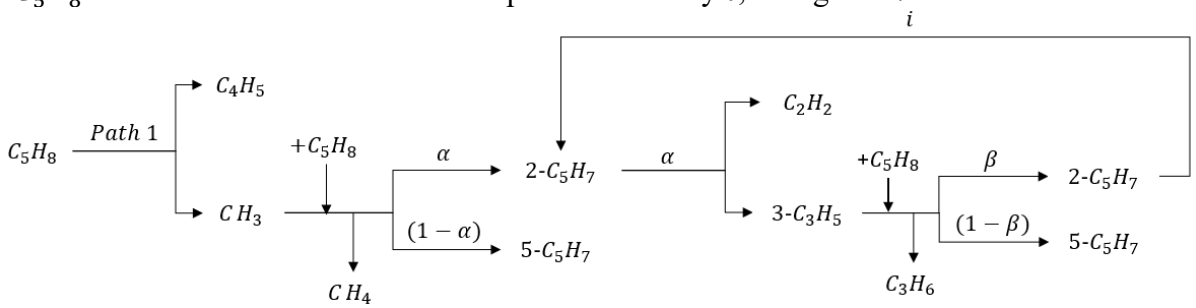

Figure 17. Radical rearrangement of isoprene with simplified fractions.

$$n_{isoprene,p1} \xrightarrow{k_{p1}} C_4H_5 + CH_3 \quad (14)$$

$$\alpha(T) = \frac{k_{p2a}(T)}{k_{p2a}(T) + k_{p2b}(T)} \qquad \beta(T) = \frac{k_{p4a}(T)}{k_{p4a}(T) + k_{p4b}(T)} \quad (15)$$

$$CH_3 + n_{isoprene,p2} \rightarrow CH_4 + \alpha(T)2C_5H_8 + (1-\alpha(T))5C_5H_8 \quad (16)$$

$$2C_5H_8 \rightarrow C_2H_2 + 3C_3H_5 \quad (17)$$

$$3C_3H_5 + n_{isoprene,p4} \rightarrow C_3H_6 + \beta(T)2C_5H_8 + (1-\beta(T))5C_5H_8 \quad (18)$$

The overall consumption path for isoprene was assumed to be:

$$n_{iso,tot} = n_{isoprene,p1} + n_{isoprene,p2} + \left(\alpha(T) + \sum_{1}^{i} \beta(T)^{\,i}\right) n_{isoprene,p4}$$

$$n_{iso,tot} \xrightarrow{k_{p1}} C_4H_5 + CH_4 + \left(\alpha(T) + \sum_{1}^{i} \beta(T)^{\,i}\right)(C_2H_2 + C_3H_6) + \left(\left(1-\alpha(T)\right) + \sum_{1}^{i}\left(1-\beta(T)\right)^{i}\right) 5C_5H_8$$

The decomposition of NR was setup, so the decomposition of polyisoprene produced the isoprene monomers which was to be decomposed, in the secondary cracking. The radicals 5-C_5H_8 was assumed to be continuing to react to create oil, creating pathway to form oil.

4.4.3 Synthetic rubber decomposition

The decomposition of synthetic rubber included the decomposition of SBR and BR, as these are the main synthetic rubbers. The amount of styrene present in SBR was assumed to be 25 wt.% as has been reported in literature but could be adjusted when using different types of blends as the underlying decomposition paths are not affected.

The primary decomposition of SBR will be dictated by the scission between butadiene-butadiene and butadiene-styrene monomers. The bonds are the longest in the groups, making them the most probable to break, splitting SBR into BR + styrene, as shown in Figure 18. The most likely outcome of the breaking according to Yang et al. is a formation of a double bond for the styrene group.

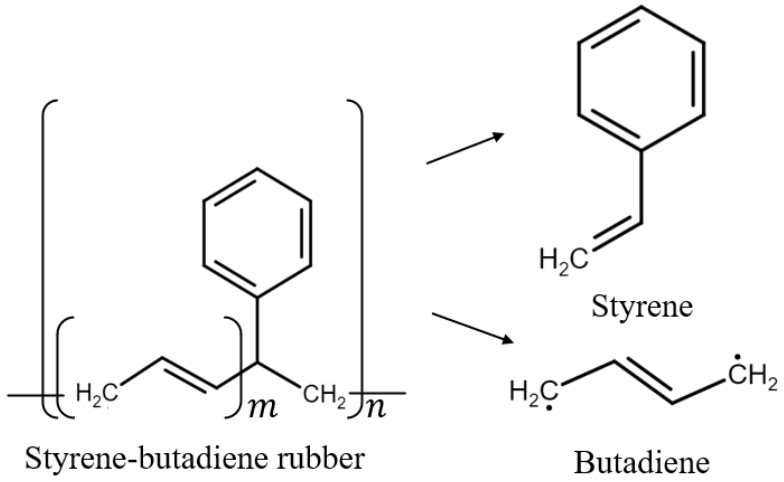

Figure 18. Primary decomposition of the SBR polymer

The primary decomposition of BR was assumed to be the breakage between monomers, as these bonds are the longest, making them the most likely to break. When they break, they release the butadiene radical, as shown in Figure 19, similarly to the SBR case.

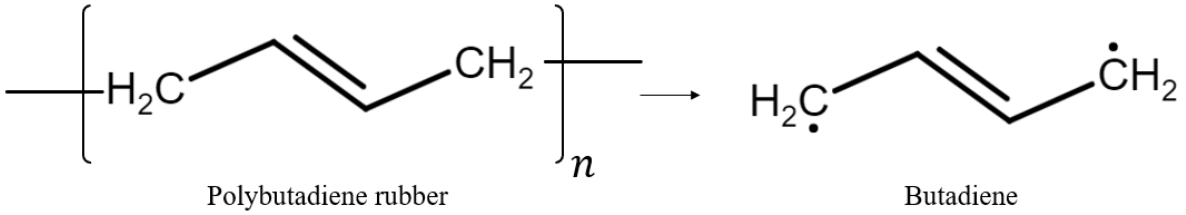

Figure 19. Primary decomposition of the BR polymer

The kinetic parameters for the primary decomposition, shown in Table 4-6, was not reported by Yang et al. so they were sourced from Lah et al. as these had individual decomposition for the two rubbers[19]. The use of these parameters includes an assumption of the primary decomposition being the creating of radicals previously discussed.

Table 4-6. Kinetic parameters for primary decomposition of synthetic rubbers.

	Pre-exponent factor [1/s]	*Activation energy [kJ/mole]*	*Reaction rate constant, k, at 500 °C [1/s]*
SBR	1.4E+14	200	5.53
BR	1.08E+7	125	3.87E-2

Due to the similarities between the two rubbers and their paths of decomposition, the radical rearrangement in the secondary zone was assumed to follow the same paths.
In the butadiene radical, the pi-bond (double bond) in the middle is most likely to break, as this is an exothermic reaction, with the lowest enthalpy change for the reaction as well as having the lowest free Gibbs energy of the potential paths [10]. A competing path is for the butadiene group to remain as a radical and continue to react. The paths in Figure 20 was suggested as the most likely to happen during the radical rearrangement. 1,3-butadiene was assumed to continue to decompose.

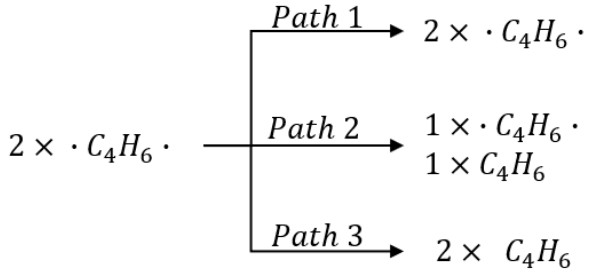

Figure 20. Butadiene radical reaction paths

As the 1,3-butadiene groups and the radicals are exposed to temperatures, they will continue to decompose. The most likely decomposition paths are shown in Figure 21 for 1,3-butadiene and in Figure 22 for the radical. The radical was assumed to decompose into C3-radicals and methyl groups, which was assumed to react instantly with free hydrogen in the mixture to form CH_4. If the hydrogen production exceeded that of the methyl groups, the hydrogen atoms was assumed to form hydrogen gas.

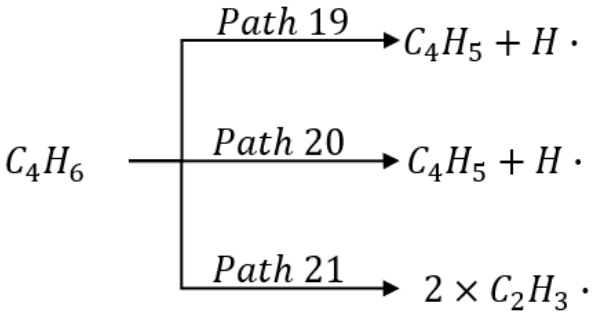

Figure 21. 1,3-butadiene decomposition

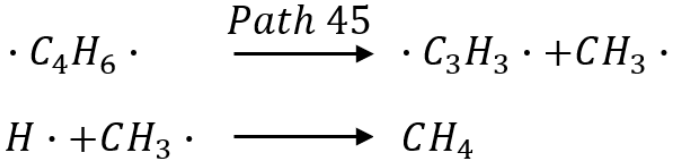

Figure 22. butadiene radical decomposition

Styrene was assumed to not react or decompose due to the activation energy was higher than that of the ones presented. This assumption was supported by the different paths presented by Yang et al., shown in Table 4-7. As the table indicated, path 2 and 3 is dominating, producing significant amount of 1,3-butadiene gas. The downstream reactions will not be as fast as the

first steps in the decomposition. The path for styrene decomposition includes one path which was in the same order of magnitude as path 45.

Table 4-7. Kinetic parameters for decomposition of synthetic rubbers

	Pre-exponent factor [1/s]	Activation energy [kJ/mole]	Reaction rate constant, k, at 500 °C [1/s]
Path1	Not presented, set to 1	83.9	2.15E-6
Path 2	Not presented, set to 1	31.5	7.4E-3
Path 3	Not presented, set to 1	20.45	4.1E-2
Path 19	Not presented, set to 1	597.33	4.29E-41
Path 20	Not presented, set to 1	435.15	3.98E-30
Path 21	Not presented, set to 1	568.86	3.68E-39
Path 45	Not presented, set to 1	474.69	8.48E-33
Path 22 (styrene)	Not presented, set to 1	495.35	3.41E-34

4.4.4 Structure of the reactor model

The computational cell setup of the model followed the transient modelling presented in section 3.7, using the Arrhenius equation with the kinetic parameters presented in this section. The SRM used one cell for the primary decomposition zone of release all the radicals from the primary decomposition instantaneously. The radicals then enter a series of computational cells, in which the radical rearrangement is occurring. The residence time in the computational cells, dt, used to estimate the consumption of reactants was estimated using the volumetric flow of nitrogen, geometries of the reactors and the volume expansion of a fluid due to temperature using equation of state.
The model was run and evaluated to see the feasibility of using the more explicit modelling.

5 Results and discussion

5.1 Solid yield and thermal size

The char yield from the different runs, shown in Figure 23, show the impact of heating conditions. The increase in heating rate shows that as the sample is heated faster, an expansion of the sample occurs as the gases are leaving the sample. This can be seen by the cracks for the sample using HR=20°C (Figure 23b) compared to when lower heating rates was used (Figure 23a). As the heating of the sample increases even further, as in the case of the T-FXBR (Figure 23c), the expansion seems to be happening at such a rate that the sample is crumbled.

a) TGA, HR = 5 °C/min *b) TGA, HR = 20 °C/min* *c) T-FXBR run, HR = ∞*

Figure 23. Samples after runs in different reactors at 550 °C hold temperature.

The thermal size of the sample in the different reactors was estimated using the Biot-number. In the TGA, the thermal size was estimated to be 4e-4, indicating the thermal size is very small, meaning a constant temperature gradient within the sample. In the T-FXBR the thermal size was 2.9, providing an indication about a temperature gradient within the sample.
The thermal size might be coupled with the expansion and shattering of the sample. For a thermally smaller particle, the temperature gradient inside the particle will be uniform. When the heat transferred to the sample, any increase in temperature will be felt by the whole sample as soon as it is applied to the surface. For the larger thermal size, the surface and the inside of the sample will not be at the same temperature. Since pyrolysis is a heat and thus temperature driven process, the differences in the thermal size and heating rate will influence if the particle shatters or not, due to a too violent expansion of the gases formed when the tars are vapourised, as presented in section 3.1.
When the heating rate increases, the heat supplied to evaporate the gases also increases, which makes the vapours to increase in size, creating pressure and thus a driving force. This driving force pushes the bubbles out of the sample, and when done to quickly, makes the sample swell too fast, or shattering. In short, internal residence time is inversely proportional to heating rate.

5.2 Trends from literature

The literature review aimed to find data to be able to find trends for the decomposition of ELTs. The product yields reported in literature, normalised on a dry-ash-free basis is shown in Figure 24. In the figure the results from the hold temperature going from 300°C to 800°C are indicated by colour. The experiments using 300°C clearly shows a very high yield of solid residue (>90 wt.%), which is to be expected as the majority of the decomposition has not yet occurred, as laid out in section 3.1. As temperature increases, the solid residue decrease, as more of the polymeric material is decomposing. While there is a clear trend towards the area of 35-45%wt_daf solid yield, the oil and gas yield have a larger variation, indicated by spread in the direction of right to left in Figure 24. This difference can be due to a few factors ranging from differences in the secondary reactions, i.e. decomposition of products after the radical rearrangement, or how the gas phase was determined, either by difference or by actual weight. The most plausible reason for the deviations is the secondary reaction, as this will break down the products into smaller compounds due to exposure to elevated temperatures over time.

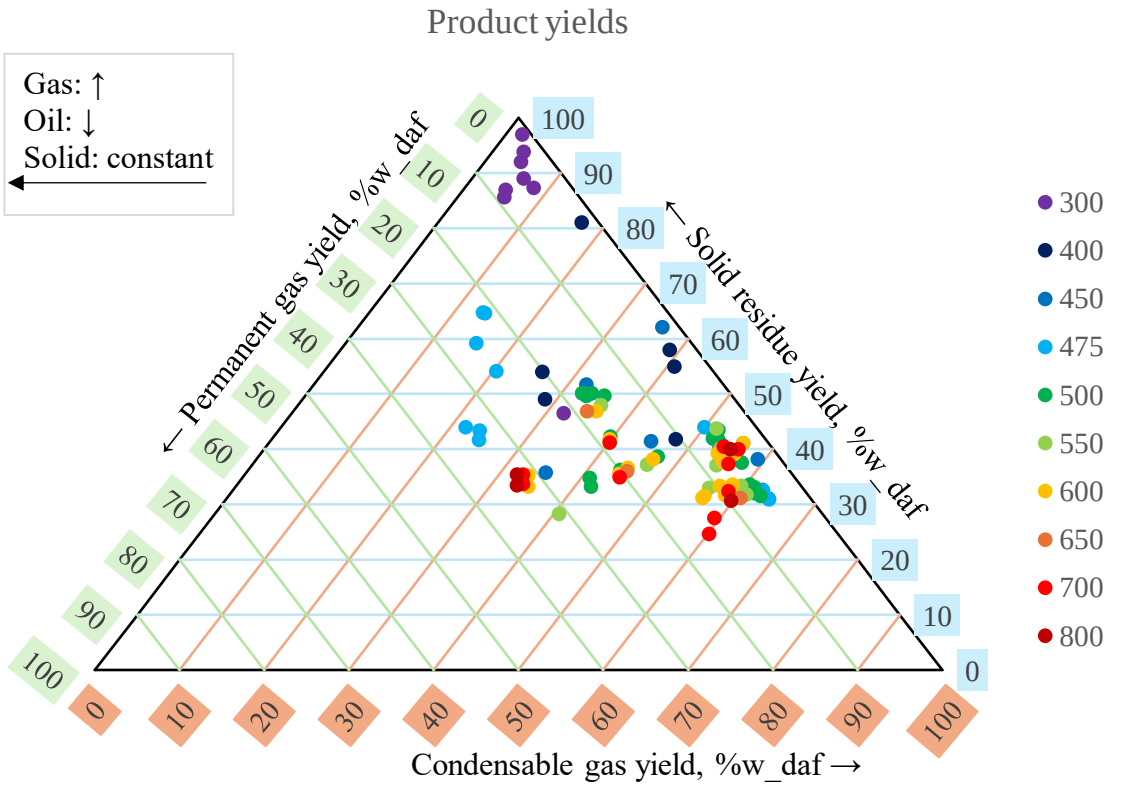

Figure 24. Product yields for all reactors on dry-ash-free basis

5.2.1 Feedstock characteristics

For authors who presented the elemental composition and proximate analysis, an average feedstock could be defined, as is shown in Table 5-1. Histograms of the individual elements in the feedstock, as reported in literature can be found in Appendix B. The results indicate a consistency of the feedstock which can be used as a generic feedstock when modelling the process. The moisture content in ELTs is shown to be of low significance, compared to biomass where it heavily influences the process. Samples are similar, but the composition of the polymeric material, i.e. rubbers and fabrics, in the feedstock is not distinguishable solely from the ultimate and proximate analysis alone. The oxygen content might be influenced by the type

of fabrics, but other compounds affect this such as ZnO, an activator used in the vulcanisation process.

Table 5-1. Average ultimate and proximate analysis of an ELT from data found in literature.

	Ultimate analysis DAF wt.%						*Proximate analysis wt.%*			
	C	H	N	S	O	H/C	FC	VM	M	Ash
Average	88.3	7.1	0.6	1.8	2.1	0.96	29.0	64.6	0.92	5.4
Abs. deviation	1.0	0.7	0.2	0.3	1.1	0.1	1.8	2.6	0.4	1.7

Since the fixed carbon within a sample is the solid residue when all the volatile matter has left the sample and ash has been removed, one can use it as the lowest yield of solid residue on dry-ash-free basis. Assuming the values in Table 5-1 represents an average ELT, a lower limit of solid yield would be 29 %w. and 31 %wt_daf when re-evaluated for the average sample. This would indicate that DAF solid residue yields above this would have some carbonisation.
As shown by the individual proximate analysis of the rubbers in section 2.1.1, the volatile matter for the polymeric material would be around 98-99 %w. The rubbers have been reported to leave a solid yield of 2-3 %w_daf, showing the tendency for the tar to carbonise to a certain extent. If carbonisation happens, the H/C value in the rest of the products will be higher, as more of the carbon content is converted to the solid yield.

5.2.2 Influence of H/C values on solid and oil yields

The H/C value is a characteristic of the feedstock directly linked to its polymeric composition, thus linked to the yield of the different phases. The trends shown for the different temperatures, presented in Figure 25, is clearly indicating that with lower H/C-value of the feedstock, the higher the solid residue will be. This is due to the amount of potential volatile matter which can leave the sample is lower, as a higher H/C value indicates more polymeric content. For 700 °C (red) there are 4 points at the same H/C-value, which is actually changes in heating rate, where the lowest solid yield is the highest heating rate at 80°C/min. This shows the correlations between heating rate and solid yields once more.

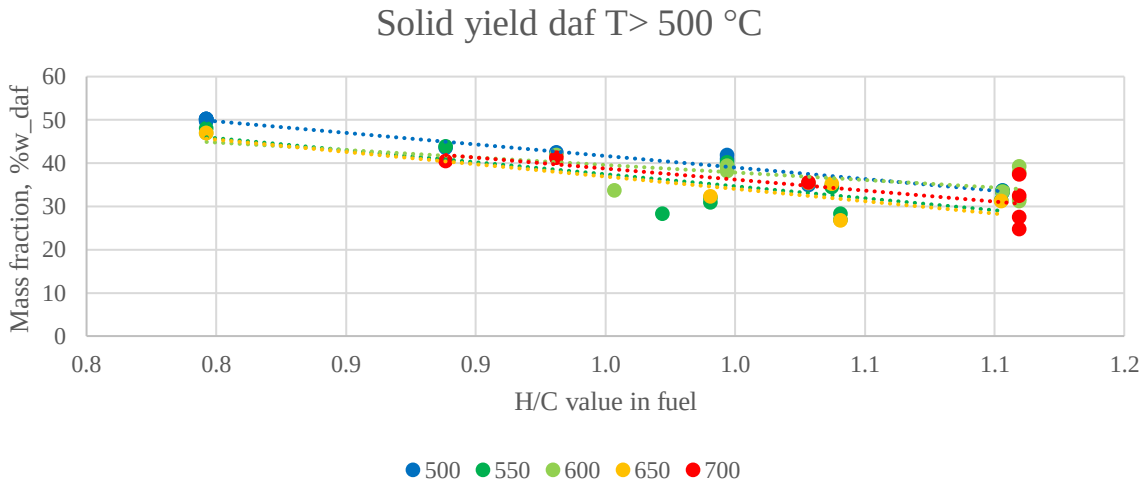

Figure 25. Solid residue correlation with H/C value of the feedstock at different pyrolysis temperatures, T>500°C.

The oil yield is not as influenced by the H/C-value, shown in Figure 26 as it has a lower spread than the solid yield, with at 55-65%w_daf. While these trends are consistent, secondary reactions of the compounds are limited, which would affect the oil and gas yields. There is a slight positive trend with higher H/C-value, which following the logic used for the solid

residue, is to be expected. With a larger fraction of hydrogen in the fuel, more of the fuel will end up as an oil, instead of being left in the solid residue.

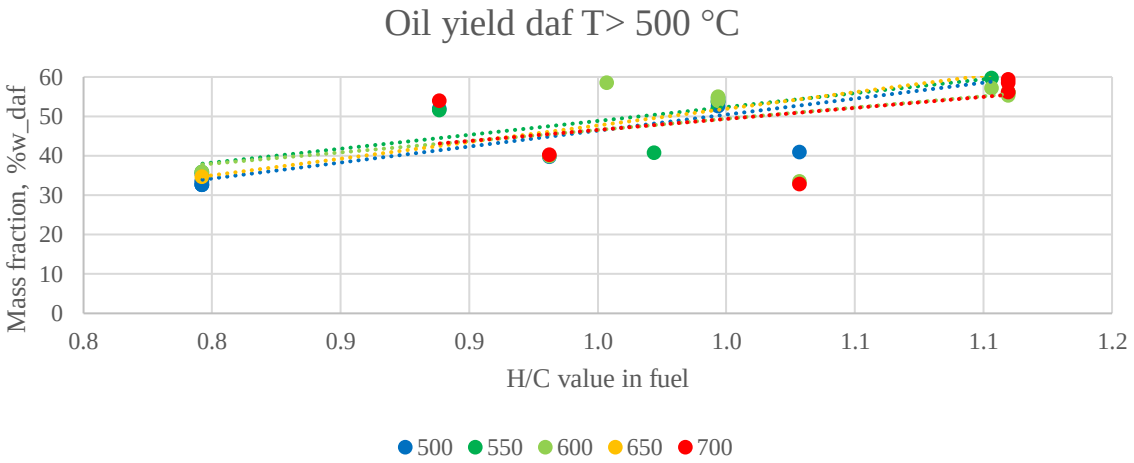

Figure 26. Oil yield correlation with H/C value of the feedstock at different pyrolysis temperatures, T>500°C

5.2.3 Influence of heating rate on solid, liquid and gas yields

The yield of solid, liquid and gas were evaluated with regards to heating rate for samples over 1.5 mm, as is shown in Figure 27. As mentioned, solid yields above 31 %w_daf could be assumed to have some carbonisation of the vapours happening as they are leaving the sample. Looking at the figure, there is a clear trend which show an increase of carbonisation occurring at lower heating rates. This can be attributed to the impact of heating rate on the particle, as shown by the increased swelling with increased heating rate. With the higher heating rate, the driving force pushing the vapours out of the particle increases, which decreases the contact time between the vapours and the solid.

The impact of the oils, seem small, as the data points are in between two red lines, indicating 50 and 60 %w_daf for the oil. The gas is increasing with the higher heating rates, alluding to secondary reactions happening with increased heating rate.

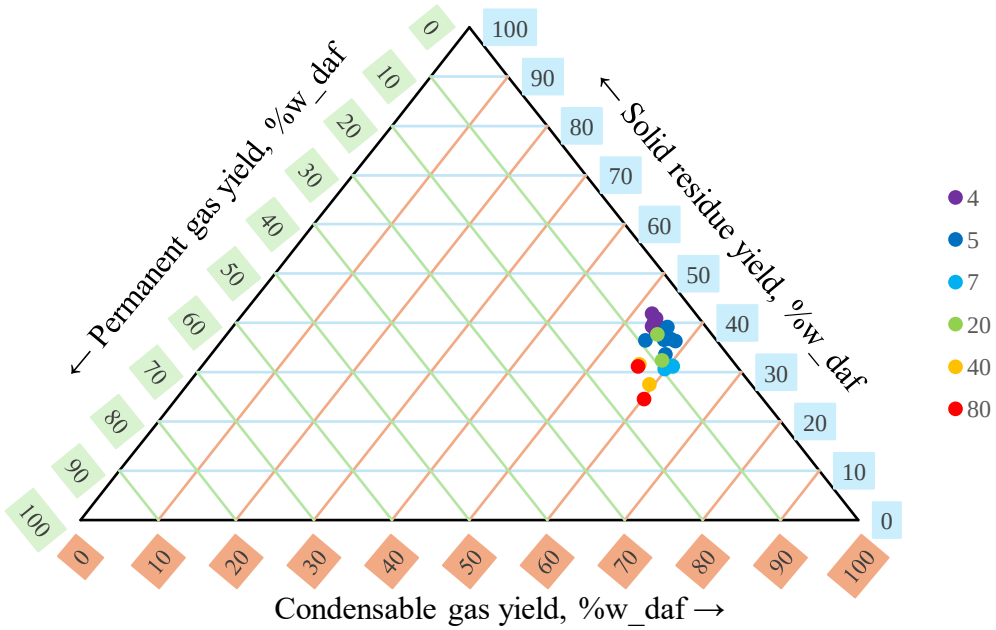

Figure 27. Heating rate influence on solid, liquid and gas yield for particles over 1.5 mm. Heating rate is shown by colour.

5.2.4 Oil phase trends

The oil phase was of interest due to the high potential for material recovery, as it can be used as a feedstock in the petrochemical industry to produce products with properties comparable to those produced with virgin feedstock.

In literature, several authors have reported the yields of oils, however, the reporting has mainly been in the form of peak area, without any information about the maximum or total area, rendering the reported results hard to decern. Due to this issue, one study using a rotary kiln rector instead of a fixed bed reactor was included. Adding to the issue, a reporting where both species in the gas phase and the oil was not found. There was one study which included this, however, only for one temperature using nitrogen as the working gas, for other temperatures steam was used[46].

The elemental composition of the oil is of importance as this can provide information regarding the compounds present within it. The conversion of carbon (CC) and hydrogen (HC) is directly related to the majority of the chemistry making up the feedstock and products. Sulphur conversion (SC) have been included due to its importance when evaluating the TDFs to be used as a fuel substitute, usually by comparing it to automotive fuels or naphtha. Figure 28 shows this conversion of the three elements with respect to temperature and heating rate.

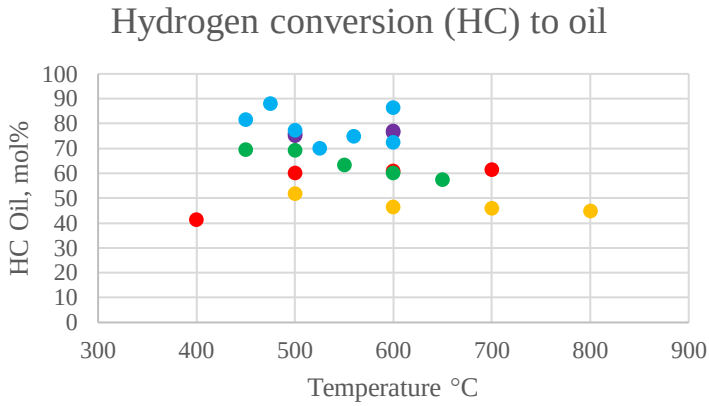

a) Hydrogen conversion to oil

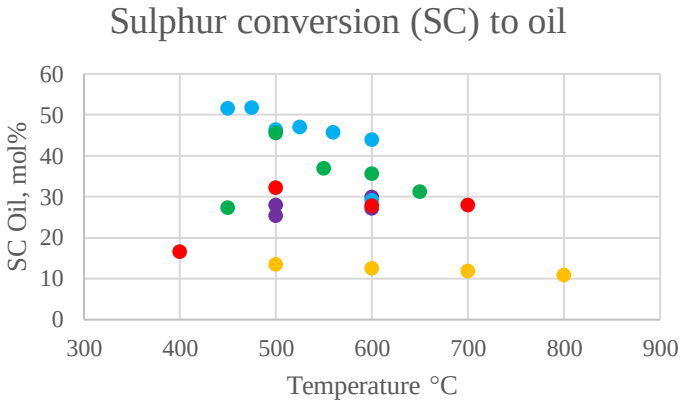

b) Sulphur conversion to oil

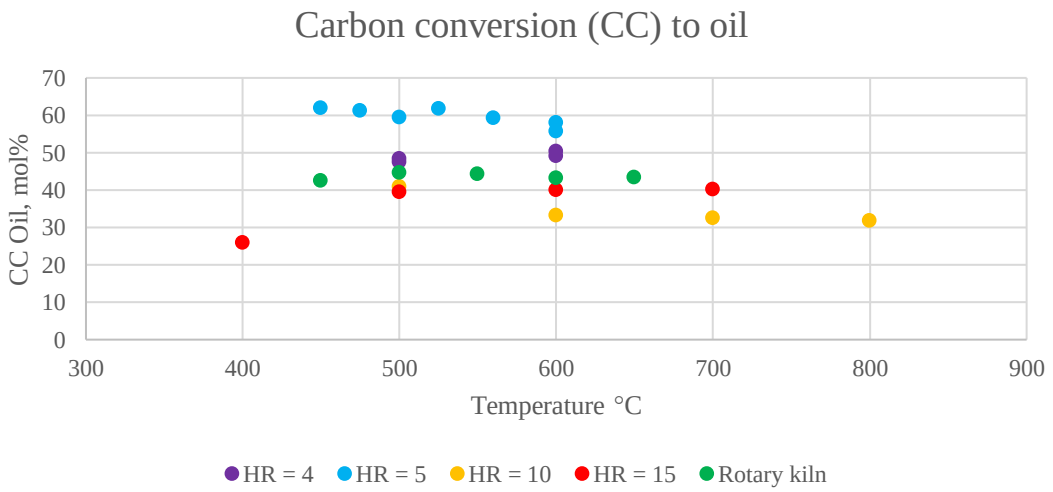

c) Carbon conversion to oil

Figure 28. Elemental conversion to oil on dry-ash-free-basis with regards to temperature and heating rate

The key take aways from the figure is the influence of heating rate used. For all the elements, the conversion to the oil is inversely proportional to the heating rate.
The trend coincides with the assumption that a lower HR will carbonise more of the oil, increasing the hydrogen and sulphur content in the volatile products. This binds more of the carbon to the solid yields, and considering the polymers being hydrocarbons with distributed sulphur atom, the hydrogen and sulphur must transfer to the rest of the products. Following this logic, the carbon conversion to the oil should be lower at lower heating rates, as more carbon is locked up in the solid. This is not seen, however. One explanation is with the higher heating rates, there is a shift of all three elements to be converted into the gas phase instead as more energy into the oil will start to break apart the aliphatic content and promote cyclisation of the dienes found in the monomers of the rubbers.
To get further insight into the oil composition, the H/C value was determined with regards to temperature and heating rate, shown in Figure 29a) and b). Increased temperature impacts the H/C value in a marginal way when looking at the trendline for the average value. However, there is great variance for a given temperature, such as for 500 and 600 °C. Heating rate influences the H/C value, as is shown in Figure 29 b), where a lower heating rate promotes a higher H/C value. This coincides with the assumption of lower heating rates promotes carbonisation of the volatile matter as the internal residence time is increased, as discussed above.

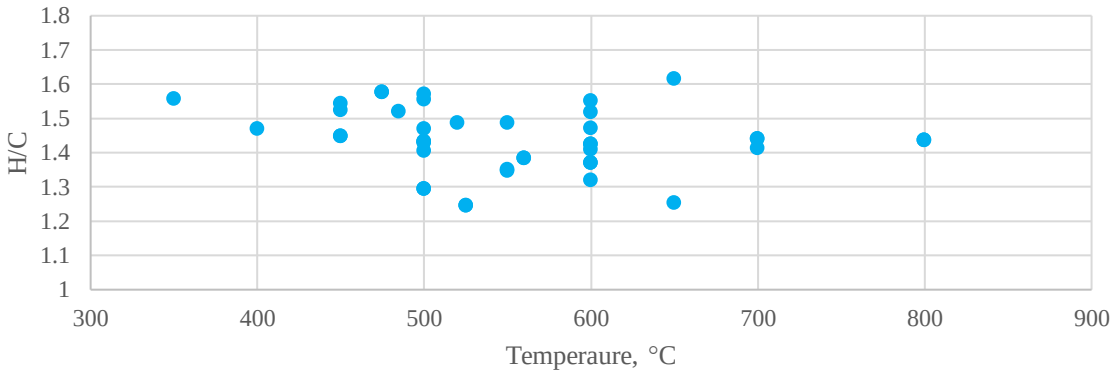

a) Any temperature, no heating rate indicated

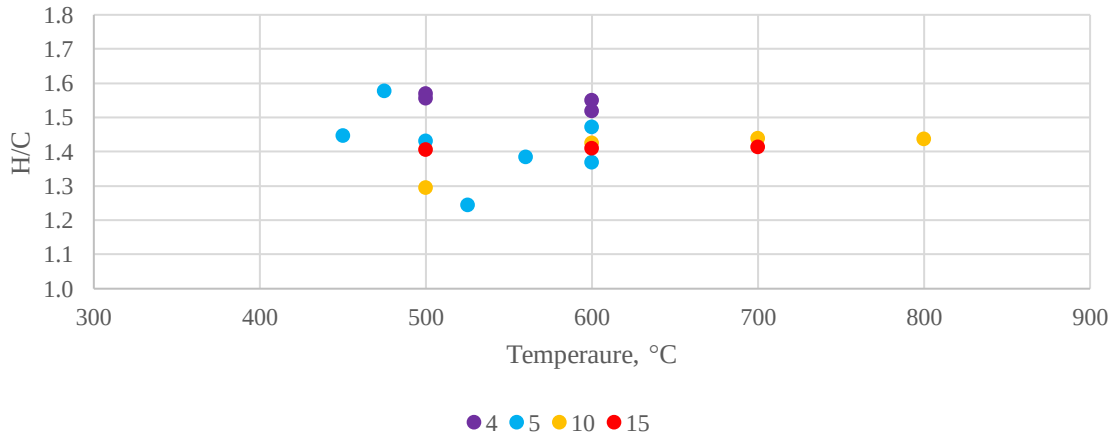

b) Heating rate indicated

Figure 29. H/C in the oil yields on DAF basis.

5.2.4.1 Aliphatic and aromatic content

The oil includes many different compounds; however, the two major groups are the aliphatic and aromatic compounds. As the vapour escaping the sample are exposed to high temperatures, they continue to react and decompose via the secondary reactions. To what extent this is happening due to increased heating rate is shown in Figure 30, where both the aromatic and aliphatic content are presented. The yields are with regards to the total amount of products. During secondary reactions, the longer chains (aliphatic content) are broken down into smaller and more stable products, such as gas products or aromatics. In Figure 30a, the aliphatic content this is shown to be happening with higher heating rate, i.e. more energy is supplied to the fuel. The secondary reactions are also shown in the increase of aromatic yields due to increased heating rate, presented in Figure 30b.

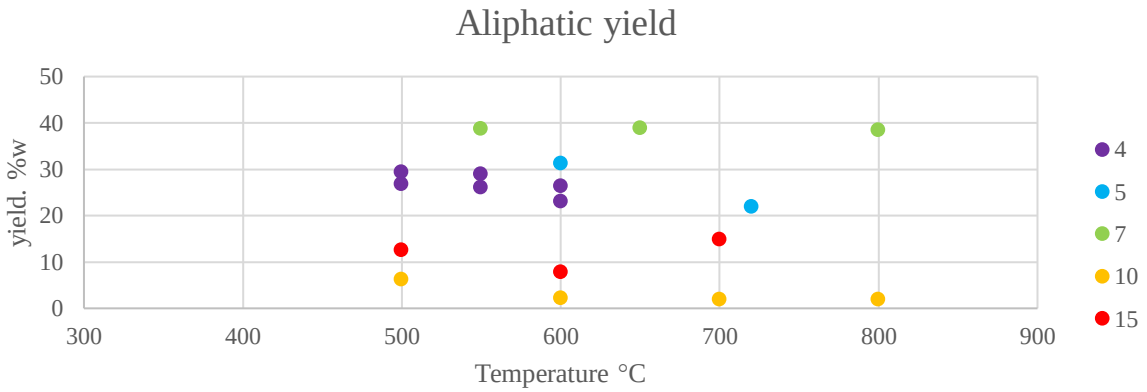

a) Aliphatic yield

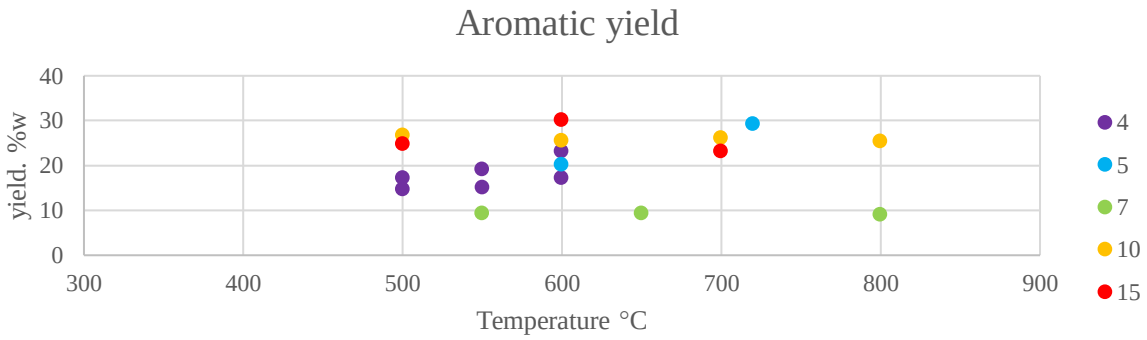

b) Aromatic yield

Figure 30. Aliphatic and aromatic compounds yield with regards to temperature and heating rate. Heating rate shown by colour.

5.2.4.2 Carbon content in oil

The carbon content in the oil was of interest as it will account for a large portion of the carbon in the vapours leaving the sample. Data found in studies for the carbon content in the oil are shown in Figure 31. The key take away is the spread, which is rather small compared to data presented earlier. Also note the slight positive trend with increased temperature, which might be due to secondary reactions, which decreases the hydrogen in the oil, effectively increasing the mass fraction of carbon in the oil.

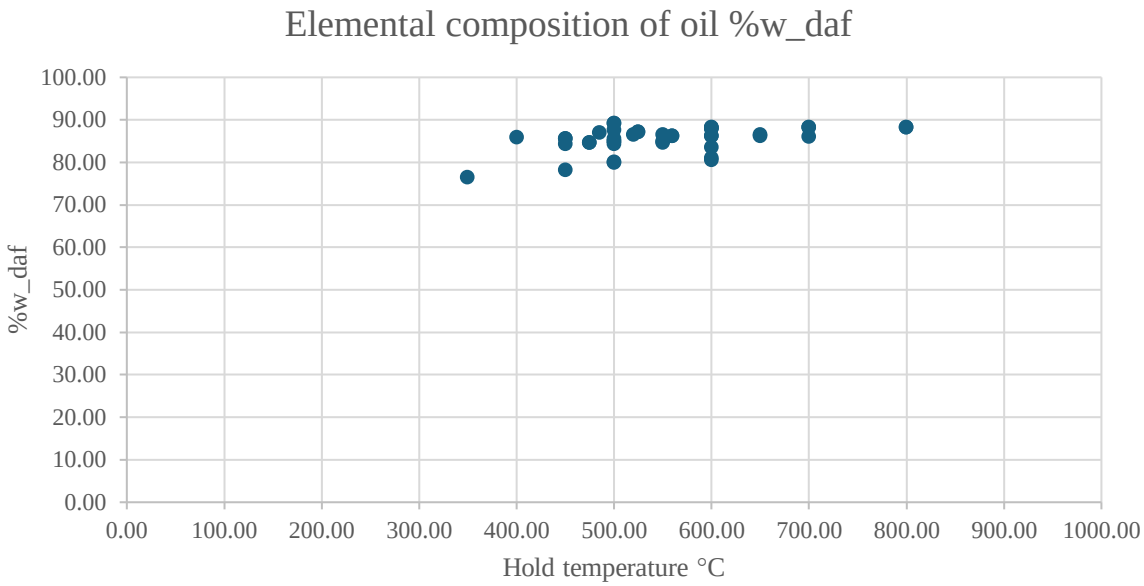

Figure 31. Carbon content in the oil on DAF basis from data found in literature.

5.2.5 Oil phase species

There were a few compounds which was of interest when determining the yields. The most prominent one was styrene, as previously described, as it is a part of the monomers in the SBR. Both benzene and limonene are also interesting compounds due to their paths of formation. Benzene is partially created by the Diels Adler reaction and dehydrogenation of the dienes found in the monomer of the rubbers, as described in section 3.8. Limonene is also produced via the Diels Adler reactions for isoprene. The influence of temperature and heating rate on the production of these three species sheds some insight on the reactions occurring. In Figure 32 the influence of heating rate and temperature on the styrene yield is shown. Due to the stark difference between the different heating rates, as shown in a), the plot is rescaled to show the individual trends for rest if the heating rates, which is shown in b).

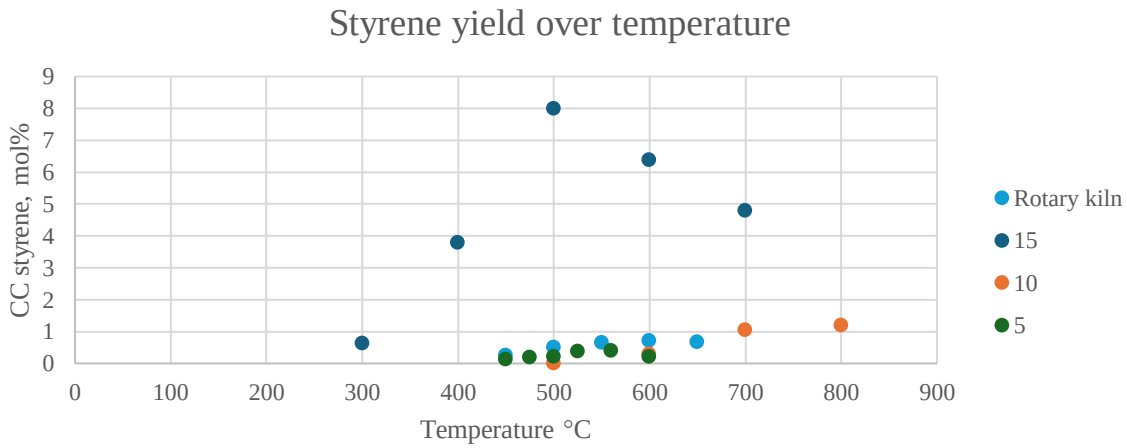

a) Carbon conversion to styrene for all four cases

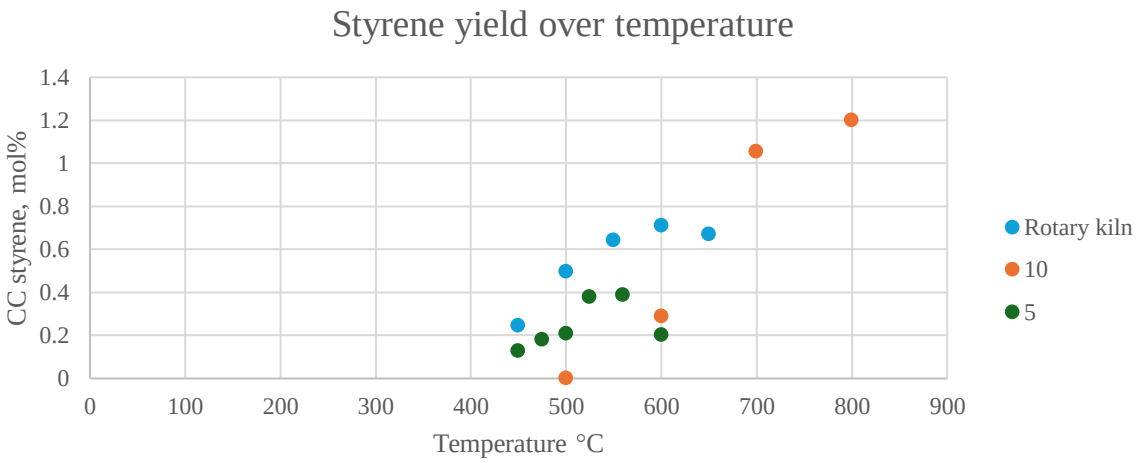

b) Carbon conversion for three cases due to rescaling.

Figure 32. Carbon conversion to styrene with regard to temperature and heating rate for fixed bed and rotary kiln reactors

The trends for styrene production, seems to have a distinct trend with regards to temperature. As the temperature is increased a parabolic behaviour is occurring for the CC to styrene. This might be due to the increased decomposition of the compounds from the SBR rubber, which increases the yield of the key specie. At higher temperatures, the decrease might be explained by the production of larger aromatic compounds such as methyl styrene and PAHs, decreasing the carbon being converted into styrene. The impact of heating rate is very distinct on styrene, as the increase in heating rate increases the carbon conversion to styrene, which might be due to the decreased internal residence time, leading to less production of the larger aromatic compounds.

The carbon conversion to benzene and limonene with regards to styrene, shown in Figure 33, shows an interesting trend. The lower heating rate will promote a high yield of benzene and a low yield of limonene. Benzene is promoted by the longer residence times within the sample, compared to styrene, which might be continuously consumed with longer residence time.

Limonene is created by the cyclisation of isoprene monomers, favoured by lower amounts of secondary reactions, as this breaks it down into smaller compounds.

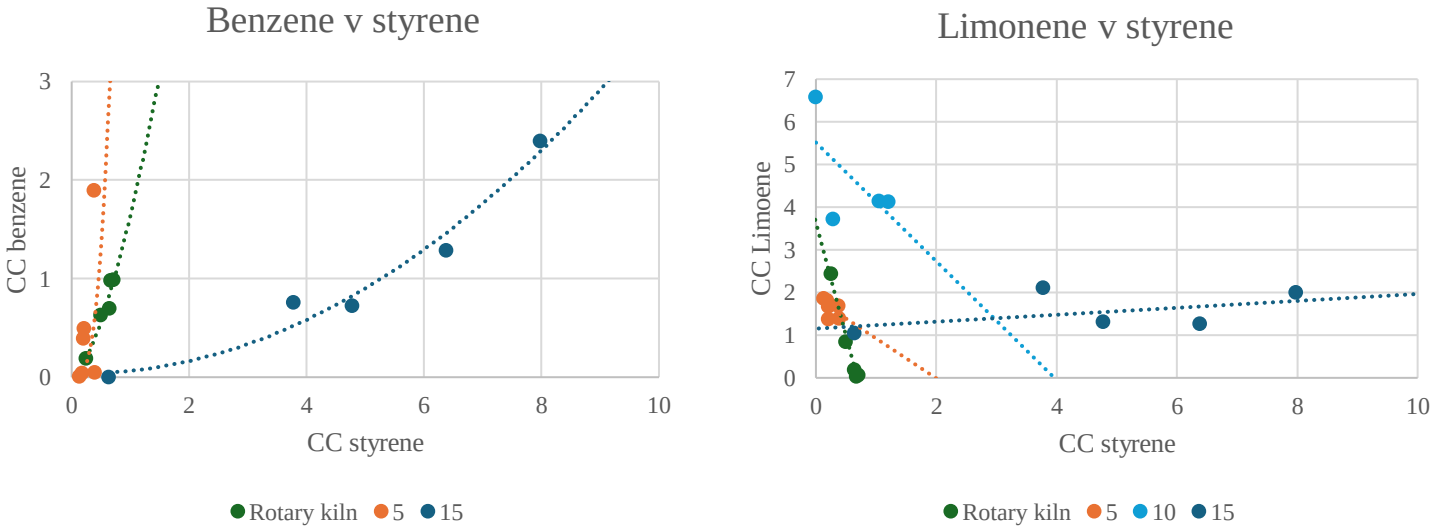

Figure 33. Carbon conversions to benzene and limonene with regards to styrene

The two compounds' decomposition with regards to temperature and heating rate is shown in Figure 34. When viewed from this perspective, an additional trend can be seen. For benzene, an increase in CC comes with the increase in energy supplied, i.e. higher heating rate. This underlines the production of smaller radicals from the secondary reactions of larger chain and aromatisation as a function of energy supplied. The trend for limonene is not a stark, which might be due to the differences in natural rubber used in the samples, as this is directly linked to the production of limonene.

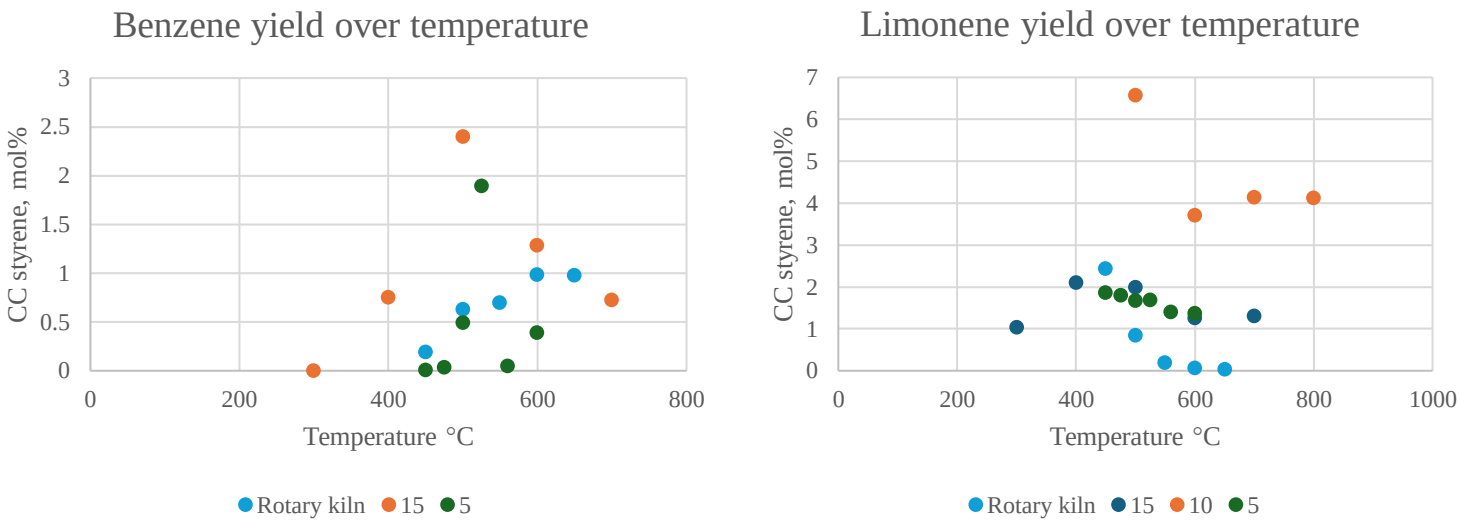

Figure 34. Carbon conversion to benzene and limonene with reads to temperature and heating rate

5.2.6 Gas phase species trends

In literature, several authors investigated the effect of operating conditions on the elemental composition of the oils, while few have looked at species present in the gases. To increase the amount of data available, a second reactor was included in the form of a fluidized bed reactor. The heating rate is significantly higher, as the temperature the sample is experiencing is dramatically increased, changing the heat transfer to the sample. In a fluidised bed the sample will be broken down by attrition caused by the bed particles, breaking away particles of the solid residue as the conversion has occurred. These differences should be kept in mind as they might affect the results, and the reactor is assigned the significantly higher heating rate of 180°C/min[41].

Two species which was of interest in the gas phase was methane and ethylene. The carbon converted (CC) from the feedstock to the compounds seems to depend on a few factors. Temperature and heating rate has an impact on the compounds produced in the process, as is shown in Figure 35. The differences in the number of colours between the two compounds comes down to the data available, for methane 5 [32], [35], [37], [41], [43] different studies had included the heating rate, while only three had done so for ethylene[37], [41], [43].

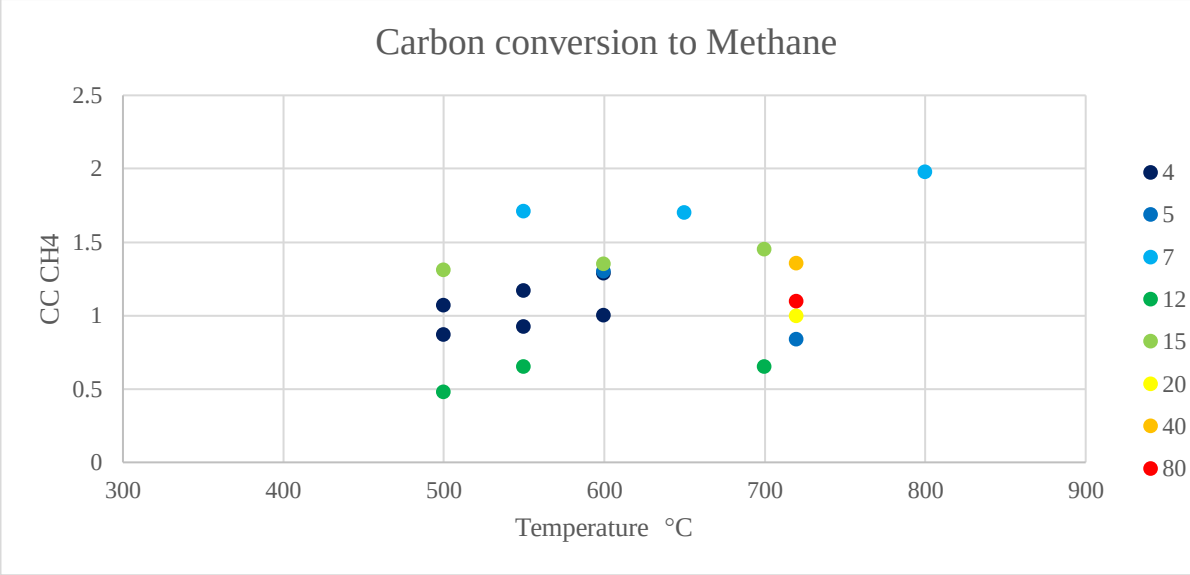

a) Carbon conversion to methane

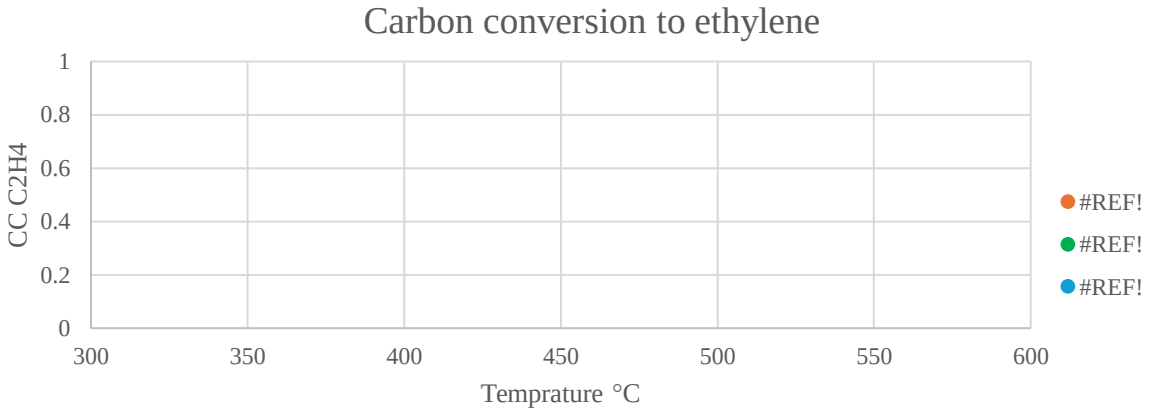

b) Carbon conversion to ethylene

Figure 35. Carbon conversion to methane and ethylene as a function of temperature and heating rate.

To see the impact of heating rate on the methane yield to find some trend, trendlines was used, as is shown in Figure 36. The impact is best showed by the angle on the lines, which is similar for the heating rates of 4-12°C/min, while it starts to increase at 15 °C/min and continues to do so for the fluidized bed reactor, assigned to be 180°C/min.

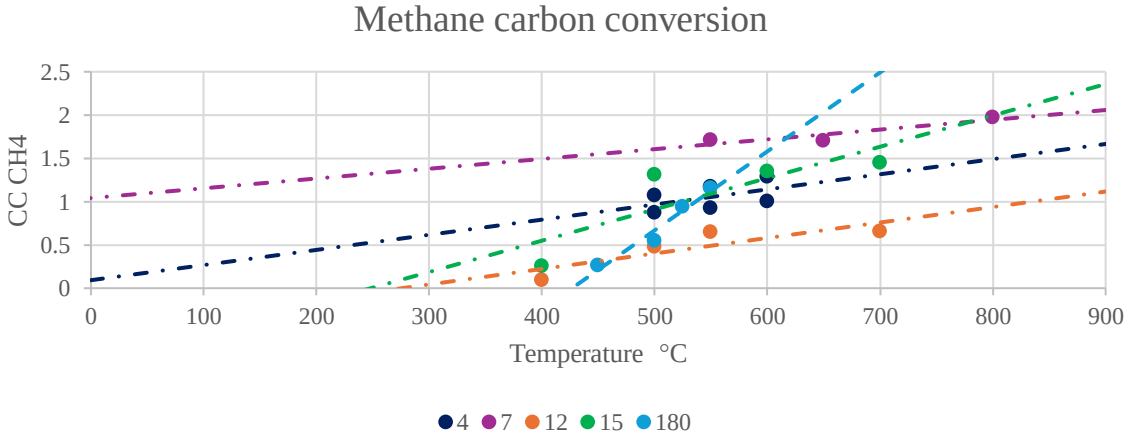

a) Methane trend with trendlines

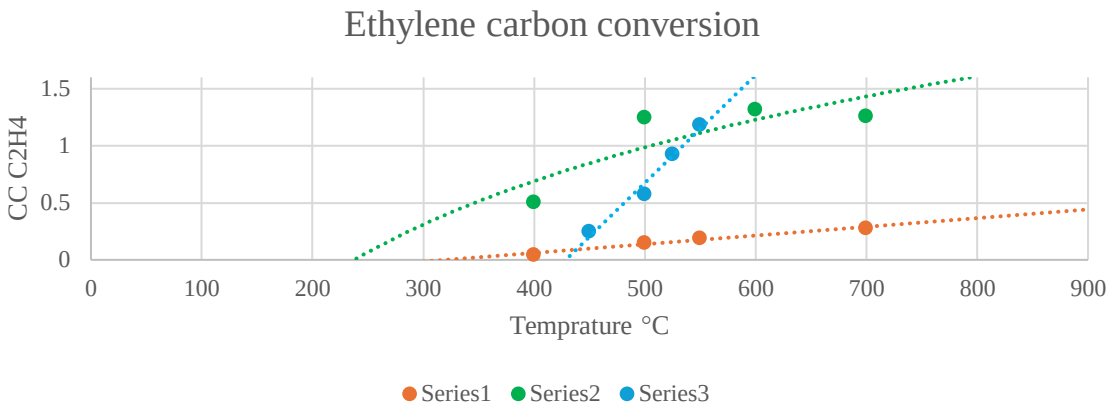

b) Ethylene trend with trendlines

Figure 36. Trendlines to showcase the impact of heating rate on CC to methane and ethylene.

The increase in lighter products aligns with the increase in energy supplied, as the extreme case of the fluidised bed is showing a clear increase in the compound when temperature is increased. Looking at the relation between ethylene and methane, shown in Figure 37, the trend is clear, where a higher heating rate will produce more methane at the expense of the longer chains, while both ethylene and methane is still produced to a larger extent at higher heating rates.

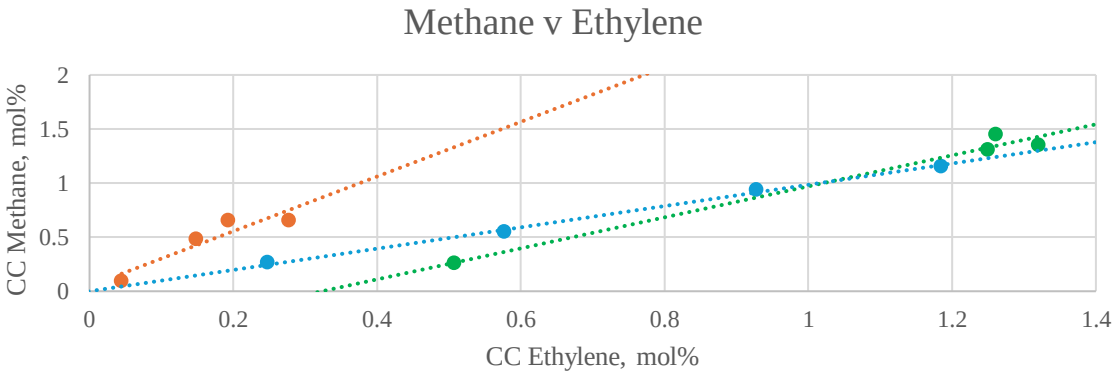

Figure 37. CC to methane and ethylene with trendline for different heating rates.

5.3 Empirical modelling

The general trends found in in the data from literature was used in the empirical model to make estimations of interest for different operating conditions. The structure of the modelling starts broader with production explicit estimations of oil and solid while implicitly modelling the gas yield, followed by carbon content in the oil and wrapping up with CC to compounds using key species.

5.3.1 Solid, Liquid and Gas estimation based on H/C- value of the feedstock

The usage of the H/C-value along with temperature to estimate the product yield introduced less spread in the results for the solid yields, compared to the oil and especially the gas yield. The solid yield is connected to the fixed carbon in the feedstock, which was shown to be of little variance, thus the solid yields will vary less even if there are carbonisation occurring. For the oil, the secondary reactions will introduce more variation for the yields, thus the increase of spread in the data, thus the errors done by the model will also be larger. The assumption defining the gas phase yield by difference, resulting in a significant under estimation of the gases, as it mainly estimated oil yield to be in the 35-60 %w_daf range with a corresponding

solid yield of 50-35 %w_daf for the same H/C values, leaving little rooms for error in the gas phase. The functions for the correlations used can be found in Appendix C and shown in Figure 38 . The errors of the functions was evaluated for all temperatures from 500-700 °C, and the r spread of the error can be found in Appendix DAppendix C.

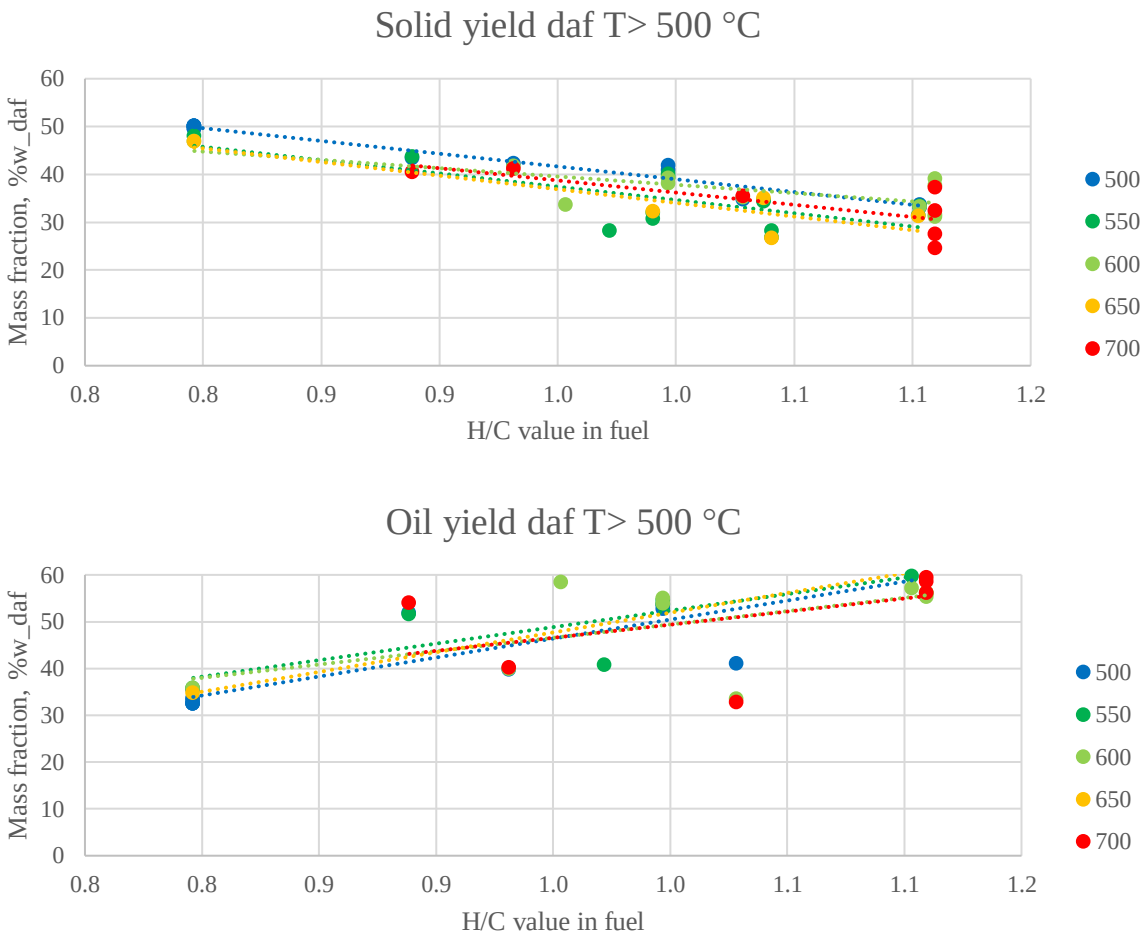

Figure 38. Yield of products based on H/C value and their corresponding trendlines.

5.3.2 Oil carbon content estimation

The elemental composition of the oil was estimated using the pyrolysis temperature, which the trend for carbon is shown in Figure 39. The function for the correlation derived from the data in literature is shown in the figure.

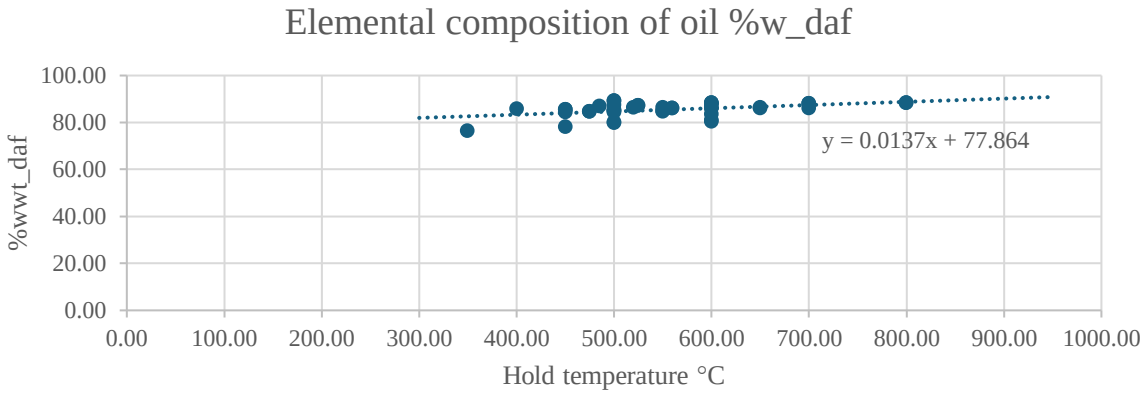

Figure 39.Carbon content of the oil based on pyrolysis temperature.

The estimation of the carbon content in the oil as a function of temperature had a maximum absolute error of 8.1%, while the majority (79%) of the estimations had an error of 4 % and below, as is shown in Figure 40. With an error of 8.1%, the correlation was deemed to be of good quality, however, additional verification is needed for it to be tested properly.

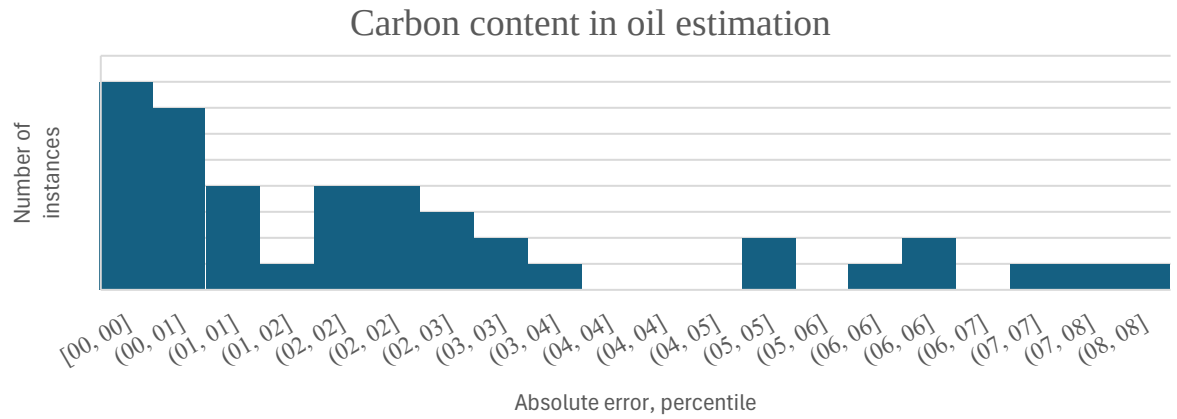

Figure 40. Absolut error of the carbon content in the oil based on temperature.

5.3.3 Gas phase estimations

The CC to species in the gas phase was estimated using ethylene as a key specie. In this subsection the correlations derived from data found in literature is presented first, then in the results from using the correlations for different operating conditions is presented, along with an evaluation of the model.

5.3.3.1 Correlation setup species gas

Ethylene was used as a key specie to estimate the yield of compounds of interest in the gas phase. The ethylene yield was dependent on the pyrolysis temperature and heating rate, as is shown in Figure 41.

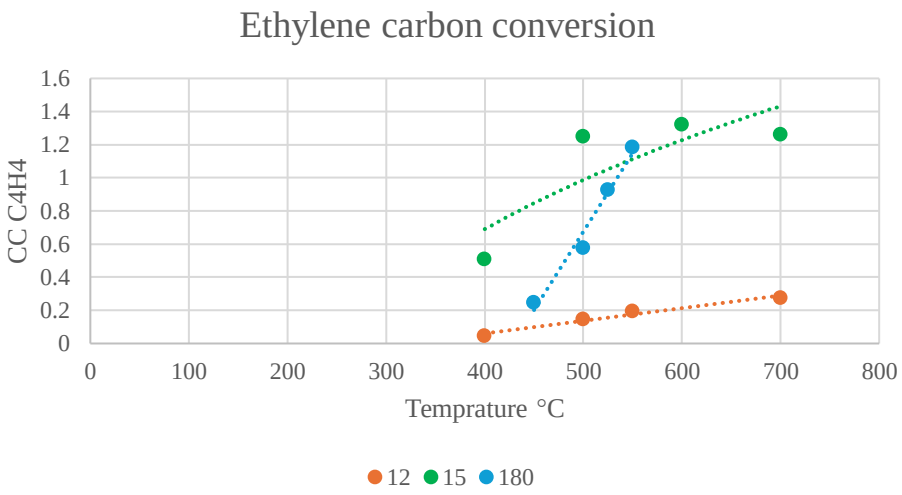

Figure 41. Carbon conversion to ethylene based on temperature and heating rate.

The CC to the compounds defined as a function of CC to ethylene can be seen in Figure 42. Since the heating rate seems to have a significant effect on the overall carbon conversion, heating rate is also considered when deriving the expression. While the correlations can be seen in the figure, the functions themselves can be found in Appendix E

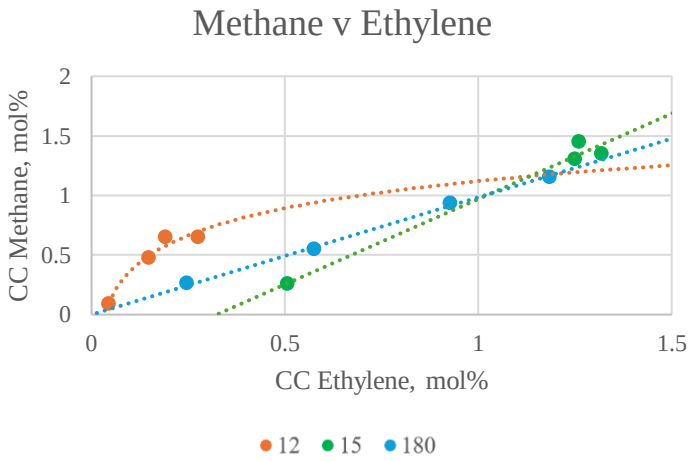

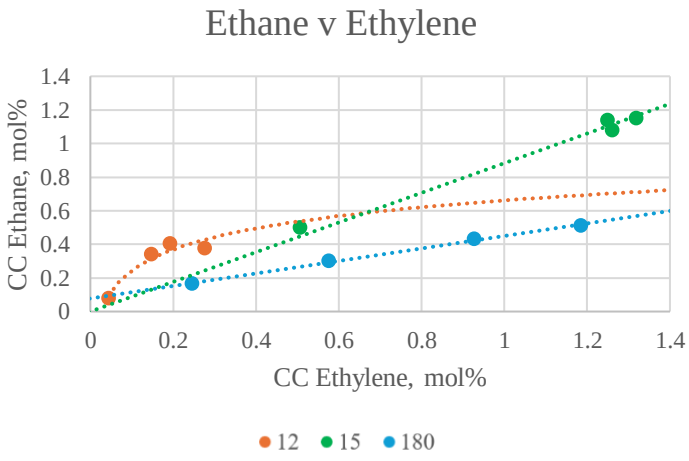

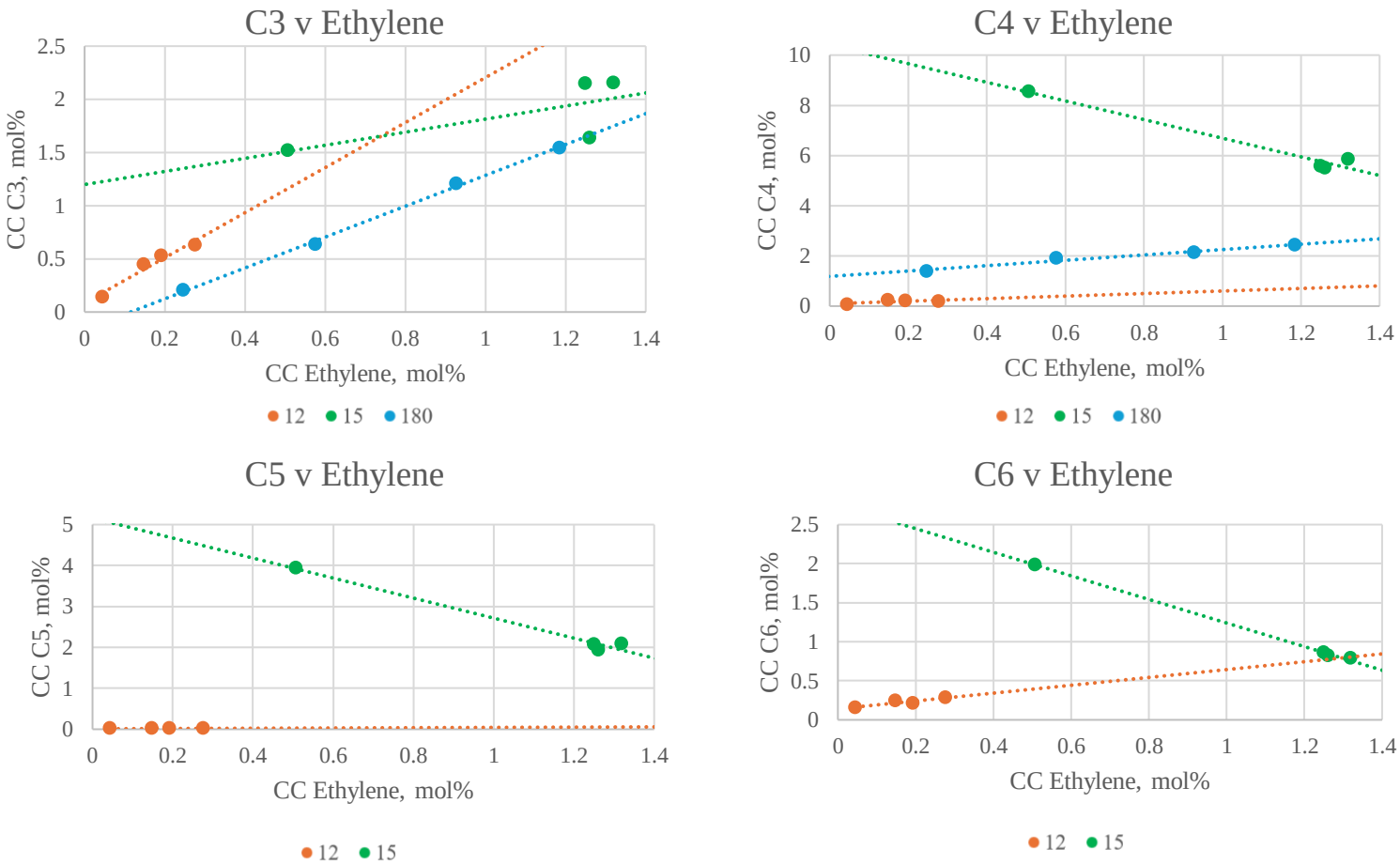

Figure 42. Compounds of interest normalised over ethylene with heating rate indicated.

For the compounds in the gas phase normalised over ethylene, some trends can be seen. The main one being for compounds up to C3, an increased ethylene production is accompanied by an increase in the compound. For C4-C6s, the trend for 15 °C/min (green line) is showing the opposite compared to the other. This might be due to the point at CC to ethylene = 0.5 begin at 400 °C, thus full conversion might not yet have been achieved. However, since the temperature is implicitly included with CC to ethylene, this deviation is included in the correlations. Compounds such as C5 and C6 was not reported in conjunction with ethylene for the HR=180°C/min, thus correlations were not possible to produce.

As previously mentioned, CO and CO_2 are a part of the total carbon balance but were assumed to be constrained by the oxygen content in the feedstock. The data and the corresponding correlations with their equations of the oxygen conversion are shown in Figure 43. As is shown in Figure 43b heating rate was considered when deriving the correlations for CO.

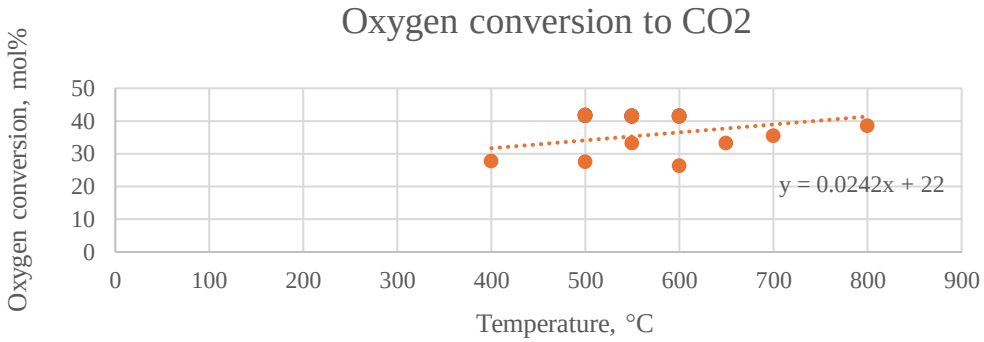

a) Oxygen conversion to CO_2

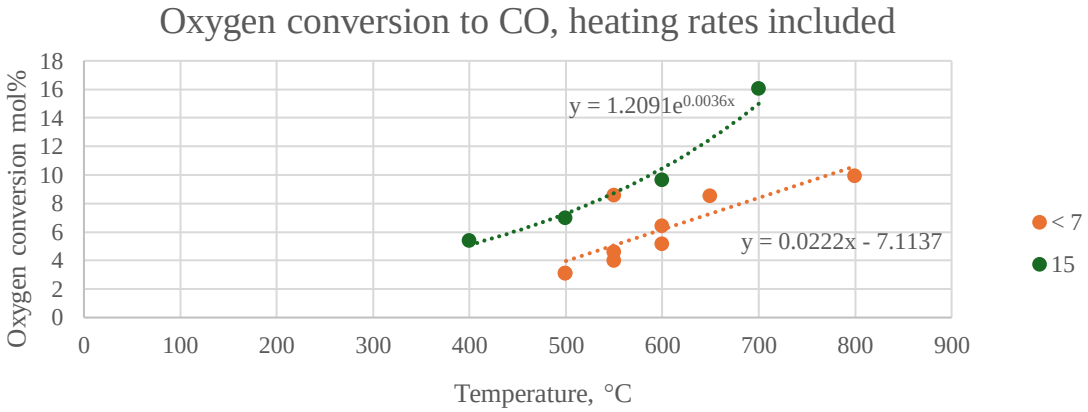

b) Oxygen conversion to CO with heating rate indicated by colour.

Figure 43. Data and correlation for oxygen conversion to CO2 and CO.

5.3.3.2 Estimation outcome from empirical model

The outcome of the estimations of the CC to compounds was carried out using temperatures in the range of 500-800°C with heating rates of 12,15 and 180 °C/min. The yield of compounds on a mass basis can be seen in Figure 44.

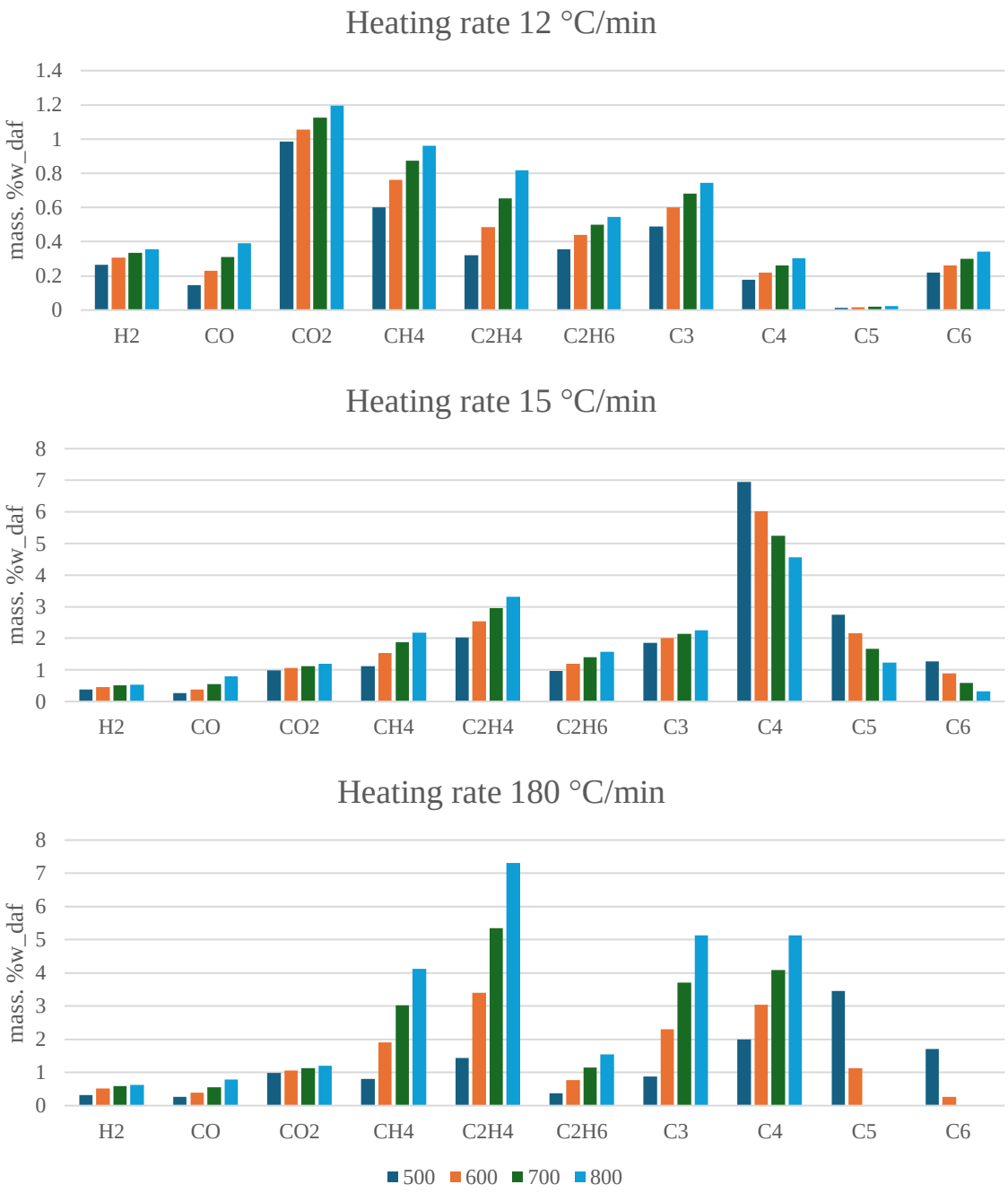

Figure 44. Product estimations for compounds up to C6

To clarify the validity of the model, ethylene and C3s can be isolated and compared to experiments presented in literature. As Figure 45 shows, the predicted and actual CC to the compounds differ. For both compounds, the predictions are in the same order of magnitude as the experiments, however they do differ significantly. In the case of ethylene, the prediction is differing 25-50% while for C3s the difference is in the range of 5-30% range.

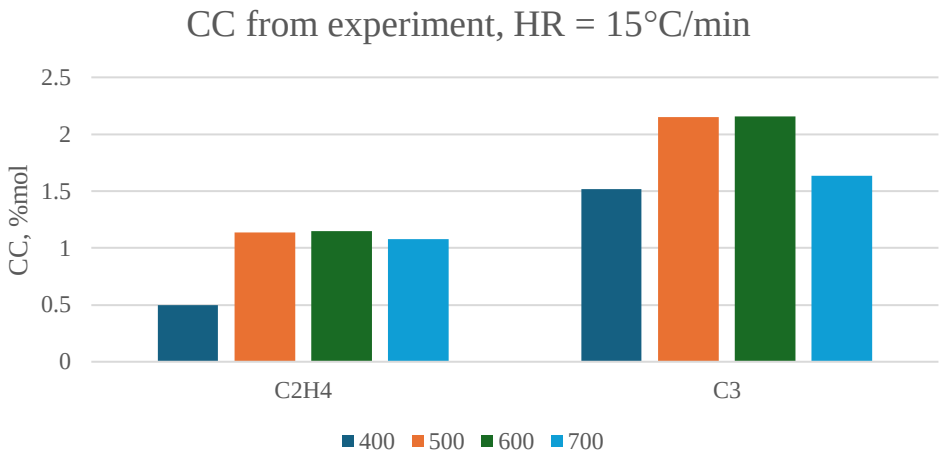

a) Experimental data for CC to ethylene and C3s

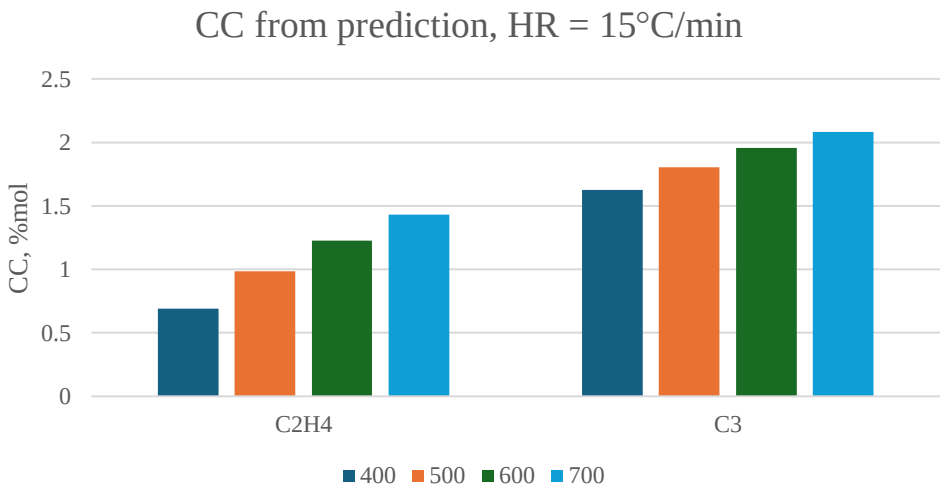

b) Prediction of CC to ethylene and C3s using empirical modelling

Figure 45. Empirical modelling(b) comparison to experimental data(a)

By estimating the carbon conversion to ethylene, CO, and CO_2, the accounted part of the carbon balance can be determined. As is shown in Figure 46, the total accounted part of the carbon balance varies slightly with temperature, but mainly with heating rate. This is due to the expressions used to estimate the yields of ethylene heavily determines the rest of the products.

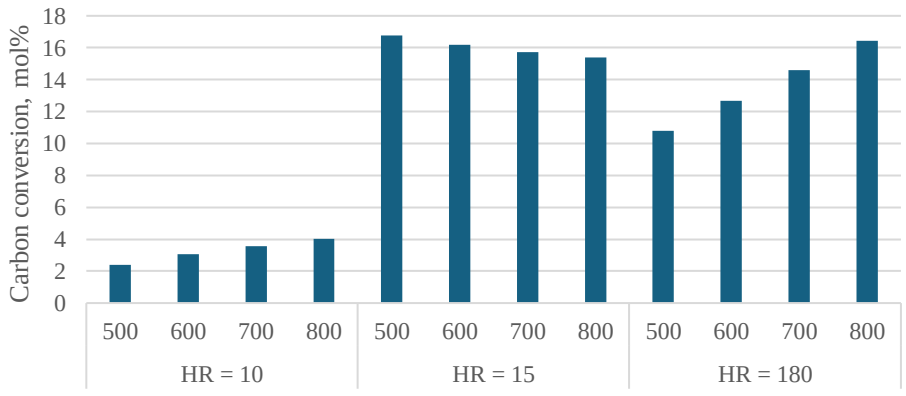

Figure 46. Carbon balance accounted for in compounds up to C6 using empirical modelling.

5.3.4 Oil phase estimates

Similar to the empirical modelling of the species in the gas phase, the oil phase utilized a key species, which was styrene. The same structure is presented here, with the correlation derived from literature first, and the predictions second along with a brief evaluation.

5.3.4.1 Correlation setup species oil

To estimate the oil yields, styrene was used as the key specie, which was modelled based on the temperature and heating rate. As previously discussed, the influence of heating rate seems to be significant. In Figure 47 the CC to styrene is shown, where the study using a HR = 15°C/min is sufficiently high to outscale the other heating rates, thus a rescaling was done, also shown in the figure.

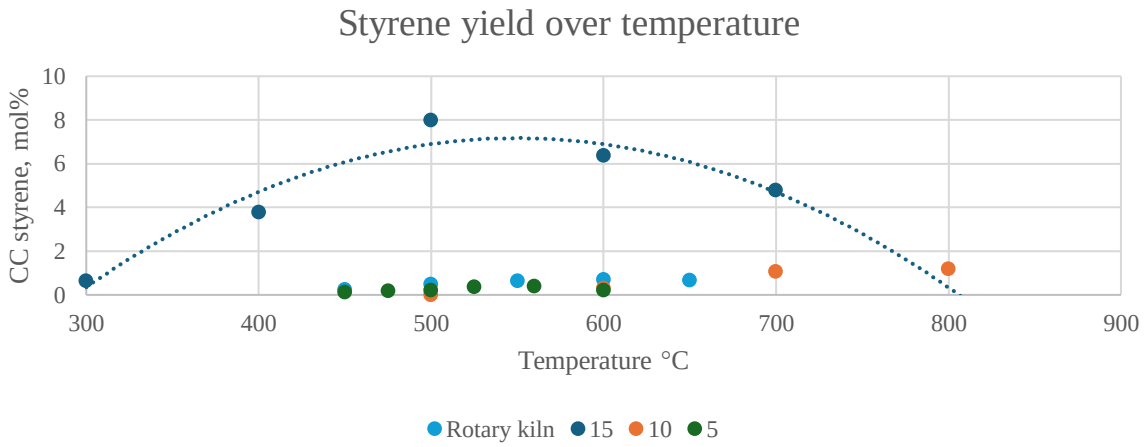

a) All studies included

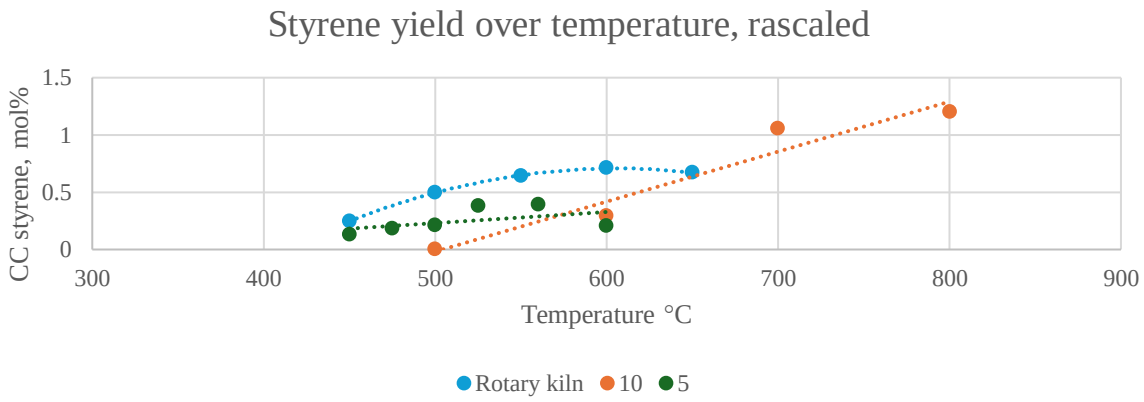

b) Study with heating rate of 15 °C/min is excluded, axis rescaled.

Figure 47. Data and correlations of CC to styrene with heating rate accounted for.

The correlations used in the empirical model is shown by the lines in Figure 47 while the functions of the correlations are presented in Appendix F. The same is done for the correlations between the compounds in the oil and the key specie styrene, as is shown in Figure 48. In the correlations there are clear trends with increased heating rate, which was accounted for.

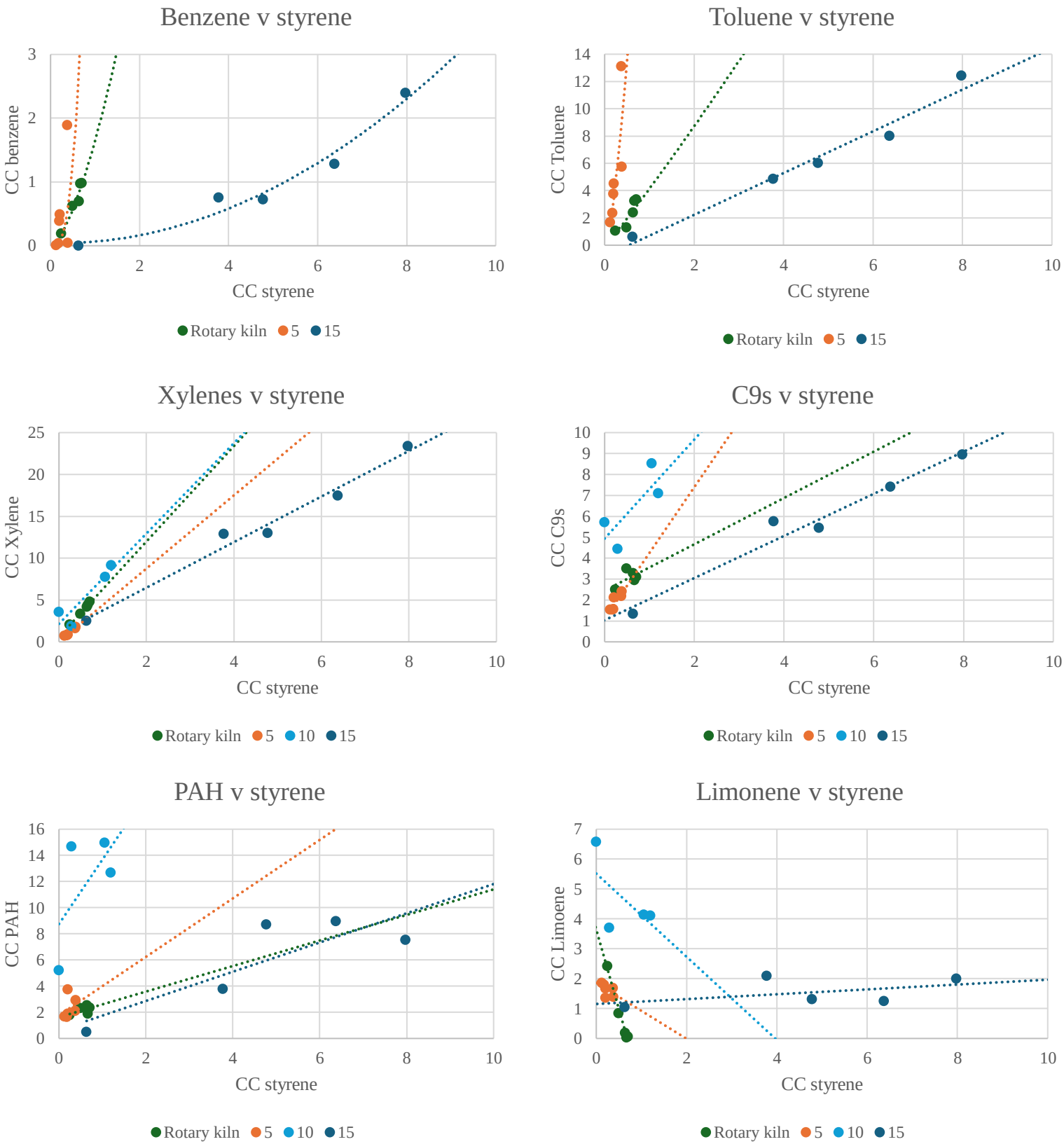

Figure 48. Compounds of interest normalised over styrene with heating rate indicated.

5.3.4.2 Estimation outcome for empirical modelling

Using the correlations presented in precious section was used to predict carbon conversion to the products in the oil. The overall carbon conversion to species in the oil can be seen in Figure 49, where parabolic expressions are occurring for both the heating rate = 15°C/min and the rotary kiln.

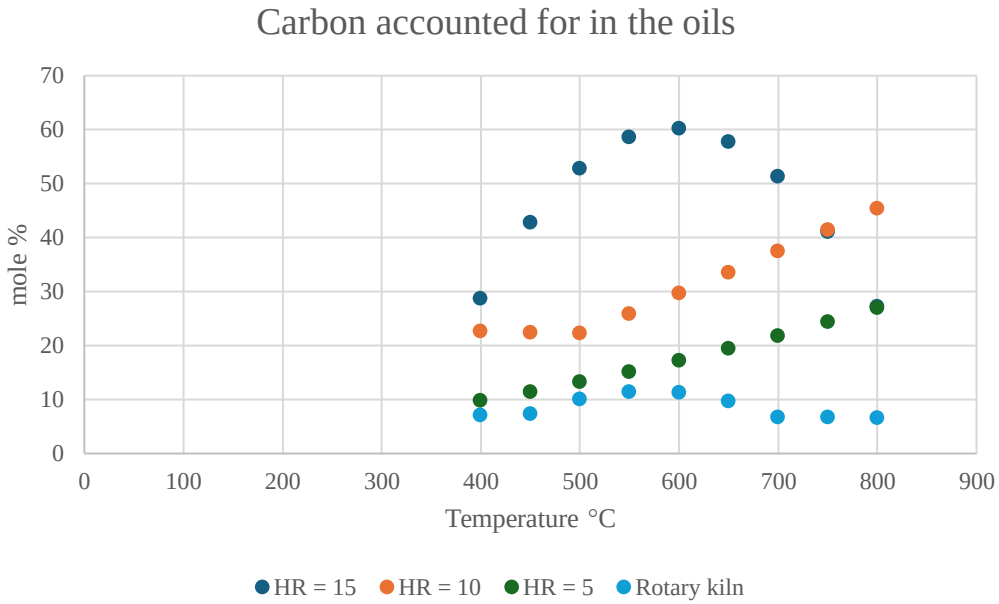

Figure 49. Total carbon content accounted for in the oil at different heating rate and temperatures.

With the known content in the oils predicted, the unknown content can be simply calculated by difference. The amount of unknowns is not unexpected, as going through the effort of individually identifying every specie would not be a good use of resources. To provide some context to the validity of this assumption, the previous work done by the author identified unknowns to be 85-80%w at 550 °C, with a decrease to around 70 %w for 650°C. While the units are not compatible, it indicates the order of magnitude of the unknown species. The carbon content can be seen to be rather close to the mass fraction in the oil, as the carbon is makes up a significantly larger portion of the mass for a compound in the oil.

Similarly to the evaluations of the gas phases, the key specie, styrene, and another compounds, benzene, is isolated to show the discrepancies between what the model predicts and what the experiments are showing. In Figure 50 the CC to styrene and benzene is shown for both experimental data and prediction of by the empirical model. Once again the discrepancy between the two is significant, indicating that the model is not sufficiently accurate to be use in a fully predictive manner.

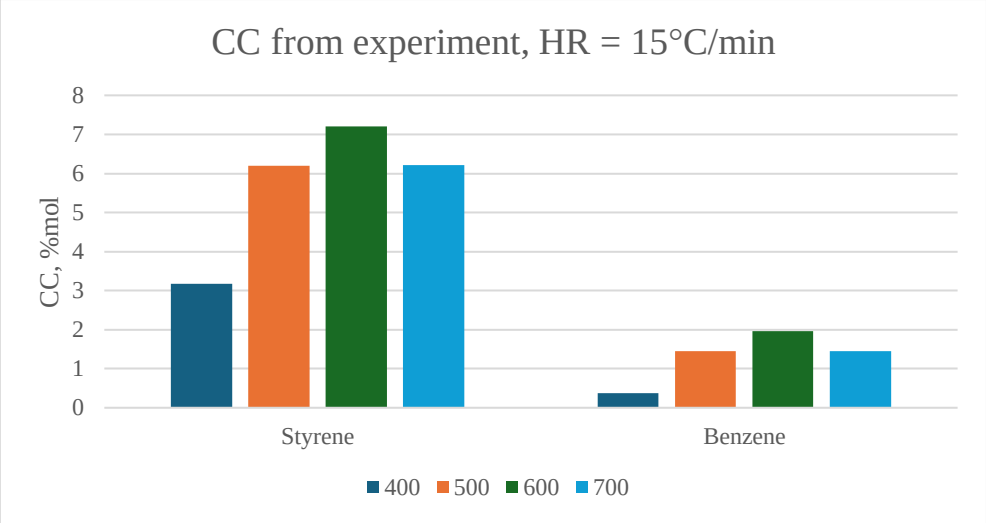

a) Experimental data of CC to styrene and benzene.

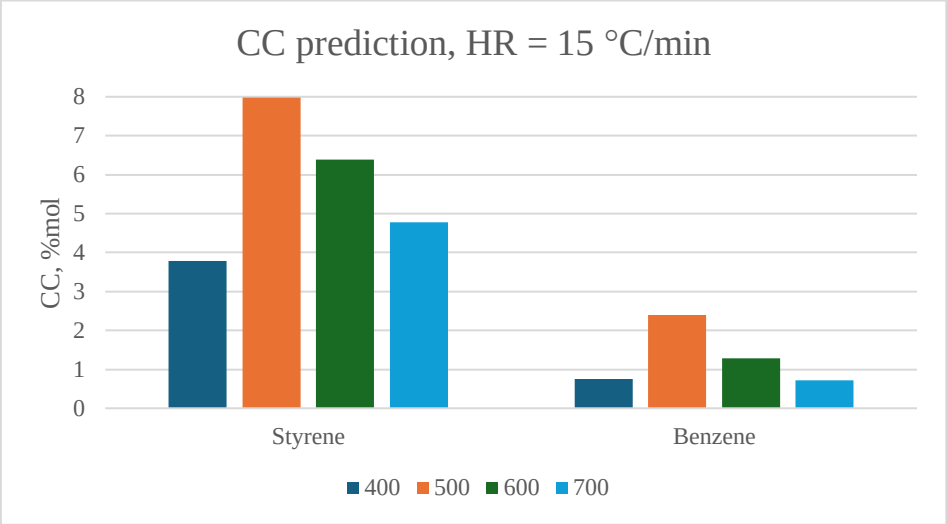

b) Prediction of CC to styrene and benzene.

Figure 50. Prediction(b) and experimental data(a) of CC to styrene and benzene for using heating rate of 15 °C/min

5.4 Simplified reactor model

The simplified reactor system was used to be able to describe the transient decomposition of ELTs, as the secondary cracking in the vapour might be of interest and might yield key species, in this case methane, to be able to model the process more accurately. The reaction pathways presented in 4.4 showed the procedure of the assumed decomposition. The reactor used to show the result is shown below, as introduced in section 4.4.1 and repeated here for clarity.

Feedstock related parameters		
Natural Rubber	X_{NR}	30wt.%
Styrene-butadiene rubber	X_{SBR}	30wt.%
Butadiene-rubber	X_{BR}	10wt.%
Carbon black	X_{CB}	30wt.%
Ash	X_{ash}	0wt.%
Reactor related parameters		
Volumetric flow	$\dot{V}_{N_2}$	10 $\frac{l}{min}$
Reactor diameter	D_R	0.1 m
Reactor height	l	5 m
Temperature	T	600 °C
Heating rate	Hr	5 °C/min

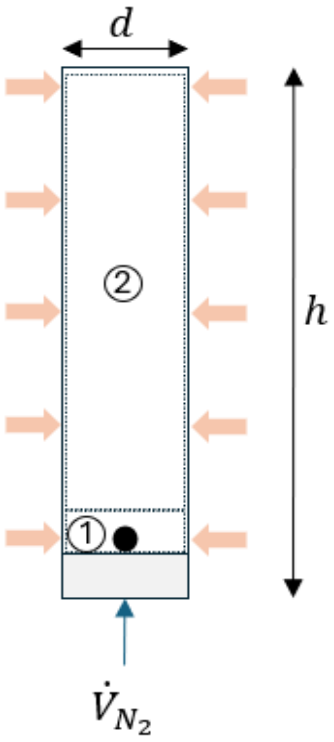

The overall decomposition of the sample is shown in Figure 51, shows the two phases of the decomposition happening indicated by the small bump, which is consistent with prior experiments presented in section 3.1. This is to be expected, as modelling a decomposition using kinetic expression are a usually a straightforward procedure.

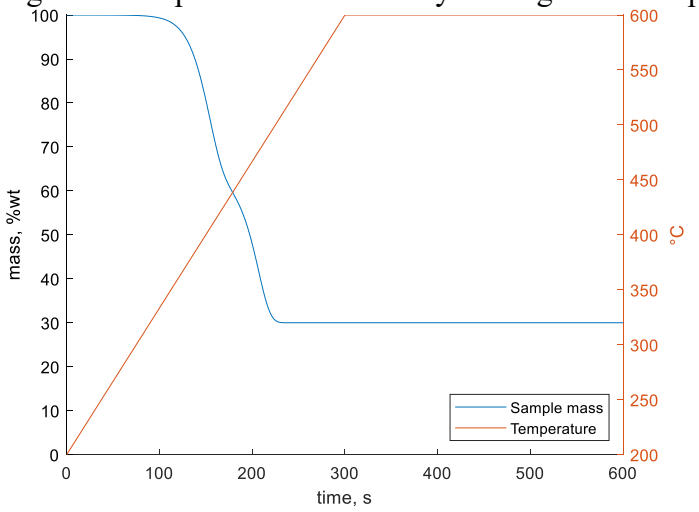

Figure 51. Decomposition of tire using kinetic modelling

Since the decomposition was assumed to not have any interactions between the compounds, the groups formed from the synthetic rubber decomposition was dominated by butadiene

monomers and 1,3-butadiene gas, while the natural rubber decomposition produced mainly isoprene monomers, as is shown in Figure 52 for the total mass at the end on the reactor (5m). Styrene is at the expected yield of 7.5%w as this is the input value of styrene in the feedstock.

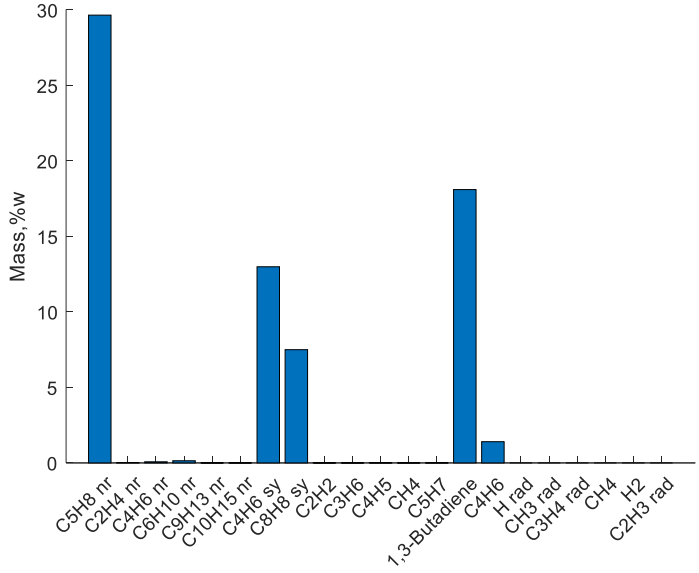

Figure 52. Compounds yield from radical reaction modelling of ELTs at 600 °C

The effect of residence time of the reactor is shown to highlight the decomposition of the butadiene monomers to produce 1,3-butadiene gas, shown in Figure 53. The figures display the transient behaviour of the compounds as they travel through the reactor. In a) the first cell is the line at the top and in b) the first cell is the one at the bottom.

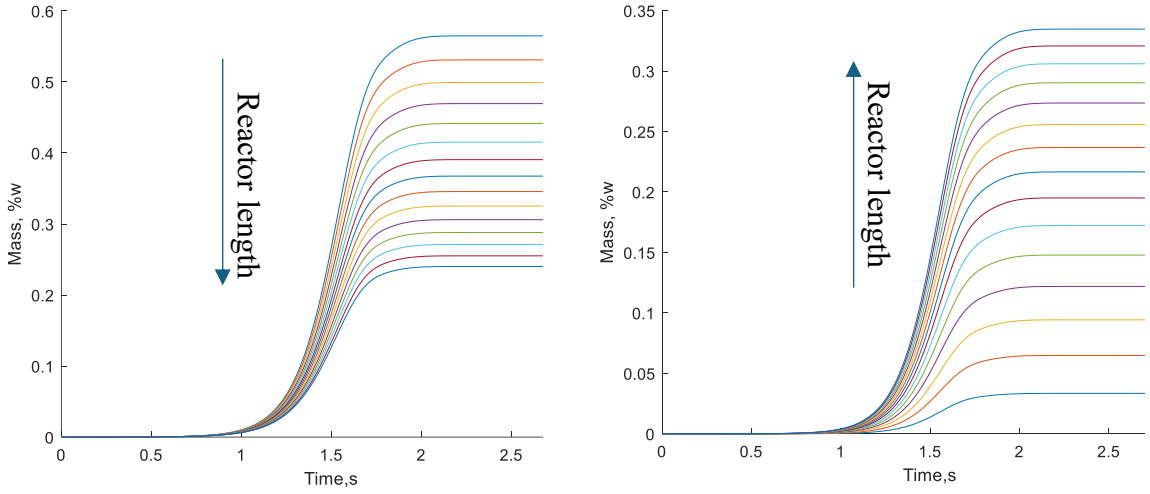

a) Consumption of butadiene radicals

b) Formation for 1,3-butadiene gas

Figure 53. Decomposition along the reactor height for synthetic rubber.

This shows how some of the reactions are happening, however, the majority of the compounds are not produced at these rates, making the overall conversion heavily skewed towards the stable monomers.

6 Discussion

6.1 Solid conversion behaviour and thermal size

The impact of heating rate has been shown to have an influence on the conversion path of ELTs. From prior experiments using a fixed bed reactor, the sample seemed to shatter due to the violent release of vapour as the tars in the sample are vapourised. Comparing this to the TGA, which aim is to have decrease the thermal size of the sample, the shattering does not occur, but a swelling of the sample is shown. The impact of the thermal size is of great interest as this might influence the solid behaviour as it is decomposed. There might be similarities to the case of biomass pyrolysis and combustion, where depending on the type of regime, the solid behaviour is greatly influenced. Since the heating rate influenced both the solid conversion and the composition of the oils, the impact on thermal size on the volatile products would be of interest.
The experiments themselves had a significant flaw, which was the preheating of the oven. By changing the heating rate so drastically compared to the TGA, the influence of thermal size is not isolated, meaning reruns of using the T-FBR would be needed to ensure the trends are valid.

6.2 Trends from data in literature

Looking at the data from literature, there are two trends which seems to be occurring at different stages, in Table 6-1 a condensed list of the trends is shown. The first is the perceived increased carbonisation with lower heating rate, which might be due to a longer residence time inside the particle. This increases the reactions between the tars produced and the carbon black. This was indicated by several things, but mainly the increase in H/C-value in the volatile matter, as less carbon bonds to the hydrogen, as well as the sulphur. This should correlate more light products or aliphatic content in the oil, which is seen, along with a decrease of aromatics in the oil.

Table 6-1. Trends based on heating rate

	Low HR	*High HR*	*Cause for increase*
Solid yield	↑	↓	Carbonisation due to longer contact time
H/C value in volatile products	↑	↓	Carbonisation due to longer contact time
H conv. Oil	↑	↓	Carbonisation due to longer contact time
C conv. oil	↑	↓	Carbonisation due to longer contact time
S conv. oil	↑	↓	Carbonisation due to longer contact time
Aromatic content in oil	↓	↑	Secondary cracking of volatile product
Aliphatic content in oil	↑	↓	Secondary cracking of volatile product
Methane and ethylene CC	↓	↑	Secondary cracking of volatile product
Methane v ethylene CC	↓	↑	Secondary cracking of volatile product
CC to benzene	↓	↑	Secondary cracking of volatile product

The second trend or stage which could be derived from the data is the increase in smaller hydrocarbons at higher heating rates, which, under the assumption that a higher heating rate corresponds to more energy input, translates well into the breakdown of longer chains. By producing the smaller compounds, more of the hydrogen will end up in the gas phase, which is seen by the increase of aromatic yield in the oil with increased heating rate, as this translates to a lower H/C-value in the oil. This breaking of longer chain is also seen by methane v ethylene, indicating that the production of methane was greater than that of ethylene, even if both of them increased with higher heating rates. This trend seems to be true when comparing the trends of benzene v styrene.

6.3 Empirical modelling

Modelling the carbon content of the oil based on the only the temperature showcases the consistency of properties of the oils. This a good example of utilising normalised data to derive more general expressions. However, as is the case of models, they need to be verified time and time again, which is true in this case as well.

To estimate the larger yields, the correlations had higher accuracy when estimating the solid yield. Since the oil and gas yield depends on to what extent the secondary reactions have occurred, and thus the system used, the estimations might not be complex enough to provide sufficient accuracy. While it can provide indications, trying to isolate parameters like internal residence time, thermal size and effective heating rate might prove to be a sufficient increase in complexity of the model.

In the modelling of key species, the data is not sufficient, as the expressions become dependent of how the correlations are selected. This introduces uncertainty twofold, firstly via the data available, as the study selected to be used have a significant impact on the correlations. Secondly, the selection was aimed to be as simple as possible, however, how the correlations should behave outside of the range of datapoints can be questioned. To expand the data available, additional studies can be found and included, however, due to inherent differences between studies, acquiring data through experimental campaigns might be a better plan of action.

The empirical model does give some validity to the use of key species, however, the key species themselves could be questioned, as they might not provide sufficient information regarding to what extent the decomposition has occurred i.e. the severity of the reaction. Utilising end products, such as methane, should be investigated as these can provide the severity and might provide better correlations to species. Ethylene might be too much of an intermediate in the conversion process, making it unfit to be a key specie. Styrene might be a good candidate; however, it is linked to the amount of SBR in the tire, introducing another free-variable to be determined. Since SBR is one of the most utilized rubbers, this might not be a big issue, as the amount of styrene from ELTs should be rather consistent, thus included when using an empirical model of an average tire.

The empirical model's strength is also its weakness. In parts where more complexity is needed, such as the case of the solid, liquid and gas yield, it suffers since it does not account for the secondary reactions. At the same time, as the carbon content in the oil showed, there is a significant advantage of using an empirical model, since the process can be condensed down to its most basic and important elements.

6.4 Simplified reactor model

Using radical reaction to explain the formation of the compounds of interest was deemed to be insufficient, as it was heavily skewed towards producing the stable monomers of the rubbers. While the main purpose of using such a model is to determine the production of key species, it left out two very important parts, which is the internal residence time and the Diels Adler reactions.

Tweaking the kinetic parameters might be of use, but since the overall residence time was not accounted for correctly, this might not be the main issue. How the internal residence time is affecting the products could prove to be of the highest significance, compared to the kinetic parameters. Tweaking should still be done, as the parameters are of different orders of magnitude. One big assumption was the first order of reaction, as this simplified the implementation of the model, and the validity of the assumption is up for debate as the reactions are very complex and have dependencies not accounted for in a first order reaction. This assumption should be investigated further.

Trying to explicitly model every reaction of the process is deemed unnecessary, as opening up this box will force us to unpack every reaction, thus needing parameters from every reaction. This issue was showcased, as the Diels Adler reaction was not accounted for, which might have led to a better representation of the process. While the internal residence time was not accounted for, the external was. The main assumption is the perfect mixing in each cell and thus the availability of isoprene. The simplified PFR reactor seemed to be a viable way of utilizing the decomposition pathways, however, the focus on vapour residence time was misplaced. Secondary reactions do occur in the vapours leaving the samples, but in industrial processes the shredded tires are placed in a pile and heated, so the vapours might interact with or condense on the surfaces of other tire pieces. How these reactions would influence the products would be very interesting to investigate. If carbonisation of the vapours is occurring, this would translate to a higher mass fraction of hydrogen present in the volatile matter, so if this would be left as pure hydrogen gas or more light hydrocarbons would be interesting. All in all, the radical reactions are deemed as a too complex step at the current knowledge base, thus focus should be placed on the

7 Conclusion and future work

This thesis shows the intricacies of accurately describing the decomposition of end-of-life tires. Due to several factors such as a lack of disclosed species in literature, extensive data collection was inhibited. As a result, general decomposition correlations could not be made to a satisfactory extent. However, the work points to several trends occurring during pyrolysis of ELTs.

The impact of heating rate, when equated to energy supplied, seems to show a clear impact on the composition of the products. The main pathways are an increase in lighter hydrocarbons, such as ethylene and methane, as well as promoting aromatisation at the expense of the longer chains. With lower heating rate, the solid will swell less, indicating a pressure increase with heating rate, with might increase the residence time inside the particle. A longer residence time within the particle correlated to a larger amount of the carbon in the feedstock will end up in the solid yields due to carbonisation.

The attempt of trying to explain the formation of key compounds via the SRM was deemed to be insufficient, as the model must be complemented by an internal residence time. With this added amount of complexity, the system becomes more sensitive to every input parameter. Instead of explicitly describing the decomposition, time might have been better spent focusing on why the broader trends found in the data, such as the elemental composition of oils, H/C-values, and production smaller compounds, exist. While some trends are explainable, being able to map more clearly the formation pathways is of great personal interest.

While there are some issues with modelling the process, clear trends of the decomposition paths are both seen and explainable. The field of tire pyrolysis is a promising way of recycling complex feedstock which when left unprocessed can be directly dangerous, as well as being the pure loss in the carbon loop of the world. Ideally all the carbon present in the feedstock could be recycled into new products, as is starting to be demonstrated on an industrial scale.

Future work in this research field is plentiful, however, two things is of personal interest. The first being the solid behaviour as the particle size has been reported to impact the pyrolysis time, which might also impact the products used. Are there distinct regimes in the case of ELT pyrolysis in a fixed bed reactor? The second is development of key species, where ethylene and styrene should be scrutinized.

8 References

[1] F. Valentini and A. Pegoretti, “End-of-life options of tyres. A review,” 2022, doi: 10.1016/j.aiepr.2022.08.006.

[2] M. Consulting, “End of Life Tyre Management: Thermal Processing Options,” 2022, Accessed: Oct. 09, 2023. [Online]. Available: www.sprep.org

[3] B. Rodgers, “Tire Engineering: An Introduction.”

[4] N. Gao, F. Wang, C. Quan, L. Santamaria, G. Lopez, and P. T. Williams, “Tire pyrolysis char: Processes, properties, upgrading and applications,” *Prog Energy Combust Sci*, vol. 93, p. 101022, Nov. 2022, doi: 10.1016/J.PECS.2022.101022.

[5] “Enviro’s recovered pyrolysis oil has been successfully processed by Neste into raw materials for chemicals and plastics - Envirosystems.” Accessed: May 11, 2024. [Online]. Available: https://envirosystems.se/investor/press-releases/enviros-recovered-pyrolysis-oil-has-been-successfully-processed-by-neste-into-raw-materials-for-chemicals-and-plastics-cid-778987D00115D609/

[6] P. T. Williams and S. Besler, “Pyrolysis-thermogravimetric analysis of tyres and tyre components,” vol. 14, no. 9, pp. 1277–1283, 1995.

[7] M. Morton, *Rubber technology*, 3rd ed. Von Nostrand Reinhold Company Inc., 1987.

[8] “Emulsion Styrene Butadiene Rubber (ESBR) Product Details | Goodyear Chemical.” Accessed: May 10, 2024. [Online]. Available: https://www.goodyearchemical.com/products/emulsion-styrene-butadiene-rubber

[9] Y. Li, Y. Wu, Y. Luo, T. W. Chan, L. Zhang, and S. Wu, “A combined experimental and molecular dynamics simulation study on the structures and properties of three types of styrene butadiene rubber,” *Mater Today Commun*, vol. 4, pp. 35–41, Sep. 2015, doi: 10.1016/j.mtcomm.2015.04.007.

[10] Q. Yang *et al.*, “Gas products generation mechanism during co-pyrolysis of styrene-butadiene rubber and natural rubber,” 2020, doi: 10.1016/j.jhazmat.2020.123302.

[11] S. Liu *et al.*, “Rubber pyrolysis: Kinetic modeling and vulcanization effects,” *Energy*, vol. 155, pp. 215–225, Jul. 2018, doi: 10.1016/J.ENERGY.2018.04.146.

[12] ETRMA, “Press release”.

[13] A. Mohajerani *et al.*, “Recycling waste rubber tyres in construction materials and associated environmental considerations: A review,” *Resour Conserv Recycl*, vol. 155, p. 104679, Apr. 2020, doi: 10.1016/J.RESCONREC.2020.104679.

[14] M. Consulting, “End of Life Tyre Management: Thermal Processing Options,” 2022, Accessed: Oct. 09, 2023. [Online]. Available: www.sprep.org

[15] P. T. Williams, “Pyrolysis of waste tyres: A review,” *Waste Management*, vol. 33, no. 8, pp. 1714–1728, Aug. 2013, doi: 10.1016/J.WASMAN.2013.05.003.

[16] J. Yang and C. Roy, “thermochimica acta ELSEVIER A new method for DTA measurement of enthalpy change during the pyrolysis of rubbers,” *Thermochim Acta*, vol. 288, p. 168, 1996.

[17] J. M. Bouvier, F. Charbel, and M. Gelus, “Gas-solid pyrolysis of tire wastes — Kinetics and material balances of batch pyrolysis of used tires,” *Resources and Conservation*, vol. 15, no. 3, pp. 205–214, Aug. 1987, doi: 10.1016/0166-3097(87)90003-4.

[18] J. Yang, P. A. Tanguy, and C. Roy, “Heat transfer, mass transfer and kinetics study of the vacuum pyrolysis of a large used tire particle,” *Chem Eng Sci*, vol. 50, no. 12, pp. 1909–1922, Jun. 1995, doi: 10.1016/0009-2509(95)00062-A.

[19] B. Lah, D. Klinar, and B. Likozar, “Pyrolysis of natural, butadiene, styrene–butadiene rubber and tyre components: Modelling kinetics and transport phenomena at different

heating rates and formulations," *Chem Eng Sci*, vol. 87, pp. 1–13, Jan. 2013, doi: 10.1016/J.CES.2012.10.003.
[20] A. K. Bhowmick, S. Rampalli, K. Gallagher, R. Seeger, and D. McIntyre, "The degradation of guayule rubber and the effect of resin components on degradation at high temperature," *J Appl Polym Sci*, vol. 33, no. 4, pp. 1125–1139, Mar. 1987, doi: 10.1002/app.1987.070330407.
[21] John. Scheirs and W. (Walter) Kaminsky, *Feedstock recycling and pyrolysis of waste plastics : converting waste plastics into diesel and other fuels*. J. Wiley & Sons, 2006.
[22] D. Neves, H. Thunman, A. Matos, L. Tarelho, and A. Gómez-Barea, "Characterization and prediction of biomass pyrolysis products," *Progress in Energy and Combustion Science*, vol. 37, no. 5. Elsevier Ltd, pp. 611–630, 2011. doi: 10.1016/j.pecs.2011.01.001.
[23] S. Andersson, P.-E. Bengtsson, B. Leckner, D. Pallarès, and H. Thunman, *Combustion engineering*, 2020th ed. Göteborg: Reproservice, CHALMERS UNIVERSITY OF TECHNOLOGY, 2020.
[24] S. W. Churchill and M. Bernstein, "A Correlating Equation for Forced Convection From Gases and Liquids to a Circular Cylinder in Crossflow," *J Heat Transfer*, vol. 99, no. 2, pp. 300–306, May 1977, doi: 10.1115/1.3450685.
[25] W. Ye *et al.*, "Formation behavior of PAHs during pyrolysis of waste tires," *J Hazard Mater*, vol. 435, p. 128997, Aug. 2022, doi: 10.1016/J.JHAZMAT.2022.128997.
[26] F. p. Incropera, D. P. Dewitt, T. L. Bergman, and A. S. Lavine, *HEAT and MASS TRANSFER*, 8th ed. Hoboken, NJ: Wiley, 2017.
[27] C. Roy, A. Chaala, and H. Darmstadt, "The vacuum pyrolysis of used tires: End-uses for oil and carbon black products," *J Anal Appl Pyrolysis*, vol. 51, no. 1–2, pp. 201–221, Jul. 1999, doi: 10.1016/S0165-2370(99)00017-0.
[28] G. S. Miguel, G. D. Fowler, and C. J. Sollars, "Pyrolysis of tire rubber: Porosity and adsorption characteristics of the pyrolytic chars," *Ind Eng Chem Res*, vol. 37, no. 6, pp. 2430–2435, 1998, doi: 10.1021/IE970728X.
[29] P. T. Williams, S. Besler, and D. T. Taylor, "The pyrolysis of scrap automotive tyres: The influence of temperature and heating rate on product composition," *Fuel*, vol. 69, no. 12, pp. 1474–1482, Dec. 1990, doi: 10.1016/0016-2361(90)90193-T.
[30] C. Berrueco, E. Esperanza, F. J. Mastral, J. Ceamanos, and P. García-Bacaicoa, "Pyrolysis of waste tyres in an atmospheric static-bed batch reactor: Analysis of the gases obtained," *J Anal Appl Pyrolysis*, vol. 74, no. 1–2, pp. 245–253, Aug. 2005, doi: 10.1016/J.JAAP.2004.10.007.
[31] A. Hooshmand Ahoor and N. Zandi-Atashbar, "Fuel production based on catalytic pyrolysis of waste tires as an optimized model," *Energy Convers Manag*, vol. 87, pp. 653–669, Nov. 2014, doi: 10.1016/J.ENCONMAN.2014.07.033.
[32] W. Ye *et al.*, "Formation behavior of PAHs during pyrolysis of waste tires," *J Hazard Mater*, vol. 435, p. 128997, Aug. 2022, doi: 10.1016/J.JHAZMAT.2022.128997.
[33] S. Xu *et al.*, "Pyrolysis characteristics of waste tire particles in fixed-bed reactor with internals," *Carbon Resources Conversion*, vol. 1, no. 3, pp. 228–237, Dec. 2018, doi: 10.1016/J.CRCON.2018.10.001.
[34] C. Díez, O. Martínez, L. F. Calvo, J. Cara, and A. Morán, "Pyrolysis of tyres. Influence of the final temperature of the process on emissions and the calorific value of the products recovered," *Waste Management*, vol. 24, no. 5, pp. 463–469, Jan. 2004, doi: 10.1016/J.WASMAN.2003.11.006.
[35] I. De Marco Rodriguez, M. F. Laresgoiti, M. A. Cabrero, A. Torres, M. J. Chomón, and B. Caballero, "Pyrolysis of scrap tyres," *Fuel Processing Technology*, vol. 72, no. 1, pp. 9–22, Aug. 2001, doi: 10.1016/S0378-3820(01)00174-6.

[36] S. Q. Li, Q. Yao, Y. Chi, J. H. Yan, and K. F. Cen, “Pilot-scale pyrolysis of scrap tires in a continuous rotary kiln reactor,” *Ind Eng Chem Res*, vol. 43, no. 17, pp. 5133–5145, Aug. 2004, doi: 10.1021/ie030115m.
[37] M. F. Laresgoiti, B. M. Caballero, I. De Marco, A. Torres, M. A. Cabrero, and M. J. Chomón, “Characterization of the liquid products obtained in tyre pyrolysis,” *J Anal Appl Pyrolysis*, vol. 71, no. 2, pp. 917–934, 2004, doi: 10.1016/j.jaap.2003.12.003.
[38] G. G. Choi, S. H. Jung, S. J. Oh, and J. S. Kim, “Total utilization of waste tire rubber through pyrolysis to obtain oils and CO2 activation of pyrolysis char,” *Fuel Processing Technology*, vol. 123, pp. 57–64, Jul. 2014, doi: 10.1016/J.FUPROC.2014.02.007.
[39] P. T. Williams and A. J. Brindle, “Fluidised bed pyrolysis and catalytic pyrolysis of scrap tyres,” *Environmental Technology (United Kingdom)*, vol. 24, no. 7, pp. 921–929, Jul. 2003, doi: 10.1080/09593330309385629.
[40] A. M. Cunliffe and P. T. Williams, “Composition of oils derived from the batch pyrolysis of tyres,” 1998.
[41] S. Ucar, S. Karagoz, A. R. Ozkan, and J. Yanik, “Evaluation of two different scrap tires as hydrocarbon source by pyrolysis,” *Fuel*, vol. 84, no. 14–15, pp. 1884–1892, Oct. 2005, doi: 10.1016/J.FUEL.2005.04.002.
[42] S. Q. Li, Q. Yao, Y. Chi, J. H. Yan, and K. F. Cen, “Pilot-scale pyrolysis of scrap tires in a continuous rotary kiln reactor,” *Ind Eng Chem Res*, vol. 43, no. 17, pp. 5133–5145, Aug. 2004, doi: 10.1021/ie030115m.
[43] X. Wei, H. Zhong, Q. Yang, E. Yao, Y. Zhang, and H. Zou, “Studying the mechanisms of natural rubber pyrolysis gas generation using RMD simulations and TG-FTIR experiments,” 2019, doi: 10.1016/j.enconman.2019.03.069.
[44] W. Kaminsky, C. Mennerich, and Z. Zhang, “Feedstock recycling of synthetic and natural rubber by pyrolysis in a fluidized bed,” *J Anal Appl Pyrolysis*, vol. 85, no. 1–2, pp. 334–337, May 2009, doi: 10.1016/J.JAAP.2008.11.012.

Appendix

Appendix A. Data collection

Reactor	Particle size	Heating rate(s) °C/Min	End Temperature(s) °C	Source
Vacuum FBR	20x30;100x120 mm	NA	485;500;520;550	[29]
Rotary kiln	0.42	5	300;400;450;500;600;700;800	[30]
FBR	2-5 cm^2	5;20;40;80	300;420;600;720	[31]
FBR	2-20 mm	12	400;500;550;700	[32]
FBR	5;20	NA	475	[33]
FBR	0.15 mm (powder)	10;20;40	450;475;500;550;600;650	[34]
FBR	>5 mm	4	550;550;600	[35]
FBR	0.42 mm (powder)	NA	350;450;550	[36]
FBR	2-3 cm	15	300;400;500;600;700	[37]
Rotary kiln	13-15 mm	NA	450;500;550;600;650	[38]
FBR	2-3 cm	15	300;400;500;600;700	[39]
FBR	1-2 mm	10	500;600;700;800	[40]
BFBR	1-1.4 mm	NA	450;500;525;550;600	[41]
FBR	150 mm	5	450;475;500;525;560;600	[42]
FBR	1.5-2 mm	7	550;650;800	[43]

FBR – Fixed bed reactor
BFBR – Bubbling fluidised bed reactor

Appendix B. Feedstock composition spread

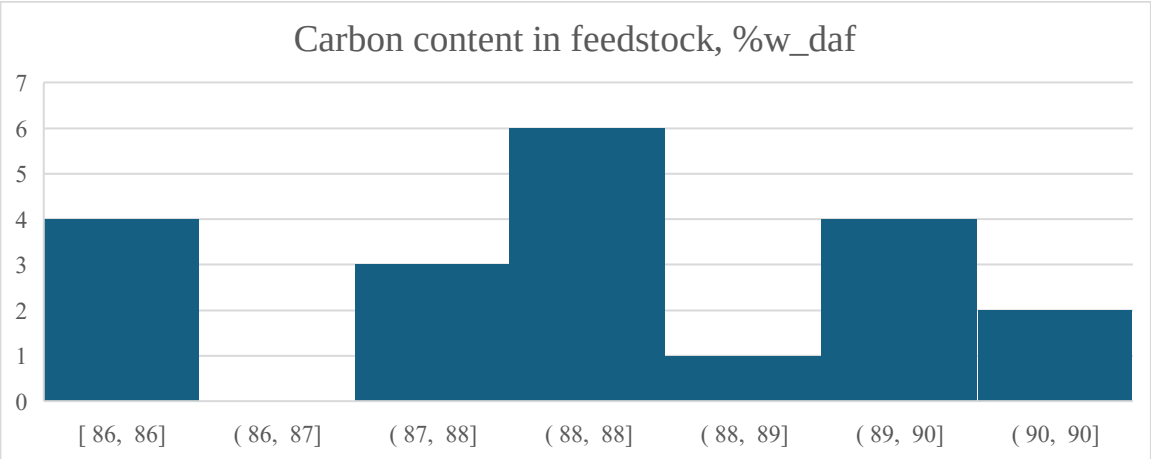

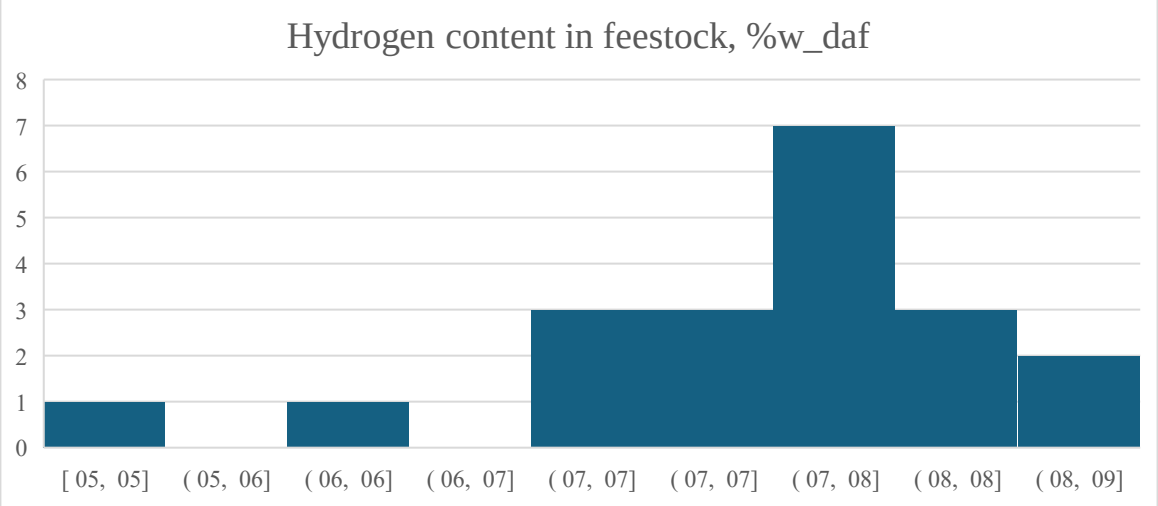

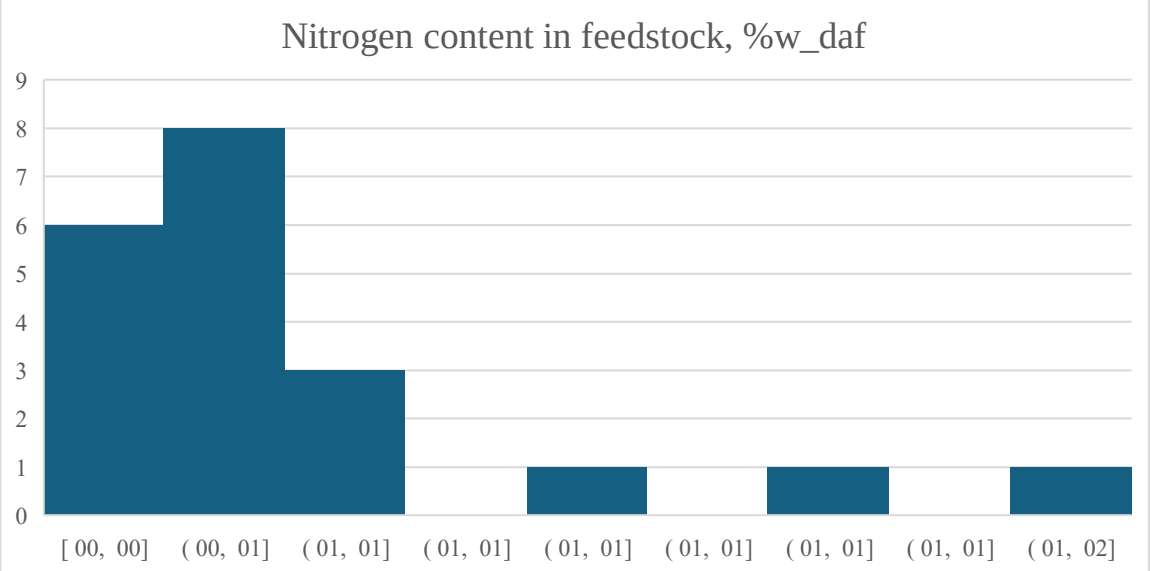

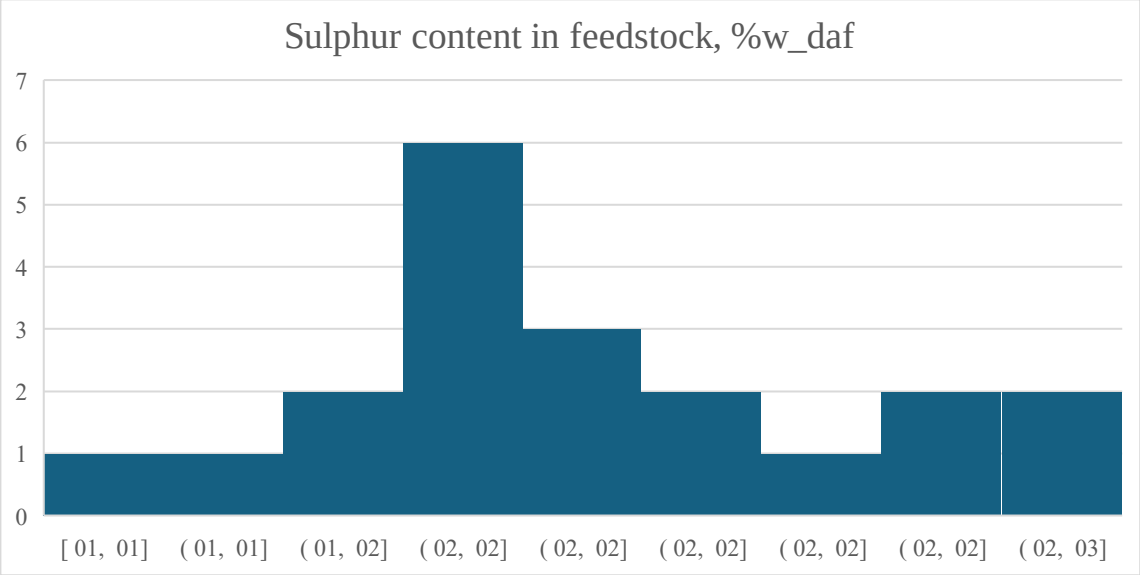
Sulphur content in feedstock, %w_daf
7
6
5
4
3
2
1
0
[01, 01]
(01, 01]
(01, 02]
(02, 02]
(02, 02]
(02, 02]
(02, 02]
(02, 02]
(02, 03]

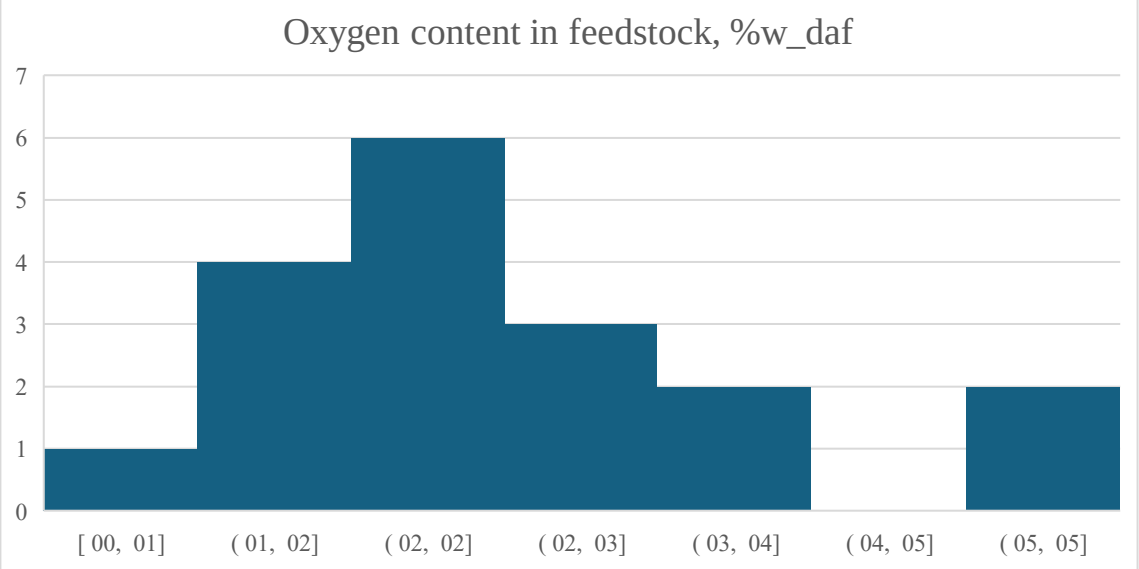
Oxygen content in feedstock, %w_daf
7
6
5
4
3
2
1
0
[00, 01]
(01, 02]
(02, 02]
(02, 03]
(03, 04]
(04, 05]
(05, 05]

Appendix C. Correlations to estimate the product yields for HC values

Product yield estimations beased on H/C- values for different temperature ranges, HC indicates the H/C value.

Temperature	Solid	Oil	Gas
500	$-53.4 \cdot HC + 92.4$	$81.1 \cdot HC - 30.6$	*By difference*
550	$-55.6 \cdot HC + 90.2$	$70.6 \cdot HC - 18.2$	*By difference*
600	$-34.7 \cdot HC + 72.5$	$57 \cdot HC - 7.6$	*By difference*
650	$-57.0 \cdot HC + 91.0$	$28.1 \cdot HC - 22.5$	*By difference*
700	$-51.0 \cdot HC + 87.1$	$55.9 \cdot HC - 6.6$	*By difference*

Appendix D. Product yield estimations error

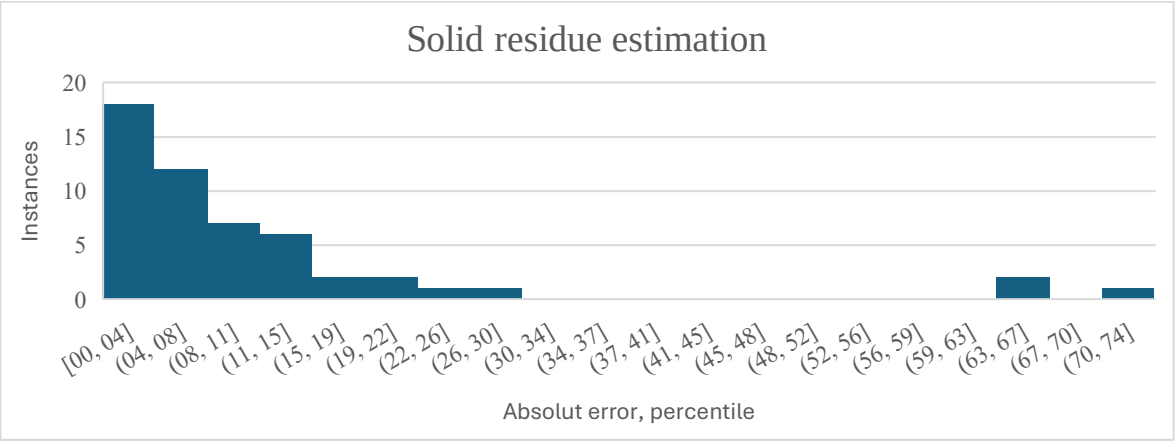

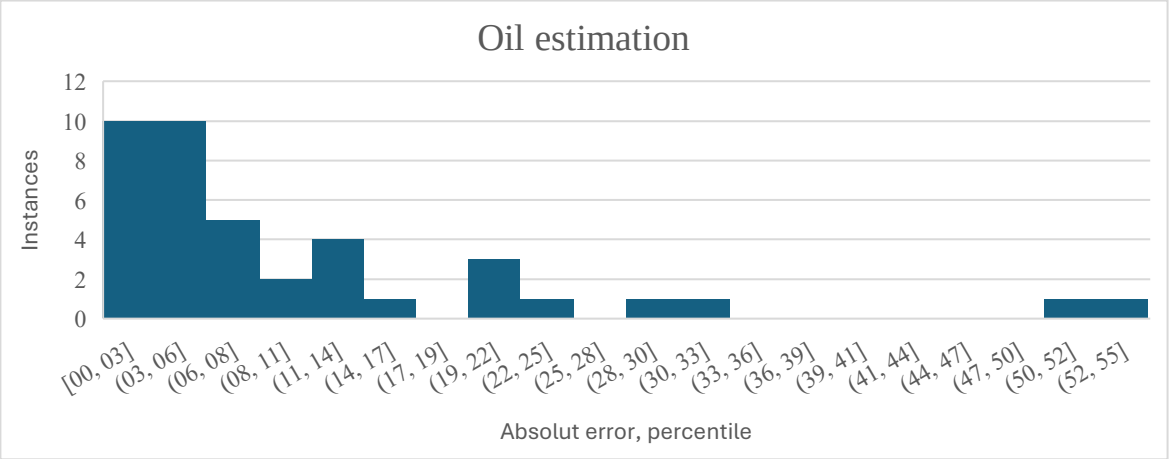

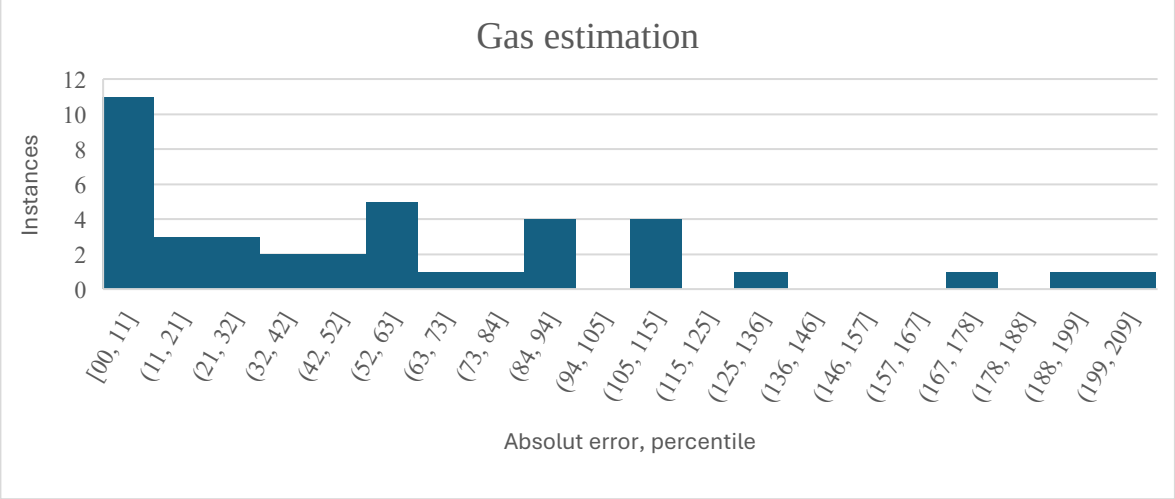

Appendix E. Correlations for CC to compounds in gas

Carbon conversion to ethylene dependent on temperature, T and heating rate.

	Fluidized bed	*Fixed bed*	
Heating rate, °C/min	180	12	15
Ethylene	$0.0095 \cdot T - 3.054$	$0.0008 \cdot T - 0.2442$	$1.325\ln(T) - 7.25$

Carbon conversion to specie dependent on carbon conversion to ethylene, CC_{Eth} and heating rate.

	Fluidized bed	*Fixed bed*	
Heating rate, °C/min	180	12	15
Methane	$0.985 \cdot CC_{Eth}$	$0.328 \cdot \ln(CC_{Eth}) + 1.120$	$1.43 \cdot CC_{Eth} - 0.464$
Ethane	$0.372 \cdot CC_{Eth} - 0.078$	$0.182 \cdot \ln(CC_{Eth}) + 0.661$	$0.883 \cdot CC_{Eth}$
C3s	$1.45 \cdot CC_{Eth} - 0.166$	$0.266 \cdot \ln(CC_{Eth}) + 0.965$	$0.615 \cdot CC_{Eth} + 1.20$
C4s	$1.07 \cdot CC_{Eth} + 1.185$	$0.51 \cdot CC_{Eth} + 0.094$	$-3.71 \cdot CC_{Eth} + 10.4$
C5s	*NA*	$0.034 \cdot CC_{Eth} + 0.009$	$-2.44 \cdot CC_{Eth} + 5.16$
C6s	*NA*	$0.50 \cdot CC_{Eth} + 0.14$	$-1.51 \cdot CC_{Eth} + 2.75$

Carbon conversion to CO and CO_2 as functions of temperature and heating rate

Compound	*HR = 7*	*HR = 15*
CO2	0.024T+22	
CO	0.0022T-7.711	$1.21e^{0.0036T}$

Appendix F. Correlations for CC to compounds in oil

	Rotary kiln	*Fixed bed reactor*		
Compounds	HR = NA	HR = 5 °C/min	HR = 10 °C/min	HR = 15 °C/min
Styrene	$-2E-05T^2+0.023T-6.23$	0.001T-0.25	0.004T-2.2	$-0.001*T^2+0.1201T-28.86$
Benzene	$1.65\ CC_{styr}^{1.536}$	$11.68\ CC_{styr}^{3.167}$	NA	$0.037\ CC_{styr}^2+0.011\ CC_{styr}-0.04$
Toluene	$4.128\ CC_{styr}^{1.077}$	$37.74\ CC_{styr}^{1.503}$	NA	$1.53\ CC_{styr}-0.83$
Xylenes	$5.70\ CC_{styr}+0.58$	$4.38\ CC_{styr}+0.01$	$5.40\ CC_{styr}+2.15$	$2.72\ CC_{styr}+1.02$
C9s	$3.14\ CC_{styr}+1.11$	$1.11\ CC_{styr}+2.45$	$2.368\ CC_{styr}+4.94$	$1.01\ CC_{styr}+1.04$
PAHs	$0.98\ CC_{styr}+1.63$	$2.24\ CC_{styr}+1.76$	$4.92\ CC_{styr}+8.75$	$1.12\ CC_{styr}+0.632$
Limonene	$-5.31\ CC_{styr}+3.64$	$-0.93\ CC_{styr}+1.86$	$-1.39\ CC_{styr}+5.52$	$0.08\ CC_{styr}+1.15$

CHALMERS
UNIVERSITY OF TECHNOLOGY

DEPARTMENT OF Space, Earth, and Environment
Division of Energy Technology
CHALMERS UNIVERSITY OF TECHNOLOGY
Gothenburg, Sweden 2024